Spring 1-1-2011

The Effects of Snow Loading on Lightweight Metal Buildings with Open-Web Steel Joists

Jamie Marie Geis
University of Colorado at Boulder, jamie.geis@colorado.edu

THE EFFECTS OF SNOW LOADING ON LIGHTWEIGHT METAL BUILDINGS WITH OPEN-WEB STEEL JOISTS

by

JAMIE MARIE GEIS

BSCE, Gonzaga University, 2009

MSCE, University of Colorado, 2011

A THESIS SUBMITTED TO THE

FACULTY OF THE GRADUATE SCHOOL OF

THE UNIVERSITY OF COLORADO

IN PARTIAL FULFILLMENT OF THE REQUIREMENTS

FOR THE DEGREE OF

MASTER OF SCIENCE

DEPARTMENT OF CIVIL, ENVIRONMENTAL

AND ARCHITECTURAL ENGINEERING

December 2011

THE EFFECTS OF SNOW LOADING ON LIGHTWEIGHT METAL

BUILDINGS WITH OPEN-WEB STEEL JOISTS

By Jamie Marie Geis

The final copy of this thesis has been examined by signatories, and we find that both the content and form meet acceptable presentation standards of scholarly work for the Department of Civil, Environmental and Architectural Engineering.

_____

(Abbie Liel) Principal Advisor

_____

(George Hearn)

_____

(Siva Mettupalayam)

Abstract

Geis, Jamie M. (M.S., Civil, Environmental and Architectural Engineering)

The Effects of Snow Loading on Lightweight Metal Buildings with Open-Web Steel Joists

Thesis directed by Assistant Professor Abbie B. Liel

The implications and consequences of snow loading on buildings can be significant, with failures resulting in damage, casualties, and building downtime. This study seeks to probabilistically quantify the effects and consequences of snow-induced building failure and to examine the behavior and performance of lightweight metal buildings with open-web steel joists to snow overloading.

One part of the study focused on the quantification of national and worldwide building failure trends. In terms of snow-induced incidents, 1,029 national and 91 international building failures revealed patterns of roof failure attributed to the amount of snow, rain-on-snow mixes, and building problems. Warehouses, factories, and commercial buildings were most commonly affected.

The second part of the study centered on the analysis of open-web steel joist roof systems, which may be particularly vulnerable to snow-related failures. Seventy-one archetypical lightweight metal buildings were identified, each with different design characteristics that may have an influence on structural response. Nonlinear simulation models for seven archetypical

buildings were developed and subjected to pushdown analyses under uniform snow loads. Each building was modeled independently and building responses were compared.

Results from the nonlinear static pushover analyses show that the open-web steel joist roof systems yield when loaded with roof snow loads about double their design roof snow load capacities. This overload capacity implies that there is an adequate level of built-in safety when considering snow overload due to extreme or unanticipated snow events, such as rain-on-snow or drifted snow. All buildings exhibited the same type of response trend, with elastic linear responses up to the point of yielding, and inelastic strain hardening responses after the point of yielding. Through a deflection-controlled static pushover analysis, one building was analyzed with increasing incremental deflections at mid-span until the joist's maximum deflection was achieved, which resulted in major in-plane yielding of the top and bottom chords and movement of the neutral axis of the joist into the top chord. Advancement and development of the building models in this study will lead to a broad and representative set of models aimed with the intention of furthering our understanding of open-web steel joist roof systems.

Acknowledgements

I would like to express my sincere appreciation to my advisor and mentor, Professor Abbie Liel. Without her continued support and guidance, this research would not have been possible. I feel honored to have had the opportunity to work with her. I would also like to thank the other members on my graduate committee, Professor George Hearn and Professor Siva Mettupalayam for their keen insight and helpful suggestions.

I am grateful for the opportunity to attend the University of Colorado and to work on this research, generously funded by the National Science Foundation. I express my appreciation to the NSF for granting me the opportunity to present my research at the 2011 CMMI Grantees Conference in Atlanta, Georgia, as well as to the numerous other professionals with whom I have worked and collaborated. Special thanks to Jim Harris for sharing his knowledge and expertise of the structural engineering field and for providing the case studies used in this project. Thanks to Judith Mitrani-Reiser and Professor Rajagopalan Balaji for their advice and collaboration.

Lastly, I would like to thank my family, friends, and research team for their continued support, guidance, and words of encouragement they shared with me during my graduate experience.

Contents

List of Tables

List of Figures

Chapter 1

Introduction

1.1 General Background

The implications and consequences of snow loading on buildings can be significant, with failures resulting in damage, casualties, and building downtime. Although snow-induced building failures are fairly uncommon, one building failure can have significant detrimental effects on businesses and communities. Climate changes have caused average temperatures to increase on a global scale, leading to more unpredictable weather patterns and severe snowstorm events. As a result, the occurrence of large, dense snowfalls is expected to increase in certain regions of the world (CCSP 2008). With the additional implications of wetter and heavier snowfalls, adequate understanding of snow design and snow-related consequences on buildings is crucial. In recent years, high profile structural collapses include the Hartford Civic Center arena in Connecticut (1978) and the C.W. Post Theater on Long Island (1978). Quantifying risks associated with snow-induced damage or collapse is critical in understanding the implications on life safety, building downtime, and economic losses.

1.2 Motivation and Objectives

In this study, we seek to probabilistically quantify the effects and consequences of snow-induced building failure and to study the behavior, performance, and susceptibility of lightweight metal buildings with open-web steel joist roof systems to snow loading. Studies have shown that due to their high snow to dead load ratios, lightweight metal and steel buildings can be particularly susceptible to snow in cases of drifting and rain-on-snow events. On the basis of these studies, the behavior of long-span, lightweight metal buildings with open-web steel joist systems to snow loading was investigated in a performance-based snow engineering context. This research contributes to the advancement of national snow load provisions and the understanding of the behavior of lightweight metal buildings with open-web steel joist systems.

1.3 Scope and Organization

Although the building response methods developed in this study can be applicable to many different types of structures, this research specifically focuses the susceptibility and behavior of lightweight metal buildings with open-web steel joists to snow loading. Included within this study is a summary of the types, history, and development of open-web steel joists and discussion of the key parameters that contribute to the overall susceptibility of buildings with open-web steel joist roof systems to snow-induced failure. National and worldwide building failure trends are subsequently investigated in order to identify key failure modes and building types shown to be susceptible to snow loading. Finally, nonlinear structural models are developed to determine the factors that contribute to the susceptibility of lightweight metal buildings with open-web steel joists to snow-induced failure and to validate failure modes exhibited through case studies with failure modes exhibited by the building models.

Chapter 2 presents how modern snow design provisions are used to predict roof snow loads from ground snow loads, based on statistical weather data and geometric and regional factors. Design standards for uniform and nonuniform roof snow loads are discussed.

Chapter 3 investigates worldwide and U.S. building failures due to snow-related causes and identifies the failure modes, building types, building activities, and loading conditions shown to be susceptible to snow-induced loading. A detailed literature review is included so as to position this study within the broader context of other research concerning snow-induced building failures.

Chapter 4 discusses the types, history, production, development, and susceptibility of lightweight metal buildings, with specific emphasis on roof systems containing open-web steel joists. Also included in this chapter is a discussion of the key differences between lightweight metal buildings and other types of buildings and identification of the specific design factors that may contribute to overall susceptibility of lightweight metal buildings to snow loads.

Chapter 5 includes a detailed methodology of the design and analysis of nonlinear building models in order to determine the factors that contribute to the susceptibility of lightweight metal buildings with open-web steel joists to snow-induced failure. Building response under snow loading is simulated using robust nonlinear models in the OpenSees software package.

Chapter 6 presents the results of pushdown analyses performed on six archetypical lightweight metal buildings with open-web steel joists. A more thorough pushdown analysis is performed on one building in order to identify how these types of buildings respond when subjected to extreme snow loads. Failure parameters of interest include globalized yielding and localized buckling of joist elements.

Finally, **Chapter 7** summarizes the important findings of this research and discusses any implications related to presently-constructed long-span, lightweight metal buildings with open-web steel joists.

Chapter 2

Conventional Building Design for Snow Loads

2.1 Background

Modern code provisions require that buildings be designed to resist snow loads. Since a portion of this project focuses on the response of buildings to snow loads, a general understanding of how buildings are designed and their requirements for resisting snow must be understood. Currently, two prominent design procedures exist for buildings: code-based prescriptive design procedures and performance-based design procedures. The main difference between these two lies in the level of uncertainty incorporated into design. Prescriptive procedures acknowledge some level of uncertainty in design through load factors and strength reduction factors. However, performance-based procedures specifically take into account the levels of uncertainty associated with defining hazards, performing design processes, and estimating consequences of failure (Tang et al. 2008). While performance-based techniques are becoming more popular for uses in lateral design, prescriptive design procedures are commonly used for snow design. As such, this project begins using prescriptive design procedures and ends using performance-based techniques. One of the major aims of this project is to contribute to future research in the advancement and implementation of performance-based techniques for snow design.

This chapter discusses the background of conventional building design for snow, as described in ASCE 7-05, and highlights important code requirements related to designing for snow loads. It is important to note that at the time of ASCE 7-10's release, this project had already begun using ASCE 7-05 as the governing code provision. Therefore, the 2005 version was used throughout the life of this project. Differences in snow design do exist between the 2005 and 2010 versions of ASCE 7, however these do not affect estimations of uniform balanced snow loads for building roofs (O'Rourke 2011). For a complete synopsis of the changes between ASCE 7-05 and 7-10, please reference Appendix 2. In this project, only uniform and balanced snow loads are used in design, therefore results should be compatible between the 2005 and 2010 versions. Any future investigation relating to this project should use ASCE 7-10.

2.2 Probabilistic Philosophy behind Snow Design

The approach behind snow design in the U.S. is probabilistic in nature. Basic snow design principles aim to reduce the risk of snow-induced failure to an acceptably low level by establishing design snow load values that meet a targeted level of reliability. In modern U.S. codes, ground snow loads having a two percent annual probability of being exceeded, otherwise known as a 50-year recurrence interval, are used in snow design. To determine the design roof snow load for a particular building, roof snow loads are calculated from these probabilistically defined ground snow loads and modified based on site conditions and building characteristics. Site conditions include exposure, while building characteristics include roof geometry, thermal considerations, building occupancy, and building function.

2.3 Ground Snow Load Values

ASCE 7-05 design ground snow load values were developed from extreme-value statistical analysis of weather data collected from 204 National Weather Service (NWS) first-order stations across the U.S. between 1952 and 1992. At every station, ground snow depths and loads were measured daily for at least 11 years during the 40-year period (O'Rourke 2007). The mathematical relationship between the snow depths and loads having a two percent annual probability of being exceeded, otherwise known as a 50-year recurrence interval, was found using nonlinear best-fit techniques and was used to estimate the two percent ground snow loads at about 9,200 other U.S. locations for which only snow depths were measured. Based on these estimated ground snow load values and additional information, such as the number of years of record available at each location, maximum observed snow loads, regional topography, elevation of each location, meteorological information available from NWS, the Soil Classification Service (SCS) snow surveys, and other sources, design ground snow load maps were constructed from the 204 first-order and the 9,200 second-order locations (ASCE 2005). The design ground snow load maps, shown in Figure 2.1, specify the ground snow load, in psf, that must be considered in design.

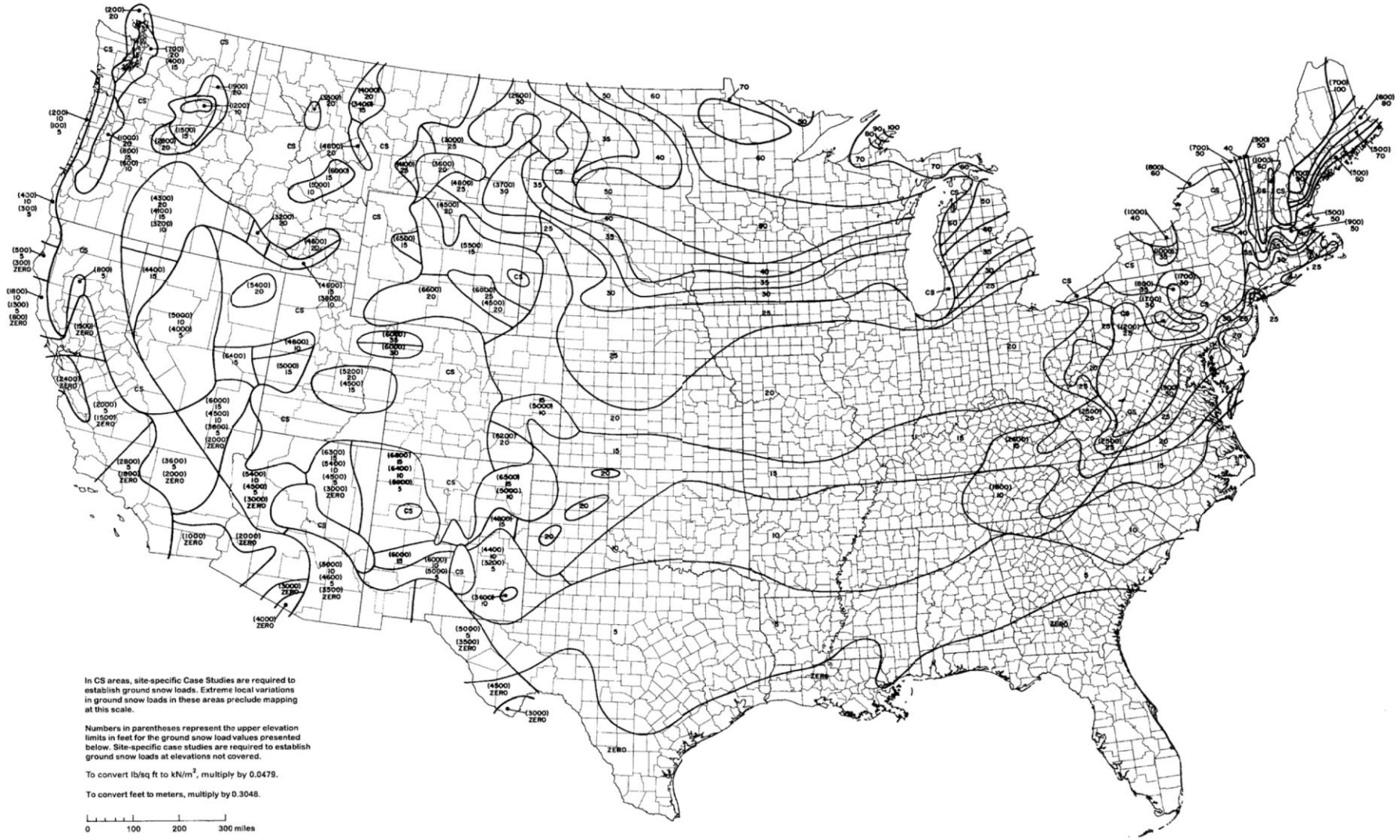

Figure 2.1– Ground snow loads, p_g, for the United States (psf) (ASCE 7-05).

Local climate and topography may heavily influence ground snow loads at site-specific locations, shown in the case study areas in Figure 2.1, denoted by 'CS'. The ground snow load values of some of these locations are shown in Table 2A.2 (see Appendix 2); for other case study regions not shown in Table 2A.2, ground snow load data from local sources should be consulted. In terms of regional variability, ground snow loads may be affected by their proximity to bodies of water and elevation. For example, a 75 psf design snow load or greater is required around regions of the Great Lakes to account for lake-effect storms. In some areas of the Rocky Mountains, the ground snow load exceeds 200 psf, and in the southern portion of the Appalachian Mountains, not far from sites where a 15 psf ground snow load is appropriate, ground loads exceeding 50 psf may be required (ASCE 7-05 2005).

2.4 Roof Design Loads

ASCE 7-05 provides a generalized procedure to calculate design roof snow loads. First, ground snow loads are determined for a geographic region. Flat roof snow loads are generated from the ground loads depending on roof exposure, roof thermal conditions, occupancy, and function of the structure. Next, roof slope and partial loading are considered. For structures with multi-step roofs or projections, snow drifts are also considered in addition to sliding snow, rain-on-snow, and ponding. Snow load design information that directly pertains to this research is included in this chapter. Additional snow load design information is included in Appendix 2.

2.4.1 Flat Roof Snow Loads

Snow loads on flat roofs (those having slopes of five percent or less) are calculated from Equation (2-1), where p_f is the flat roof snow load, p_g is the ground snow load, C_e is the exposure factor, C_t is the thermal factor, and I is the importance factor.

$$p_f = 0.7\, C_e\, C_t\, I\, p_g \tag{2-1}$$

In this basic conversion equation between ground snow loads and roof snow loads, the 0.7 factor accounts for the average exposure of roofs to wind and sunlight. The exposure factor, thermal factor, and importance factor are determined from Table 2.1, Table 2.2, and Table 2.3, respectively.

The exposure factor, C_e, accounts for specific roof exposure and surrounding terrain characteristics. Exposure factor values range from 0.7 to 1.2, as indicated in Table 2.1. Buildings that are fully exposed, or are in other words, not sheltered by trees or other structures, have the smallest exposure factors, leading to reductions in roof snow load values by 10% to 30%. Other buildings that are partially exposed have exposure factors between 0.8 and 1.0 and sheltered buildings have exposure factors greater than 1.0 (leading to an increase rather than a reduction in roof design snow loads). It is important to note that different parts of building roofs may have different exposure factors based on stepped roofs or other roof obstructions.

Table 2.1 – Exposure Factor, C_e (ASCE 7-05).

Terrain Category	Exposure of Roof[a] Fully Exposed	Partially Exposed	Sheltered
B (see Section 6.5.6)	0.9	1.0	1.2
C (see Section 6.5.6)	0.9	1.0	1.1
D (see Section 6.5.6)	0.8	0.9	1.0
Above the treeline in windswept mountainous areas.	0.7	0.8	N/A
In Alaska, in areas where trees do not exist within a 2-mile (3 km) radius of the site.	0.7	0.8	N/A

The thermal factor, C_t, accounts for the effects of heated or unheated structures; generally, more snow will be present on cold roofs than on warm roofs. Thermal factor values range from 0.85 to 1.2, as indicated in Table 2.2. Typical heated structures have a thermal factor of 1.0, while other unheated structures or structures kept just above freezing have a thermal factor of 1.1 or 1.2. Roof snow load values of continuously heated greenhouse are reduced by 15% with a thermal factor of 0.85.

Table 2.2 – Thermal Factor, C_t (ASCE 7-05).

Thermal Condition[a]	C_t
All structures except as indicated below:	1.0
Structures kept just above freezing and others with cold, ventilated roofs in which the thermal resistance (R-value) between the ventilated space and the heated space exceeds 25 °F× h× ft^2/Btu (4.4 K × m^2/W).	1.1
Unheated structures and structures intentionally kept below freezing.	1.2
Continuously heated greenhouses[b] with a roof having a thermal resistance (R-value) less than 2.0 °F× h× ft^2/Btu (0.4 K × m^2/W)	0.85

The importance factor, *I*, accounts for the need to relate design loads to the consequences of failure. Importance factors for buildings depend on the occupancy and function of the building. Occupancy categories can be found in Table 2A.1 in Appendix 2. Structures with higher consequences of failure have higher category numbers, and thus higher importance factors (see Table 2.3). In consequence, while the flat roof snow load is increased by 20% for hospitals and emergency facilities, the flat roof snow load is decreased by 20% for minor structures such as agricultural buildings and garages. If occupancies and building functions are classified as normal, the importance factor equals 1.0. For any case of *I* equaling 1.0, the design snow load procedures are intended to give roof snow load values with 2% annual probabilities of being exceeded (ASCE 2005). Roof snow load values for flat roofs must be greater than or equal to $I \cdot p_g$ if the ground snow load is less than or equal to 20 psf. If ground snow loads exceed 20 psf, flat roof snow loads must be greater than or equal to $20 \cdot I$ (ASCE 2005).

Table 2.3 – Importance Factor, *I* (snow loads) (ASCE 7-05).

Category[a]	I
I	0.8
II	1.0
III	1.1
IV	1.2

2.4.3 Sloped Roof Snow Loads

For roofs with slope greater than 5 degrees, sloped roof snow loads are converted from flat roof snow loads by multiplying by a roof slope factor, C_s (Equation (2-2)):

$$p_s = C_s\, p_f \tag{2-2}$$

In most cases, roof snow loads decrease as roof slope increases because wind and sliding reduces the amount of snow on the roof. The roof slope factor, C_s, varies for warm roofs, cold roofs, curved roofs, and multiple roofs. Roofs with smoother surfaces, such as metal roofs, will have a smaller roof snow load than roofs with rougher surfaces, such as shake or asphalt roofs (ASCE 2005).

2.4.4 Snow Drift Loads

Snow drifting can cause snow to accumulate around roof obstructions (i.e. parapet walls, mechanical equipment, or multi-level roof steps as shown in Figure 2.2a, Figure 2.2b, or Figure 2.2c). Other types of roof geometries may also experience snow drifting, such as where snow drifts from the upper roof accumulate in the leeward face of the lower roof step (Figure 2.2e). When an addition is added to the building, the change from one roof shape to another can allow drifted snow to accumulate between the two roofs, as shown in Figure 2.2d.If the separation between the building and another structure or terrain feature is 20 feet or less, the roof of a building might be adversely affected by snow. This phenomenon is shown in shown in Figure 2.2f, where taller building is built within 20 feet of a smaller building (ASCE-7 2005). Refer to Appendix 2 for more detailed information on the calculation of drifted snow loads. Thus far, the buildings designed for this study did not consider drifting loads.

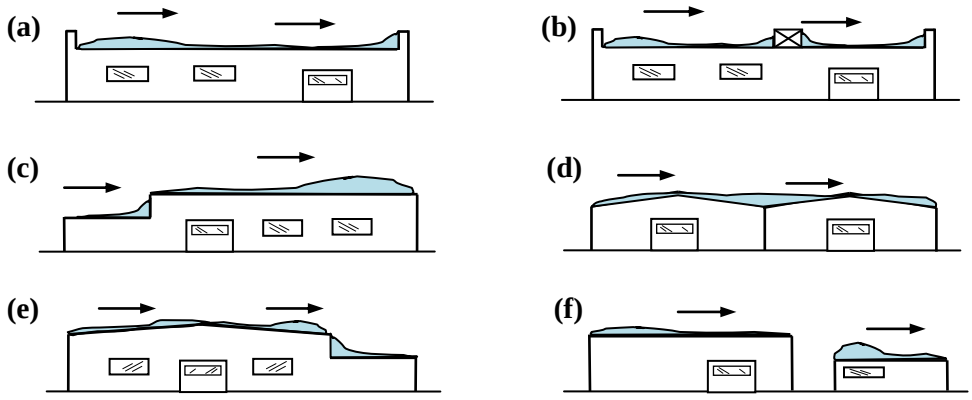

Figure 2.2 – Elevation views depicting the effects of snow drifting around roof obstructions on lightweight metal buildings with (a) parapets (b) mechanical equipment and parapets (c) multi-step roofs (d) low-sloped gable roofs (e) low-sloped gable, multi-stepped roofs (f) neighboring buildings.

In addition to snow drifting, additional considerations should include partial loading, rain-on-snow surcharges, ponding, and drifted snow around parapets and mechanical equipment. See Appendix 2 for more detailed information.

2.4.5 U.S. and Canadian Building Codes

While the U.S. snow load provisions are based upon the *National Building Code of Canada's* (2010) snow design provisions, many differences exist between the two (ASCE 2005). Instead of being based on many years of frequently measured loads, the Canadian provisions are based on measured snow depths and regionalized densities based on four or fewer measurements per month. An additional rain load is added to the ground snow load to account for the infrequency of density measuring. In the U.S. snow design provisions, if the ground snow load is greater than 20 psf, an additional rain load is not required in the calculation of the roof snow load because the effects of rain are sufficiently captured in the data set (ASCE 2005). If the ground snow load is less than or equal to 20 psf and the roof slope is less than *W*/50, an additional 5 psf rain-on-snow surcharge load must be added to the roof. Ground snow loads for the U.S. and Canada are both based on a 50-year recurrence interval.

The basic ground to roof snow load equation (Equation (2-1)) in the U.S. has a 70% reduction factor, and has five terrain categories, three roof exposure categories, and four thermal categories options. In contrast, the Canadian code has an 80% basic exposure reduction factor with three exposure categories and no thermal distinctions. Differences between the basic conversion equation and associated categories in the U.S. and Canada do not indicate differences in safety, but rather differences in the number of exposure and thermal classifications of roofs. ASCE 7-05 includes a greater number of options in these classifications than the Canadian building code in order to lessen the impact of difference in opinion when choosing an exposure category. If one designer subjectively selects a category slightly different than another designer, the associated change in the design factor is smaller using the U.S. provisions than Canada's. This error is about 10% in the U.S. (using the 12 options in categories) and is about 25% in Canada (with three exposure categories) (ASCE 7-05 2005).

2.5 Summary

Snow design provisions for buildings in the United States are based upon Canadian building codes, but are developed more specifically for regional and terrain characteristics in the U.S. They are probabilistic in nature, and take into account the uncertainly associated with the occurrence of a particular snow event—in the U.S., that being a ground snow load having a two percent chance of being exceeded. This project uses both prescriptive-design to design open-web steel joist roof systems and analyzes them using performance-based design procedures. Engineers should design buildings with discretion and care, according to provisions set by ASCE 7 and other national building codes.

Chapter 3

Snow-Induced Building Failures

This chapter is a study of snow-induced building failure and damage trends in the U.S. and abroad. It is a version of a paper accepted for publication by the *Journal of Performance of Constructed Facilities* in February, 2011. The paper was written by Jamie Geis[1], Kristen Strobel[2], and Abbie Liel[3]. Identifications of the failure modes, building types, building activities, and loading conditions shown to be susceptible to snow-induced loading are discussed.

3.1 Abstract

This study examines 1,029 snow-induced building failure incidents in the United States between 1989 and 2009 and 91 international incidents between 1979 and 2009. Incidents were identified through newspaper archives, including 1,345 articles from 883 sources. Most U.S. incidents occurred in New York, New Hampshire, and Massachusetts. Findings show that 37% of all buildings experiencing snow-induced failure incidents in the U.S. were of metal/steel construction and another 37% were of timber, while 53% of international incidents were metal/steel and 17% were concrete. Warehouses, factories, and commercial buildings were the most common buildings affected. Failures were attributed to the amount of snow, rain-on-snow

[1] Graduate Student, Univ. of Colorado, Boulder, CO 80309
[2] Undergraduate Student, College of Engineering's Discovery Learning Apprenticeship, Univ. of Colorado, Boulder, CO 80309
[3] Assistant Professor and Corresponding Author, Department of Civil, Environmental and Architectural Engineering, Univ. of Colorado, Boulder, CO 80309

mixes, and building problems. Monetary impacts included building damages ranging between $1,000 and $200 million and business interruption associated with an average building closure of four months. Nineteen fatalities and 146 injuries were reported for the U.S., while 293 fatalities and 586 injuries were reported internationally. These findings describe building failure trends which may be significant, considering potential impacts of accelerating global climate change on the patterns of snowfall frequency and density.

3.2 Introduction

Extreme snow loading can cause significant damage to buildings and lead to roof collapse, sometimes requiring costly repairs, interrupting business, damaging building contents, or endangering occupants. High profile American building failures due to snow have included the Hartford Arena in Connecticut (1978) and the C.W. Post College Theater on Long Island (1978) (Levy and Salvadori 2002); recent international failures include the collapse of the Basmanny Marketplace in Russia and the Katowice Exhibition Hall in Poland, both of which occurred in the spring of 2006, killing a total of 131 people. Snow-induced building failures can also have significant economic and societal impacts on businesses and communities. In January 1996, a large winter storm damaged buildings from Kentucky to Maine, including shopping malls, manufacturing facilities, supermarkets, theater complexes, and sports facilities (DeGaetano et al. 1997). Similarly, a March 1993 snowstorm caused damages and business disruption exceeding $200 million (1993 dollars) in the southeastern U.S. (O'Rourke and Auren 1997). More recently, three blizzards in February 2010 damaged buildings in Mid-Atlantic and New England states, including an ice rink and corporate jet hangars at both Manassas Regional and Dulles International Airports in Virginia (Kiser 2010). Some states, including New York, require yearly inspections of school roofs to prevent failure, but oftentimes there is no obligation

that building owners inspect or monitor roofs of other building types (Fish 1994). Although a number of studies have examined general trends in building failures, studies of snow-induced building failure incidents are limited.

This paper examines the risk of building failure and damage due to snow loading, characterizing the relative susceptibility of different types of structures and the human and economic impacts of these incidents. The research methodology examines snow-induced building failure incidents in the U.S. between 1989 and 2009 and worldwide between 1979 and 2009 using records of building damage and impacts gathered from databases of archived newspaper articles. These incidents include not only high profile building failures, like the Hartford Civic Center Arena, which have been investigated through detailed forensic studies, but also warehouses, strip malls, and other structures whose failure generally garners little attention—but may have significant impact on business and communities. By collecting and analyzing data regarding snow-induced building failure incidents, this study uncovers patterns of failure, damage, and risk and considers the implication of these results for design and assessment of buildings subjected to extreme snow loads.

3.3 Past Research on Snow-Related Building Failures

A number of studies have investigated major trends in building failures, including Hadipriono (1985), Hadipriono and Diaz (1988), Eldukair and Ayyub (1991), Wardhana and Hadipriono (2003), and others. Eldukair and Ayyub (1991), for example, found that 41% of building failures in the U.S. between 1975 and 1986 were the result of severe weather. Wardhana and Hadipriono (2003) analyzed 225 U.S. buildings that failed due to weather, poor maintenance, or construction deficiencies from 1989 to 2000, concluding that low-rise buildings were the most likely to fail, constituting 63% of all cases, with multistory buildings the second

most susceptible category. In addition to noting that the number of failures per year increased over the 11-year period, that study also confirmed Eldukair and Ayyub's (1991) observations of the significant role of weather in causing building failures. However, neither classified nor quantified the effects of these failures or distinguished snow from other weather events. O'Rourke et al. (1983) found that snow-related roof failures for industrial buildings exceeded those due to rain loads, structural deterioration, and other causes, contributing to 55% of all roof-related insurance claims from 1974 to 1978.

A few studies have looked specifically at the relationship between snow loading and building failures. O'Rourke et al. (1982) showed that the conversion factors to determine roof snow loads from ground snow loads in U.S. building codes lead to conservative estimates of design roof loads. Following two large January 1996 snowstorms in the Mid-Atlantic and New England states, DeGaetano et al. (1997) showed that snowfall exceeded the 50-year snow loads, which are the basis for snow loads in design standards, contributing to the building collapses during those storms. A follow-up study by DeGaetano and Wilks (1999) found that most of the buildings damaged during the 1996 storms were not engineered correctly or were built prior to the establishment of stringent building codes. Meløysund et al. (2006) examined existing buildings in Norway after an unusually large number of collapses took place during the winter of 1999—2000, concluding that older Norwegian buildings have reduced safety against snow-induced collapse in comparison to buildings meeting Norwegian modern code provisions. These findings were based on data from insurance companies and government agencies, calculations of design loads at the time of construction, and structural analyses, but due to differences in design codes, it is unclear whether the results are also applicable to older U.S. buildings.

Other studies have used numerical building simulation to evaluate the reliability of structures subjected to large snow loads. Takahashi and Ellingwood (2005) found that simply-supported structures having high snow to dead load ratios in design had a higher risk of failure than heavier structures. Likewise, Holicky (2007) examined current European design procedures, again concluding that the reliability of structural members is highly variable, with lightweight (low dead load) roof systems failing to meet a specified target reliability level. A follow-up study by Holicky and Sykora (2009) found that insufficient code provisions for lightweight roofs and human and design errors were the most common causes of the large number of roof failures in Europe during the 2005—2006 winter.

With regard to specific snow-related building failures, major U.S. case studies include the Hartford Civic Center and the C. W. Post College Dome Auditorium collapses. The collapse of the steel space frame roof of the Hartford Civic Center has been attributed to overconfidence in computer analysis. Excessive deflections that occurred during construction were ignored by engineers, who claimed that discrepancies between actual and theoretical deflections were expected. In fact, these excessive deflections were found to be the result of design and construction errors, specifically inadequate lateral bracing and weak supports of the roof members (Martin and Delatte 2001). The C.W. Post Auditorium, a shallow, rectangular steel mesh dome, collapsed due to uneven loading associated with drifting snow and ice, resulting in the overstressing of structural members (Levy and Salvadori 2002). Significant studies into international snow-induced building failures in recent years investigated the Bad Reichenhall Ice-Arena (Germany) in 2004 and the Katowice Exhibition Hall (Poland) (Biegus and Rykaluk 2009). Mistakes in structural calculations, defective construction, and lack of maintenance contributed to the failure of the cross-girder timber roof system of the Bad Reichenhall Ice-Arena

(Winter and Kreuzinger 2008). The Katowice Exhibition Hall's steel truss roof system was shown to have collapsed due to insufficient strength and stiffness of main structural elements and overloads from a thick layer of ice and snow (Biegus and Rykaluk 2009).

Although these studies have investigated general building failure trends, forensics of specific snow-related building failures, and code compliance, the authors are aware of no previous study attempting to create a database of snow-induced building incidents as a means of investigating the patterns and significance of these types of failures.

3.4 Study Design

Snow-related building incidents and failures were identified and classified using newspaper reporting on snowstorms and their effects. The database of U.S. incidents was developed by searching the 'U.S. Newspapers and Wires' references in *LexisNexis Academic* (2010). This source consists of major U.S. newspapers and wire services, from which more than 60% of the stories originate in the United States (including the well-known *Associated Press*). Snow-related building failure incidents were identified using "snow and roof and collapse" as the search criteria; articles containing these terms, but not relevant to snow-related building failure, were eliminated. A total of 1,221 articles from 131 newspapers in 37 states were identified to satisfy the search and relevance criteria in the study period between January 1, 1989 and December 31, 2009. Reporting in the selected articles covered descriptions of snow and weather events, effects on city systems and infrastructure and, most importantly for this study, impacts on buildings and other structures, including damage, economic impacts, and other factors. Before selecting *LexisNexis Academic*, a variety of sources known to publish information on snow-related building incidents were investigated. With a total of 687 sources and newspapers from all states and major cities in the U.S., *LexisNexis Academic* is sufficiently comprehensive for this

investigation and, in addition, included references to all critical incidents found in a review of other sources, including *Engineering News-Record*. Insurance data, while useful, is not publically available and was therefore not used in this study.

LexisNexis Academic was also used to identify international incidents of snow-induced building failures, searching 'Major World Publications'. This database contains 752 full-text news sources, including newspapers, magazines, and trade publications (2010). Since *LexisNexis Academic* produced a limited number of hits for international incidents, the *Factiva* (2010) database was also used to search 'Major News and Business Publications', which includes key publications with large circulation. Major U.S. publications were excluded from the search, and only English language articles were included. Together, *LexisNexis Academic* and *Factiva* produced 124 relevant articles from 39 different international newspaper sources published between January 1, 1979 and December 31, 2009. A longer study period was considered for international incidents to increase the number of relevant articles.

Articles were coded according to a set of instructions for identifying and classifying reported snow-related failure incidents. As shown in Table 3.1, each article meeting search and relevance criteria was assigned a unique *source index* and pertinent article information including date, newspaper, and byline was recorded. Each snow-related building failure (which may have been reported in one or more articles) corresponds to a unique *incident index*, and the details about date and location of incident are recorded in Table 3.2. Table 3.1, Table 3.2, and Table 3.3 include examples of the information gathered, representing a subset of the database created in this research.

Table 3.1 – Article Source Details (from U.S. database).

Source Index	Incident Indices	Newspaper	State	Date	Byline	Title	Section	Page	Word Count
1	1	Spokesman Review	WA	8/14/09	Boggs	Old School...	A	1	729
2	1	Lewiston Morning	ID	7/25/09	—	Idaho Offi…	—	—	127
3	1	The Associated Press	—	7/24/09	—	Displaced…	B	—	135
4	2	The Associated Press	—	7/10/09	Robbins	Company…	C	—	676
…continued for source indices 5 to 1,221									

Table 3.2 – Incident Identification (from U.S. database).

Incident Index	Source Indices	Building Name	City	State	Date
1	1, 2, 3	Lakeside Elementary	Worley	ID	7/15/09
2	4, 5, 6	Philadelphia Regional…	Philadelphia	PA	1/31/09
3	5, 6	Warehouse Building	Fort Plain	NY	1/31/07
…continued for incident indices 4 to 1,029					

Table 3.3 – Incident Classification (from U.S. database).

Incident Index	Damage	Collapse	Closure	Evacuation
1	—	—	—	1
2	1	—	—	1
3	—	1	1	—
…continued for incident indices 4 to 1,029				

Basic terminology used in this study is defined as follows. Any building that was damaged, collapsed, closed, or required occupants to be evacuated as a result of snow loading is referred to as an *incident.* Therefore, every incident represents a building whose structure, contents, or occupants have been impacted by snow loads. *Collapse* refers to any incident in which the roof's structural system fails and a portion of the roof falls in, while *damage* refers to the loss of integrity of any structural or nonstructural component not resulting in collapse (e.g. cracking, rotting, deflection of structural members, broken pipes, or water damage). Incidents could be classified as either damage or collapse, but not both. In other cases, *warnings*, such as cracking of structural members, deflections, or creaking noises, notified occupants of danger previous to damage or collapse. Building *closure* identifies those structures that were closed following an incident for repair or maintenance. Closure is distinguished from *evacuation*, which refers to the suspension of operation to ensure occupant safety. Evacuation can occur before any

damage. Incidents classified as experiencing closure, evacuation, or warning may or may not have also been characterized as damaged or collapsed. In Table 3.3, a "1" is used to identify those classifications that are associated with a particular incident.

In total, 1,029 incidents and 840 (77% of the total) collapses were recorded in the U.S. database over the 1989—2009 study period. The international database consists of 91 incidents occurring between 1979 and 2009, of which 80 (88%) were collapses. In the U.S., 182 (18%) incidents reported evacuation, 587 (57%) reported closure, and 32 (3.1%) reported both evacuation and closure; internationally, 25 (28%) incidents reported evacuation, 14 (15%) reported closure, and 4 (4.4%) reported both evacuation and closure. Only 6.7% (69) of U.S. incidents and 16% (12) of international incidents were associated with warnings reported in newspaper articles.

Additional details provided about each incident were classified according to major themes, including *(1) building characteristics*, *(2) loading and damage*, *(3) attributed causes*, and *(4) disruption and impacts*. *Building characteristics* recorded include the activity of the building (i.e. recreational facility, school, warehouse, church, etc.), the construction type (i.e. metal/steel, timber, masonry, fabric, etc.), and the age of the building at the time of incident. Construction type corresponds to the type of building, which may have one or more different roof systems. *Loading and damage* details recorded in the database include the amount of snow or severity of storm and the physical impact of the snow load on the building. In the *attributed causes* section (shown in Table 3.4), the database lists the causal factors identified by the article as contributing to each incident. As shown in Table 3.4, common incident causes include the amount of snow, rain-on-snow, drifting snow, melting snow, building problems, person on the roof, and drainage issues. Drainage issues include ponding and blocked or frozen drains. The

disruption and impacts section records the consequences of the incident in terms of building downtime, monetary impacts, legal implications, disabled infrastructure systems, and other factors (Table 3.5). An entry of "1" signals that the cause (Table 3.4) or disruption (Table 3.5) shown was discussed in incident reports.

Table 3.4 – Attributed Causes (from U.S. database).

Incident Index	Amount of Snow	Rain-on-Snow Mixes	Drifting Snow	Melting Snow	Building Problems	Person on Roof	Drainage Issues
1	—	1	—	—	1	1	—
2	1	—	1	—	1	—	—
3	—	—	—	1	—	—	1
…continued for incident indices 4 to 1,029							

Table 3.5 – Disruption and Impact (from U.S. database).

Incident Index	Closure	Closure Time	Evacuation	Evacuation Time	Repair	Demolition	Rebuild	Economic Impact	Legal Implication
1	—	—	1	4 hrs	1	—	—	—	—
2	1	13 days	—	—	1	—	1	$20,000	Lawsuit
3	1	—	—	—	—	1	—	—	—
…continued for incident indices 4 to 1,029									

To verify consistency of the coding procedures, two individuals independently implemented the coding instructions for nine randomly selected articles, including 27 incidents. Although the degree of agreement was good, the procedure was subsequently updated to eliminate discrepancies and ensure repeatability in coding the remaining articles.

To examine the relationship between storm severity and building failure, snowfall records were collected for three U.S. states: Massachusetts, Ohio, and Washington. These states were selected because they reported a relatively large number of snow failure incidents and represent three distinct climatic and cultural regions of the country. Using the National Climatic Data Center's Storm Events Database, snowfall data was gathered from January 1, 1993 to September 31, 2009 (NCDC 2009). No snowstorm data was available before 1993, so the period between 1989 and 1993 could not be examined. Snow data collected relevant to this study includes storm

date, storm location by county and state, reported property damage, and smallest and largest reported snow accumulations per storm.

3.5 Results: U.S. Snow-Related Building Failure Incidents

Information about snow-related building failures collected from newspaper reports is used to identify and describe trends in the U.S. and abroad. This analysis of failures, closures, and warnings provides information to characterize when and where snow-related building failures may occur and the types of buildings that are most at risk, accounting for construction type, activity, and age. In addition, incident data provides insight into the most frequently cited causes of failure and impacts on buildings, property damage, business interruption, and life safety.

3.5.1 Regional and Seasonal Variation

Factors such as building location, time of year, and weather patterns affect a building's susceptibility to extreme snow loads. Incidents were reported in 42 states, as shown in Figure 3.1, and clustered, as expected, in northern regions of the country. The majority of reported incidents (58%) occurred in the Mid-Atlantic and New England states, indicated by the white hatching in Figure 3.1. The highest numbers of database incidents per state were from New York, New Hampshire, and Massachusetts with 149, 99, and 87, respectively, comprising in total just under one-third of all U.S. incidents. Eight states had no recorded snow-related building damage or failure incidents: Alabama, Arizona, Florida, Hawaii, Louisiana, Mississippi, South Carolina, and Tennessee.

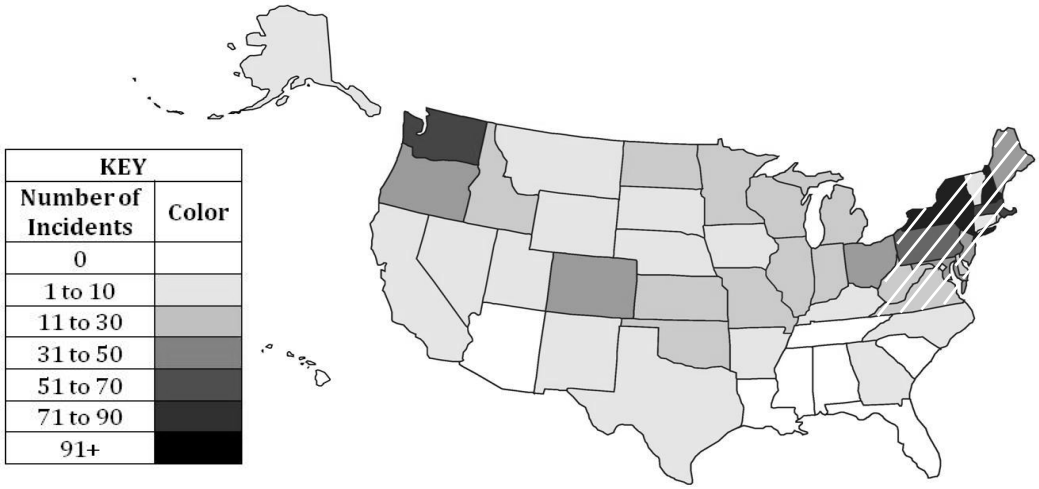

Figure 3.1 – Distribution of U.S. Database Incidents by State.

Although reported incidents appear to be concentrated in more populous states, the data shows only a weak positive correlation between population and incident occurrence. New Hampshire, Maine, and North Dakota had the highest ratio of snow-related building failure incidents relative to population size (based on 2008 data from the U.S. Census Bureau). Maine and North Dakota only had 39 and 13 reported incidents, respectively, but the number of incidents relative to these states' small population and building stock indicates a higher susceptibility to snow-induced failure than other states. Similar patterns were observed comparing the number of incidents to building stock data on a state-by-state basis (Census 2009).

Not surprisingly, 94% of reported snow-induced failure incidents occurred in the winter months of December, January, February, and March, as shown in Figure 3.2. Database incidents in June, July, August, and September were generated from newspaper reporting on building problems including design deficiencies, deterioration, and damage observed during building inspections. More incidents occurred in January and February (61% of total incidents) compared to December and March (34% of incidents), which is consistent with the Northeast States Emergency Consortium's observation that the most severe winter storms typically occur during January and February (NESEC 2008).

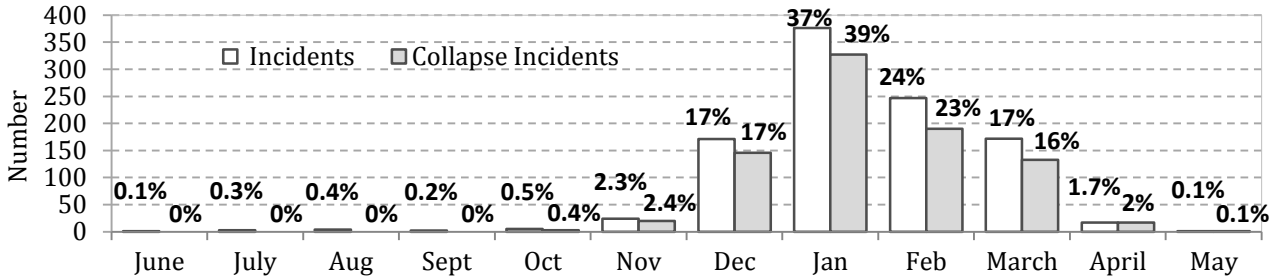

Figure 3.2 – Distribution of U.S. Database Incidents by Month, with Percentages of Total Incidents and Collapse Incidents.

The number of incidents greatly depends on weather patterns for a given year. In years with the greatest number of incidents—1996, 2003, and 2008—major snowstorms occurred. One large storm may dominate the incident total for a particular year. The Blizzard of January 1996, for example, deposited as much as 48 inches of snow in some places, impacting a region from Kentucky to Maine. This storm alone contributed to 86 of the 136 (63%) incidents reported that year. Such a large percentage may indicate uneven coverage of news sources due to the tendencies of newspapers to respond to sensation. To examine the effect of individual storms, 'major' snowstorms were classified as those causing at least ten database building failures. This analysis showed that 19 major snowstorms occurring between 1994 and 2009 contributed to 571 incidents, just over half of all reported incidents in this period. The majority of incidents can therefore be attributed to a small number of large storms.

The relationship between snowfall data and building incidents was further investigated using the storm and snowfall data collected for Massachusetts, Ohio, and Washington. To summarize this data, the depth of snow on the ground in each state was estimated from storm accumulations included in weather data for the first half (days 1 – 15) and second half (days 16 – end) of each month. The estimations were approximated by taking the average of the minimum and maximum snowfall values reported for each storm at the various weather stations, which is a very broad generalization since snow is often localized and might not be distributed over the

entirety of the state. The snow was assumed to have no cumulative effect, (i.e. the snow was assumed to completely melt between bimonthly periods). Each state was taken as a uniform unit, neglecting geographic variation in snowfall. The semimonthly windows were chosen to approximately represent the amount of snow on the ground at any given time. As shown in for Massachusetts, a positive relationship is observed between snowfall in a semimonthly period and the number of incidents in a semimonthly period, with increasing snowfall tending to be associated with a larger number of incidents. Data points along the y-axis showing incidents without any record of snowfall may reflect snow build-up on roofs over days or weeks before the incident, or the additional weight from rain and ice in addition to snow, which could not be determined from available weather data. Large snow depths causing no incidents (i.e. x-axis data points) may represent snow falling on unpopulated areas, or less-dense or quickly-melting snow that imparts smaller loads to buildings. Using the available weather data, it was not possible to determine whether or not snow loads exceeded code design loads for any particular incident. The most impactful storm recorded in the Massachusetts data is the 1996 Blizzard, which deposited an average snow depth of 37.5 inches across the state from January 7—15, leading to 19 reported incidents statewide. The snow depth from this blizzard, combined with the snowfall from a January 2 storm, produced the largest semimonthly value plotted in Figure 3.3 for Massachusetts (48 inches of snow and 19 reported incidents). Similar trends were observed for Ohio and Washington.

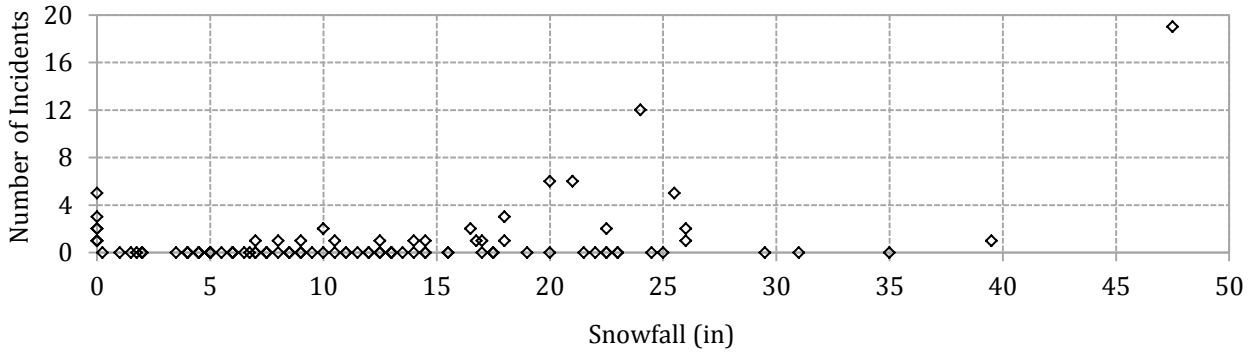

Figure 3.3 – Massachusetts Database Incidents vs. Snowfall for Semimonthly Periods between 1993 and 2009.

3.5.2 Characteristics of Impacted Buildings: Structure, Function, and Age

Of the 233 (23%) incidents with information about building construction type, the majority of impacted buildings are identified as metal/steel (37%) and timber (37%) construction, as shown in Table 3.6. Metal/steel buildings appear frequently in the database because they are commonly used in industrial and retail applications. Their construction consists of various combinations of cold-formed and hot-rolled steel members for roof systems with different types of walls. Certain types of metal/steel construction with high snow to dead load ratios, such as those with lightweight roof and/or wall systems (open-web steel joists, metal roof decking, light-gauge steel walls, etc.) may be particularly at risk under snow loads. Other significant construction types identified in the incident database include masonry (11%) and air-supported structures (9.4%). The number of air-supported structures reported in the database is notable, given that these structures make up a relatively small percentage of the overall U.S. building stock. Air-supported structures and fabric structures seem to be especially susceptible to collapse (21 of 23 and 4 of 5 incidents reported involved collapse, respectively) due to their small dead load, vulnerability to uneven loading, and difficulty associated with clearing snow and ice when overloaded.

Table 3.6– Classification of the Number of Database Incidents by Building Construction Type and Incident Type.

CONSTRUCTION TYPE	All Incidents		Collapse Incidents		Damage Incidents		Closure Incidents		Evacuation Incidents	
	U.S.	Intl.	U.S.	Intl.	U.S.	Intl.	U.S.	Intl.	U.S.	Intl.
Metal/Steel	91	19	78	18	11	1	69	4	14	2
Concrete	6	6	4	6	1	0	4	1	2	1
Masonry	28	3	21	2	6	1	23	3	2	0
Timber	91	3	76	2	15	1	74	2	10	1
Fabric	5	2	4	1	1	1	3	1	0	1
Air-Supported	23	3	21	3	1	0	19	3	2	0
TOTAL [a]	**244**	**36**	**204**	**32**	**35**	**4**	**192**	**14**	**30**	**5**

[a] 11 U.S. and 2 international incidents reported multiple construction types. The total double-counts these buildings (i.e. 244 total incidents includes 233 unique events; 11 are associated with more than one construction type).

Table 3.7 categorizes incidents by building activity, which was reported for 95% of U.S. incidents. The four most commonly reported building activities were industrial (accounting for 20% of all incidents and 24% of collapses), retail and commercial (17% of incidents and 15% of collapses), government and public (16% of incidents and 8.0% of collapses), and minor structures and garages (11% of incidents and 13% of collapses). The government and public building category includes schools, colleges, and universities. In both the U.S. and international databases, educational buildings made up a large percentage of incidents within the government and public building category, accounting for 65 incidents in the U.S. database or 39% of all government and public building incidents. Emergency and medical facilities accounted for 22 U.S. incidents (2.1%), with 55% of these resulting in collapse. These findings illustrate the large number of commercial and institutional incidents as compared to residential incidents, which account for only 7.2% of database entries.

Table 3.7 – Classification of the Number of Database Incidents by Building Activity and Incident Type.

BUILDING ACTIVITY	All Incidents		Collapse Incidents		Damage Incidents		Closure Incidents		Evacuation Incidents	
	U.S.	Intl.	U.S.	Intl.	U.S.	Intl.	U.S.	Intl.	U.S.	Intl.
Agriculture	101	-	100	-	1	-	71	-	2	-
Churches	28	1	18	1	9	0	18	1	4	0
Emergency & Medical Facilities	22	-	12	-	4	-	5	-	8	-
Government & Public Buildings	165	21	82	17	41	2	70	10	70	4
Industrial	207	16	202	16	4	0	136	1	14	1
Minor Structures & Garages	110	3	110	2	0	1	63	0	5	0
Office Buildings	6	18	1	16	4	2	1	6	4	2
Parking Garages	1	1	1	1	0	0	1	0	0	1
Public Attractions	19	5	17	5	0	0	18	0	1	0
Residential-Single Family	37	-	36	-	1	-	19	-	1	-
Residential-Multi Family	37	9	27	6	7	2	19	2	13	3
Restaurants	17	1	15	1	2	0	13	0	1	0
Retail & Commercial	177	2	128	1	28	1	92	1	52	1
Recreational Facilities	56	13	50	12	5	1	43	3	7	2
Stadiums	6	2	4	2	0	0	3	2	2	1
Vacant	46	-	44	-	1	-	29	-	0	-
Not Enough Information/Other	48	1	41	1	4	0	17	0	3	0
TOTAL [a]	**1,083**	**93**	**888**	**81**	**111**	**9**	**618**	**26**	**187**	**15**

[a] Total double-counts 53 U.S. and 2 international incidents that reported multiple building activities.

Figure 3.4 illustrates the number of incidents recorded for each year of the study. On average, 44 incidents and 35 collapses (represented by the solid and dashed lines in Figure 3.4, respectively) were reported for U.S. buildings each year (with an additional 5 incidents per year associated with minor structures such as garages). These data correspond to an average annual incident rate of at least 4.1×10^{-7} [incidents per building] and an average annual collapse rate of at least 3.3×10^{-7} [collapses per building]. In other words, one out of every 2.4 million buildings nationwide has a newspaper-reported snow-related failure incident each year and one out of every 3.0 million buildings nationwide has a newspaper-reported snow-related collapse each year. If we assume the average service life of a structure is 50 years, one out of every 48,000 buildings nationwide reports an incident over its lifetime. (These calculations use the 2007 building stock, which indicate that the U.S. has approximately 106 million buildings, excluding minor structures (Census 2009).) Incident rates should be taken as lower bounds because there are failures that are unreported each year; the impact of reporting biases and trends are discussed

in more detail below. The small number of incidents in the early years of the study most likely reflects news reporting trends and the growth in the building stock since 1980, rather than fewer actual incidents. If only the most recent decade is included (1999—2009), the average number of incidents per year is 57 (excluding minor structures). Census data from 1989 to 2008 show that the number of buildings in the U.S. has increased at an average rate of 1.5 million buildings (approximately 1.5%) per year (Census 2009). These rates are lower bounds since reporting biases will exclude some failures, leading to an underestimation of the number of incidents.

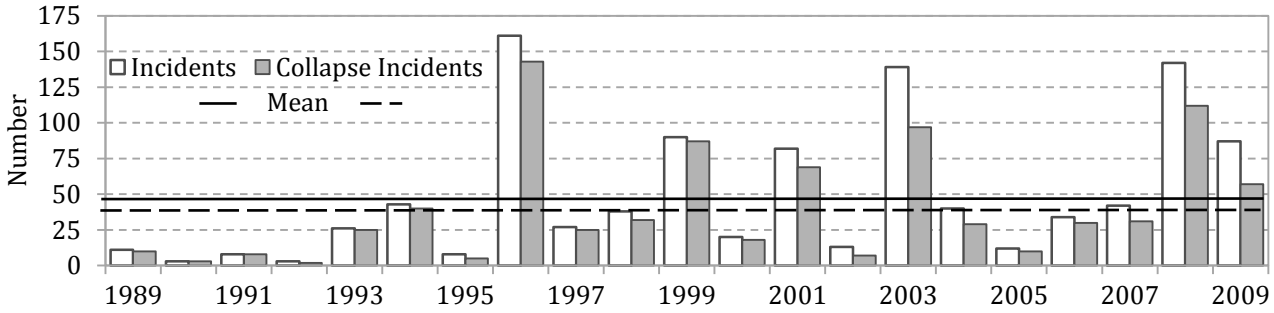

Figure 3.4 – Distribution of U.S. Database Incidents by Year.

According to Census data, the U.S. has approximately 128 million total housing units (defined as single-family dwellings, multi-family dwellings, and mobile homes) and 4.6 million non-residential buildings (Census 2009). The Census also provides 2007 data on the number of units (homes) per residential building, leading to an estimation of approximately 5.1 million multi-family residential buildings and 101 million residential buildings total (Census 2009). Of the 44 incidents reported on average annually, 32 collapses were reported for non-residential buildings, corresponding to an average annual snow-induced non-residential collapse rate of at least 6.9×10^{-6} collapses/total number of buildings. In other words, one out of every 145,000 non-residential buildings reports a collapse each year. The residential failure rate is lower at 3.0×10^{-8} collapses/total number of residential buildings (one out of every 34 million residential buildings each year). Residential construction may have lower susceptibility to snow-related failure.

However, residential building failures may also be less likely to be reported in newspaper articles than buildings with commercial activities. For comparison, seismic safety assessments find that older concrete buildings have a collapse rate of about $75x10^{-4}$ and modern buildings conforming to code requirements may have an annual collapse rate of $3.5x10^{-4}$ in high seismic regions (Liel et al. 2010). Earthquake loading is more uncertain and infrequent than snow loading, perhaps accounting for higher building collapse rates. Under gravity loading only, Ellingwood and Tekie (1999) estimate the annual probability of failure of normal buildings at 6 to $8x10^{-4}$, though failure is defined as yielding, so the likelihood of structural collapse is probably much lower.

Certain types of incidents are more likely to be newsworthy because of their high occupancy, community, or economic significance. Newspapers tend to publish articles reporting on more noteworthy events, such as high-profile roof collapses or roof collapses involving casualties, with less emphasis on garage roof collapses or similar events. Consider the percentage of non-collapse incidents for each building activity category, inferred from Table 3.7. Incidents in high-visibility buildings, such as government and public buildings, retail or commercial buildings, or emergency and medical facilities, were far more likely to be reported when the incident did not constitute building failure. A large percentage of these non-collapse incidents were related to design deficiencies, deterioration, and damage reported by building inspections, and minor snow-related damage, evacuation, or closure. Low occupancy or importance buildings, such as agricultural structures and minor structures and garages, were only press-worthy if significant damage or collapse occurred. As shown in Table 3.7, 99-100% of all reported incidents for agricultural or minor structures were collapses. Other types of structures that were reported in the news only if collapsed include: parking garages, industrial buildings, single-family residential buildings, and vacant structures.

Newspaper articles reported building age for 188 incidents (18% of the total) and these structures ranged in age from newly constructed to 177 years old. As Figure 3.5 illustrates, building age was classified into three rough categories: new (buildings 10 years or younger), mid-age (buildings between 10 and 50 years old), and historic (buildings older than 50 years). The average building age at time of incident was 50 years. Since a significant number of snow-related incidents were reported for structures built within the last ten years, it can be observed that snow-related failures and incidents are not confined to old or deteriorating structures and that even new buildings, designed according to modern code provisions, may be susceptible to extreme snow loads. Four incidents were reported as failing during construction, with little detail as to the specific cause. We hypothesize that age was more likely to be reported for both new and historic building failures since details about building age is more noteworthy in these cases.

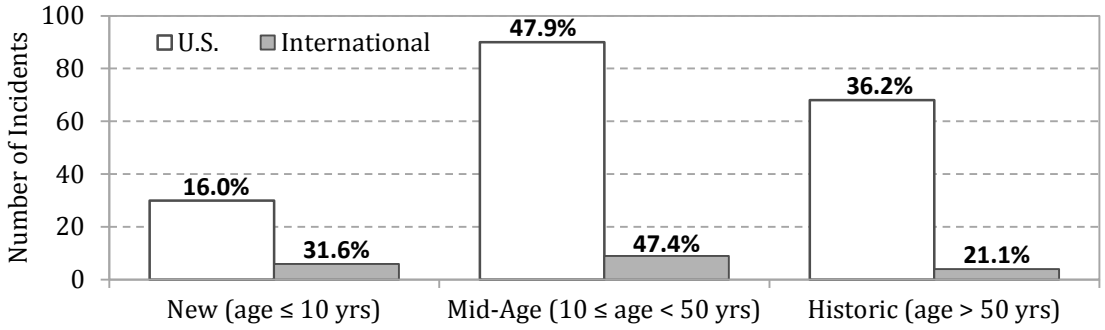

Figure 3.5 – Distribution of Database Incidents by Building Age. The percentages shown refer to the fraction of U.S. and international incidents that were new, mid-age, or historic buildings.

3.5.3 Principal Causes and Failure Modes

Each database incident was further characterized according to the cause(s) the newspaper article(s) attributed to the damage or failure. Table 3.8 shows the relationship between building age and attributed cause. For many incidents, news stories described more than one underlying cause. The most commonly reported causes of snow-related failures reported were excessive snow (89% of total incidents), rain-on-snow (13% of total incidents), and building problems

(9.0% of incidents). As buildings age, structural members experience deterioration and may become damaged. A higher percentage of incidents in older buildings were attributed to building problems, including 28% of historic building incidents and 26% of mid-age building incidents, compared to 5.4% of new building incidents in the U.S. dataset. Other incidents were attributed to melting snow (6.8%), drifting snow (3.2%), drainage issues (1.0%), and people on the roof (1.0%). For 32 incidents (3.1%), articles described no specific cause.

Table 3.8 – Classification of Incidents by Attributed Cause and Age.

CAUSE ATTRIBUTED	U.S.				International			
	Total Reported	New	Mid-Age	Historic	Total Reported	New	Mid-Age	Historic
Amount of Snow	919	26	76	48	73	4	5	3
Building Problems	93	5	24	26	13	2	4	2
Melting Snow	70	2	7	9	10	0	2	1
Rain-on-Snow Mixes	136	3	15	11	7	1	0	0
Drifting Snow	33	2	4	1	2	0	1	0
Person on Roof	10	0	1	0	2	0	0	0
Blocked Drains	10	0	1	1	0	0	0	0
TOTAL [a]	**1,261**	**38**	**128**	**96**	**107**	**7**	**12**	**6**

[a] Total double-counts 249 U.S. and 15 international incidents with more than one failure cause.

More detail about building problems, such as design and construction flaws, is indicated by articles reporting legal action for 23 (2.2%) incidents; most common were lawsuits against the general contractor or building designer for improper design or construction procedures leading to the collapse (9 incidents). Information about construction type was available for 52 of the 93 incidents related to building problems; timber, masonry, and metal/steel contributed to 27%, 11%, and 8.6% of these incidents, respectively, while 44% of the buildings had unknown construction type. Interestingly, 36% of the U.S. incidents reported as associated with building problems were government and public buildings. Since it seems unlikely that these structures have higher prevalence of design and construction flaws compared to other structures, the data appear to indicate a higher rate of reporting for these structures.

Other failures were attributed to specific snow and weather conditions. The high number of incidents attributed simply to a large amount of snow may represent, in part, the large number of incidents from northeastern states, which tend to see relatively heavy snowfall. Twenty-percent of incidents were reported to be caused by either melting snow or rain-on-snow, suggesting that the additional weight from high water content can be critical in causing snow loads to surpass building capacity. In many states, particularly those near the Great Lakes—Illinois, Missouri, Indiana, Ohio, and Pennsylvania—rain-on-snow may contribute significantly to building failures by increasing the weight on the roof. Of the 70 incidents of melting snow, 74% caused the building to collapse. The most commonly affected building types were retail and commercial (21%), followed by government and public buildings (16%). An additional 1% of incidents were attributed to blocked drains and were probably also associated with melting snow. The effects of ponding can be severe; 90% of incidents with drainage issues resulted in collapse. Of the 33 incidents (3.2%) reported due to drifting snow, 30 led to collapse, and 57% of these incidents were industrial, retail, or commercial buildings. Investigations of insurance data by O'Rourke et al. (1983) found that, of the 55% of all industrial roof failure insurance claims being attributed to snow, 75% of the failures were due to drifting on multilevel roofs, which is significantly larger than the 3.2% determined in this study. Differences in the importance of snowdrifts may be attributed to the generalizations made in reporting of failure causes.

In addition to information regarding the causes of collapse, the extent of building damage was also recorded in some cases. Reported details show that roof collapses ranged in severity from six to 160,000 square feet, comprising anywhere from one to 100% of building area. Based on the 139 incidents reporting collapse area, the average collapse area was 10,000 square feet (e.g. 100 ft. x 100 ft.). Although details were not always provided, a few selected collapse modes

are described to illustrate the relationship between snow loading, structural characteristics, and structural response. One example of progressive collapse is the March 7, 2001 failure of the 10,000 square-foot Westford Bible church (MA), built in 1973. Following the previous day's storm, the gable roof collapsed under approximately four feet of wet, drifted snow. One of the roof's timber scissor trusses, which supported the inclined cathedral ceiling over the main sanctuary, buckled due to a defect. The remaining trusses were unable to transfer the additional weight and failed, eliminating the lateral support to the concrete walls (Martinez 2001; Willhoit 2002; Burns 2002). In St. Paul, MN, the collapse of the steel roof of a distribution center warehouse in December 1991 illustrates a different failure mechanism. In this failure, four to five feet of compacted snow had drifted to one side of the flat roof against a taller adjacent structure. The steel beams were unable to hold the weight from this non-uniform load on the roof and a 50 ft. x 100 ft. section of the metal roof fell (deFiebre and Duchschere 1991). A third example is provided by a 40-year old structure housing Toys 'R' Us in Lanham, MD. On Feb 22, 2003, the lightweight metal joist roof structure of the 45,000 square-foot building caved in without warning. That day, over two inches of rain fell on the two feet of snow that had already accumulated that week. A combination of rain, snow, and ice clogged drains on the flat roof. At the location of ponding, the lightweight metal roof girders suddenly deformed and pulled away from the reinforced-masonry walls, beginning a progressive failure that propagated from the back of the store to the front. In less than eight seconds, 60-70% of the roof area had failed (Manning 2003; Tucker and Wiggins 2003; Cella and Prince 2003). These examples illustrate the progression of structural failure during snow-induced collapse incidents and the role of load transfer, redundancy, and connection adequacy in resisting failure.

3.5.4 Human and Socioeconomic Impacts

Casualties were reported for 71 (6.9%) incidents, and included a total of 19 fatalities and 145 injured persons; 26 of the injuries (18%) were serious enough to require hospitalization. These 19 fatalities occurred in 18 separate incidents and only one incident (the failure of the Lusk's Disposal recycling center in Princeton, WV in 1998) caused more than one fatality. The most commonly reported injuries were cuts, bruises, broken bones, and head injuries. Somewhat surprisingly, minor structures and garages had the largest percentage of incidents involving casualties (including 25% of minor structure incidents), indicating that these non-engineered buildings may be susceptible to failure and damage without sufficient warning. In addition, incidents involving minor structures and garages may only be reported by newspapers if casualties occur. In many other cases, warning noises or structural distress alerted occupants, providing time for them to vacate the building. In four incidents, lawsuits were brought against the building owner by victims or their families. In other cases, newspaper stories reported Occupational Safety and Health Administration investigations of workplace safety violations.

Newspaper accounts reported a variety of economic impacts from damage or collapse, including costs to repair, rebuild, or demolish; damage to building contents, such as vehicles, manufacturing equipment and warehouse goods; and death and injury to livestock. In all, 37% of incidents reported economic impacts related to property and building damage, with estimates ranging from $1,000 (for the repair of a shed roof and walls) to $30 million (for the replacement of antique trains at the B&O Rail Museum in Baltimore, MD); it is likely there were unreported economic impacts for many other incidents. Demolition may be expensive and several articles described legal action to determine who was financially responsible for this cost. Incomplete data exists about the fraction of overall costs covered by insurance and it likely differs according to

the type of construction. Of the 82 buildings for which insurance status was reported, only 8.5% were not covered by insurance. Despite the apparent prevalence of insurance, coverage was reported to be inadequate in many cases, including the B&O Rail Museum and the Plymouth Sports Dome (MA).

Reported indirect economic impacts included permanent or temporary layoffs of employees and profit loss due to business interruption. Of all U.S. database incidents, 587 (57%) buildings were temporarily closed. Closure times reported for 115 incidents varied from one day to three years with an average closure time of 122 days or just over four months. Long closure times may significantly impact business profits or viability, especially for small companies. An additional 150 buildings were evacuated before the incident took place and stayed closed while repairs, rebuilding, and inspections took place; the average evacuation length was 31 days (obtained from data for 56 incidents). All told, the data implies that 737 buildings (72% of all incidents) were either evacuated or closed, while 11 buildings were closed permanently. Although insufficient data exist to directly quantify their impacts, indirect costs of these business interruptions likely contribute significantly to total economic impact (Comerio 2006). It is also worth noting that newspaper articles often publish the day after an incident occurs, when closure and evacuation information is limited, and rarely publish follow-up articles, so actual closure times may vary from original estimates.

3.6 Results: International Snow-Related Building Failure Incidents

Additional data on international snow-induced building incidents is included to examine differences between U.S. and international building failures and reporting trends.

3.6.1 Regional and Seasonal Variation

The compiled international database consists of 91 incidents in 16 countries spanning four continents, as detailed in Table 3.9. The majority of reported incidents occurred in North America with 51 incidents (56%) from Canada, mostly from the provinces of Ontario, Quebec, and British Columbia. Europe reported the second highest continent total with 29 incidents (32% of total international incidents), while Asia and Australia reported 6 incidents (7%) and 5 incidents (6%), respectively. The large number of Canadian incidents relative to other countries may reflect the focus of the English-language international press, rather than a particularly high risk of failure in Canada. Russia had the second highest country total with eight incidents. Certainly, there are a large number of incidents in other countries not reported. For example, one article from the *South China Morning Post* reported that 1,200 houses had collapsed and 1,900 more had suffered damage in China after unusually large snow storms occurred in late 2009 causing damages of more than $497 million (Clem 2009). Without specific information about each building, however, these incidents were not included in this study.

Table 3.9 – Distribution of International Database Incidents by Continent and Country.

EUROPE		NORTH AMERICA*		ASIA	
Austria	3	Alberta, Can.	1	China	3
Belarus	1	British Columbia, Can.	8	Japan	2
Czech Republic	4	Manitoba, Can.	3	Lebanon	1
England	2	Newfoundland, Can.	1	**TOTAL**	**6**
France	2	Nova Scotia, Can.	3		
Germany	1	Ontario, Can.	17		
Italy	1	Prince Edward Isl., Can.	2		
Norway	3	Quebec, Can.	16	AUSTRALIA	
Poland	2			New South Wales, Aus.	3
Romania	2			South Australia, Aus.	1
Russia	8			Victoria, Aus.	1
TOTAL	**29**	**TOTAL**	**51**	**TOTAL**	**5**

*excluding U.S.A.

As with the U.S. database, most of the international incidents (86%) occurred in December, January, February, and March. On average, three incidents were reported each year over the 30-year database period, as shown by the solid line in Figure 3.6. The increasing number of incidents over time likely represents a larger number of references in search databases for later years, leading to more reported incidents. The greatest number of incidents in a given year was 10 incidents in 2009.

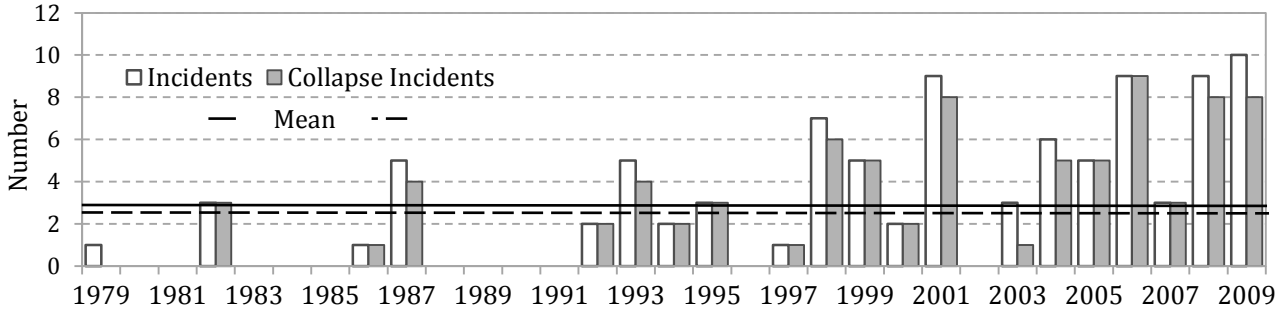

Figure 3.6 – Distribution of International Database Incidents by Year.

3.6.2 Characteristics of Impacted Buildings: Structure, Function, and Age

As with the U.S. database, international incidents were classified by construction type and building activity (Table 3.6 and Table 3.7). Of the 34 incidents (37%) whose building construction type was reported, metal/steel (53%) and concrete (17%) construction made up the majority of building incidents. Masonry, timber, and air-supported structures each accounted for approximately 8% of the building incidents. Metal/steel buildings were much more prominent in the international database (53% of incidents) compared to U.S. incidents (37%). The easy availability of timber in the U.S. may account for its relatively greater contribution to American incidents (37% in U.S. database vs. 8.3% in international database). A much larger percentage of incidents involved concrete buildings in the international database compared to the U.S. database (17% vs. 2.5% of U.S. incidents). Articles reported construction errors (e.g. insufficient reinforcement), design flaws (e.g. failing to account for temperature loads), and inadequate

maintenance (e.g. extensive rebar corrosion and concrete cracking) as the main causes of collapse in concrete buildings.

As shown in Table 3.7, the three most commonly reported building activities for international incidents were government and public buildings (23%), office buildings (20%), and industrial buildings (18%). No emergency or medical facility failure incidents were identified. While the U.S. incident database includes all types of building activities, the international database includes only large-scale buildings whose incidents were significant enough to be recorded in the international English-language press. Information on building age was available for 20 (22%) international incidents and ranged from new to 186 years old at the time of failure, as shown in Figure 3.5. The average building age at the time of reported incident was 44 years. However, the percentage of new buildings is double that of the U.S. database. In addition to demonstrating that even new buildings may be susceptible to snow-induced building incidents, the greater contribution of new building failures in the international database may indicate differences in building code provisions and compliance in other countries.

3.6.3 Principal Causes

As shown in Table 3.8, international incidents were most commonly attributed to the large amount of snow (80%), building problems (14%), melting snow (11%), or rain-on-snow (7.7%). The most likely cause in both databases was the amount of snow, while a larger percentage of U.S. building incidents were attributed to rain-on-snow mixes and a larger percentage of international incidents were attributed to building problems. Six (46%) of the 13 international incidents reported as having building problems were recreational facilities. The design of recreational facilities appears to be particularly susceptible to design and construction flaws that may increase risk of failure under large snow loads.

3.6.4 Human and Socioeconomic Impacts

Eight hundred seventy-nine casualties were reported in the international database, resulting from 27 incidents. These casualties included 293 fatalities and 586 injuries, a much larger number than in the U.S. database, demonstrating the severity of reported international incidents and the fact that major world publications tend to report international failures with human or economic significance. On average, 9.6 casualties occurred per incident internationally; no single U.S. incident was reported as causing more than nine casualties and the U.S. database failures led to a mean of 0.16 casualties per incident.

Approximately 35% of international incidents described the economic impact of building failure. The dollar value of these impacts was often significant, with total property and building damages ranging from a few thousand dollars (for repair of ceilings and structural members) to $200 million (for replacement of the BC Place Stadium retractable roof in Vancouver, British Columbia). Of all international database incidents, 35 buildings (38%) were unusable for some period of time, ranging from one day to two years. One building was closed permanently as a result of collapse. International and U.S. articles reported similar average closure lengths of 111 days (just over three and a half months) and 122 days, respectively.

3.7 Reporting of Snow-Related Building Failure Incidents

Article length and placement in the newspaper provides an indication of the prominence of snow-failure stories within a day's headlines. The first section in a newspaper generally includes major news stories, while the second section usually focuses on local and regional news. Generally, articles about U.S. roof collapses are in a position of regional prominence, with 14% of articles appearing on the front page, 60% reported in the first two sections, and 6.5% found in subsequent sections. (For 14% of articles, the position in the newspaper was unknown). In 68%

of articles only one incident was reported, demonstrating their significance to the news story. Most (40%) of the U.S. articles were from mid-size papers (with circulation between 100,000 and 750,000), while 33% were from small papers with circulation less than 100,000, 17% were from wire reports, 1.8% were from large papers with circulation over 750,000, and 8.2% were from unknown sources. According to the Annual Report on American Journalism (Project for Excellence 2004), small and mid-size papers have an average article length of less than 600 words and 800 words, respectively. The average length of articles was 558 words in the U.S. database, approximately consistent with the average article length.

Worldwide, 4% of articles appeared on the front page, 51% were in the first two sections, 5.6% were included in later sections, and 40% of articles had unknown placement. Most of the articles (66%) were from mid-size papers, 17% were from wire reports, 15% were from small papers, 2% were from other or unknown sources. The high number of mid-size international papers reporting snow-related incidents may be attributed to the fact that this type of publication is more likely to cover (and translate) notable snow-induced building failures. International articles about building failure incidents had an average length of 341 words.

Study findings are inherently constrained by the type of information about building failures that tends to be included in newspaper and wire reports. Many articles did not include all desired information or omitted engineering details on construction type, building age, and cause of failure pertinent to this study. The emphasis on drama related to casualties and victims in newspaper reporting, at the expense of discussion of factors related to risk, has been observed in reporting on other types of events, including vehicular crashes (Rosales and Stallones 2008). In the articles examined as part of this study, personal recounts of the collapse or plans to rebuild were frequently reported. In addition, different size news outlets tend to emphasize and report on

different characteristics and the impacts of these biases on the findings are difficult to quantify. Nevertheless, newspaper reports present the greatest number of sources for snow-related incidents presently available and significantly expand our knowledge about failures in common types of commercial, residential, and industrial facilities.

3.8 Conclusions

The findings of 1,029 U.S. and 91 international snow-related incidents reveal patterns of building failure, damage, and risk due to extreme snow loads. The comprehensive incident database, gathered from a study of newspaper reports, was coded to classify information about construction type, building activity, building age, type of incident (failure, evacuation, etc.), and physical and socioeconomic impacts. The U.S. data includes incidents from 1989—2009, while the international data spans the time frame 1979—2009.

On average, at least one out of 3.0 million buildings nationwide suffers a snow-failure collapse each year. The collapse rate of non-residential buildings is much higher than that of residential buildings in the U.S., with at least one out of 145,000 non-residential buildings suffering collapse each year. Although newspapers do not report all failures, especially for minor structures, the data indicates a number of snow-related building failures each year.

New York, New Hampshire, and Massachusetts have the highest number of U.S. snow-related building failure incidents; if the number of incidents in each state is normalized by population and building stock, New Hampshire, Maine, and North Dakota are identified as the most susceptible to building-related snow incidents. From both U.S. and international incidents, categories of industrial, government and public, retail and commercial, and minor structures such as garages, contribute most significantly towards incident classifications. In terms of construction type, metal/steel, timber, and masonry buildings are particularly susceptible in the

U.S., while metal/steel and concrete buildings show up most frequently in the international database. The impacts of these failures have included: casualties, especially in large structural failures occurring outside the U.S.; business interruptions due to closure and evacuation, lasting four months on average; and repair costs of up to $200 million. Approximately 72% of U.S. incidents and 38% of international incidents caused the disruption of building activities for some period of time due to evacuation or closure. The high number of incidents reported for new buildings (i.e. those constructed in the last ten years) in both the U.S. and international data sets indicates that a risk of snow-related failure can occur even in modern buildings designed according to current codes. The data also shows that snow-related building incidents increase with increased snowfall. Besides the amount of snow being reported as the main cause of incidents, rain-on-snow mixes and building problems were commonly attributed as causes in the U.S. and building problems and melting snow were commonly reported as causes internationally.

This study attempts to enhance our understanding of snow-related failure and damage trends, particularly structural design issues that may contribute to snow-induced building failures. The data gathered here indicates that buildings may be at risk of failure due to large or uneven snow loads, and that his susceptibility is particularly apparent in certain types of building construction, as well as those structures that are poorly maintained or designed. The susceptibility associated with different building systems disproportionately impacts economic and social activities that tend to concentrate in these buildings, for example retail and industrial activities in metal/steel buildings. These observations lead to a variety of possible risk mitigation strategies. Building owners, especially those with high-value structures, contents, or those sensitive to business closure, may be able to use data on the impacts of failures to value preventative maintenance. Quantitative differences in risk associated with different types of

building construction motivates further examination of the consistency of reliability provided by current building code snow load provisions. In addition, the large number of failures attributed to rain-on-snow may also indicate the need for more carefully considering this phenomenon in design procedures.

The observed relationship between snow failures and snowfall is of particular interest given changes in global climate occurring worldwide, leading to increases in average temperature. Although the overall frequency of snowstorms is expected to decrease on a global scale, snowstorms have become increasingly more severe since the 1950s (CCSP 2008). As a result, the occurrence of large, dense snowfalls is expected to increase in certain regions of the world. Ongoing work investigates the application of performance-based design and assessment methods to quantify risk of snow-related failures in buildings using nonlinear simulation and improved weather data.

Chapter 4

Lightweight Metal Roof Systems under Snow Loads

4.1 Overview

Current code provisions calculate roof snow loading conditions based on a variety of factors related to location, snowfall intensity, building type, roof geometry, and drifting effects. For many structures, these estimates are sufficient and further study is not warranted. However, recent studies like those described in Chapter 3 have revealed a significant number of snow-induced roof collapses of metal/steel buildings in the U.S. and abroad. Of all the buildings experiencing snow-induced failure incidents in the study, 37% in the U.S. were of metal/steel construction and 53% outside of the U.S. were of metal/steel construction (Geis et al. 2011). It is likely that many of these structures have steel joist roof systems or other cold-formed steel roof systems. Other types of buildings, such as those with wood construction and those with fabric construction also experienced snow-induced failure incidents in Chapter 3, which raise questions as to whether certain types of buildings are particularly at risk under snow loading compared to other types of buildings. Although there is no particular indication that lightweight metal buildings are the most vulnerable to snow loading compared to other types of buildings, they show up frequently in the database in Chapter 3 and provide the basis for the remaining chapters of our study. The following chapter discusses the types, history, production, development, and susceptibility of lightweight metal buildings, with specific emphasis on roof systems containing

open-web steel joists. Also included in this chapter is a discussion of the key differences between lightweight metal buildings and other types of buildings, identification of the specific design factors that may contribute to overall susceptibility of lightweight metal buildings to snow loads, and structural behavior of these types of buildings built according to modern code provisions.

4.1.1 Types of Lightweight Metal Roof Systems

Lightweight metal buildings most commonly include a combination of hot-rolled and cold-formed steel elements. Hot-rolled sections are manufactured through heating and casting processes (Marotta 1997), while cold-formed sections are manufactured from sheet steel through cold rolling, brake pressing, or folding (Macdonald 2008). Examples of hot-rolled elements include wide-flange beams, I-beams, and HSS sections, shown below in Figure 4.1a, Figure 4.1b, and Figure 4.1c, respectively, while cold-formed elements include metal roof decking, siding, channels (Figure 4.1d), and Z-shapes (Figure 4.1e). Channels and Z-shapes are most commonly referred to as purlins, where a purlin is defined by the Steel Joist Institute (SJI) as a "horizontal structural member that supports roof deck and is primarily subjected to bending under vertical loads such as dead, snow, or wind loads" (Canam 2010). Some structural members contain elements manufactured by hot-rolling and cold-forming processes. Open-web steel joists, for instance, are made of a variety of hot-rolled (i.e. angles and rods) and cold-formed elements (i.e. plates and bent angles). Hot-rolled sections are designed in accordance with the American Institute of Steel Construction's (AISC) *Specification for Structural Steel Buildings* and cold-formed sections are designed in accordance with the American Iron and Steel Institute's (AISI) *North American Specification for the Design of Cold-Formed Steel Structural Members* (SJI 2005).

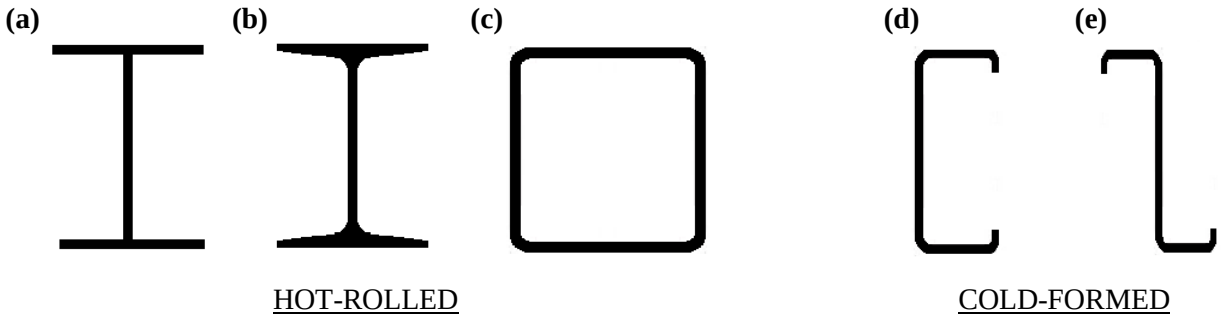

Figure 4.1 - Basic steel sections used in lightweight metal building construction, including hot-rolled steel (a) W-beams, (b) I-beams, and (c) HSS-beams, and cold-formed steel (d) C-shapes and (e) Z-shapes.

Much variation exists within roof systems of lightweight metal buildings, especially with regard to material selection and overall structural design. It is more common for the structural system of older buildings to include channels or Z-sections acting as joist-like members and wide-flange sections acting as girders, compared to the roof systems of newer buildings, which typically use wide flanges or joist girders to support open web steel joists.

Open web steel joist roof systems are popular in commercial and industrial applications and are typically used for strip malls, warehouses, and manufacturing facilities. SJI describes steel joists and joist girders as "open web, parallel chord, load-carrying members suitable for the direct support of floors and roof decks in buildings, utilizing hot-rolled or cold-formed steel, including cold-formed steel whose yield strength has been attained by cold working" (SJI 2005). The scope of this study is limited to lightweight metal buildings with roof systems consisting of open web steel joists, wide flange girders, and metal decking. Roof systems consisting of channels and Z-shaped primary members are excluded from this study. The overall layout of such buildings generally consists of open floor plans with moderate ceiling height and even column spacing along the lengths and widths of the building. Roof framing generally consists of open web steel joists, joist and/or wide-flange girders, metal decking, and diaphragm supports, while vertical support systems generally incorporate masonry, steel siding, and columns. Roof

construction is generally made up of metal decking, concrete, felt, tar, or gravel roofing. Floor systems are generally reinforced concrete slabs-on-grade. Typical design characteristics of these buildings are shown in Figure 4.2.

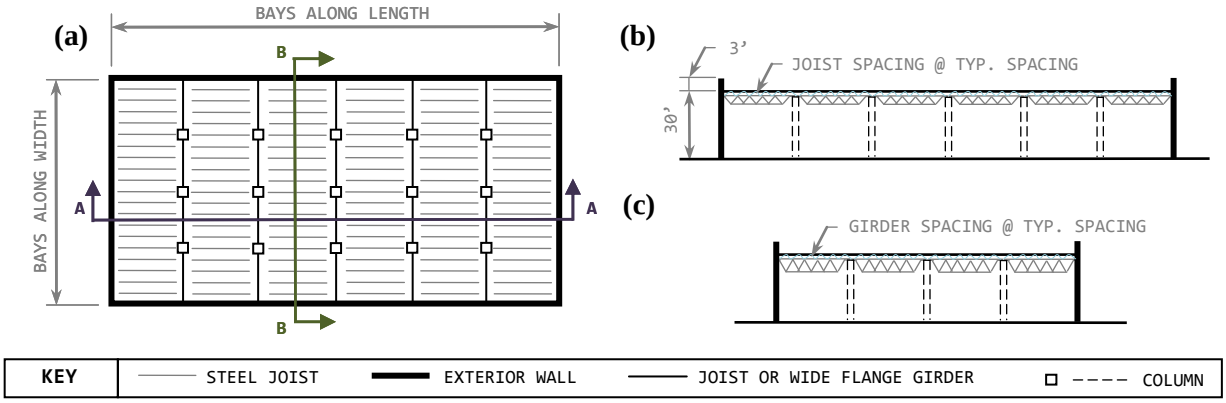

Figure 4.2 – (a) Plan view, (b) front elevation view (section A-A), and (c) side elevation view (section B-B) depicting typical lightweight metal building design characteristics.

4.1.2 History, Production, Development, and Specifications of Open Web Steel Joists and Joist Girders

The first open web steel joist was developed in 1923 and utilized the 1848 Warren Truss design shown in Figure 4.3a, which consists of a continuous bent web member connecting the top and bottom chord truss elements (SJI 2005). Other types of open web steel joists were developed soon after, such as the Neville (Figure 4.3b), Pratt (Figure 4.3c), and Howe trusses (Figure 4.3d) (Maple Valley Truss Company, Inc. 2011). The Warren Truss gains its strength from the use of equilateral triangles—in contrast to the Neville Truss which uses isosceles triangles—and limits its members to axial forces. The Howe and Pratt Trusses, developed in 1840 and 1844, respectively, are similar in design to each other (Boon 2011). The only difference is the alignment of the interior web members. In the Howe truss, the longer, angled members are in compression, while the shorter, vertical members are in compression in the Pratt

Truss. Because of the geometry, the Pratt Truss results in larger forces on the top and bottom chords than the Howe Truss. Therefore, the Howe Truss is more suitable for long-spanned structures (Boon 2011). Warren trusses are most commonly used for open web steel joists and joist girders (Vulcraft 2011, Canam 2010).

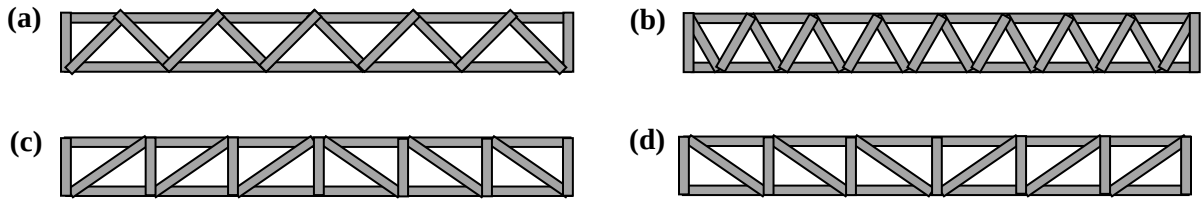

Figure 4.3 – Different types of trusses developed in the late 1800s and early 1900s, including (a) the Neville Truss, (b) the Warren Truss, (c) the Howe Truss, and (d) the Pratt Truss.

Due to varying designs and material properties among manufacturers during the early 1920s, it was difficult to compare individual manufacturers' capacities and strengths. In 1928, the SJI was formed to address these deficiencies and regulate the design and implementation of steel joist standards in industry (SJI 2005). SJI's first publication of standard specifications and load tables in 1928 and 1929, respectively, allowed building designers to select sections based on standardized capacities if loading conditions and clear spans were known. This publication was significant since it required no further analysis to reconfirm materials and sizes of steel joists after sections were selected to meet design capacities specified in the tables. Since the 1930s, SJI has adopted and adapted specifications and load tables for a variety of open web steel joists and joist girders, discussed in the following section. Today, SJI is a nonprofit organization of active joist manufacturers and other individuals whose purpose is to set standards and develop regulations for the steel joist industry (SJI 2005). Products promoted and developed by SJI are approved by the American National Standards Institute (ANSI) and meet all AISC standards (SJI 2005).

J-Series Joists: In 1928 and 1929, SJI published the first standard specifications and load tables, entitled the *Standard of Specification of Steel Joists, SJ-Series*. SJ-Series Joists were the first open web steel joists standardized in industry. The joists were designed with allowable strength design and had allowable tensile stresses of 18 ksi. Thirty years later, the *Introduction to the S-Series Joists* replaced SJ-Series Joists with higher allowable tensile stresses of 20 ksi, joist depths expanded to 24 inches, and spans increased to 48 feet. Two years later, allowable tensile stresses again increased to 22 ksi (steel had minimum yield strengths of 36 ksi) with the replacement of the S-Series with the J-Series. In 1965, SJI and AISC (American Institute of Steel Construction) developed a single specification for both the J- and H-Series Joists (SJI 2005).

LJ-Series Joists: SJI continued its advancement of load tables and specifications with the 1953 *Introduction to Longspan Steel Joists, L-Series* for spans up to 96 feet, depths through 48 inches, and allowable tensile stresses of 20 ksi. L-Series joists were jointly approved by AISC. Eight years later, the L-Series Joists were replaced with the LA-Series Joists so that maximum tensile stresses of 22 ksi could be achieved. As steel behavior became better understood through the development and advancement of different manufacturing techniques, higher strengths could be achieved through the use of low-alloy steels (McCormac 2008, Gustafson 2007). In 1966, SJI and AISC used 36 ksi minimum yield strength steel in the development of the LJ-Series Joists, which soon replaced the lower strength LA-Series. The LJ-Series Joists were eliminated with the J-Series Joists in 1978 (SJI 2005).

K- and KCS-Series Joists: The *Introduction of the H-Series Joists* was developed by SJI in 1961 so that allowable tensile stresses of 30 ksi could be achieved using steel with a minimum yield stress of 50 ksi. At the time, H-Series Joists could achieve the highest stresses than any

other steel joists on the market. It was not until 1986 that the H-Series Joists were replaced by K-Series Joists. Initially, K-Series joists were created to achieve greater economies by using lighter sections and to offer specific joists used for frequently used spans and loading conditions. Later, they were manufactured to meet demands for roofs with lighter loads at depths between 8 and 30 inches and to eliminate the use of heavy joists in medium depths for which there was little demand. In 1994, the specifications and load tables for K-Series Joists expanded with the addition of KCS-Series Joists, developed for cases with constant moment and shear. KCS-Series Joists were economical alternatives for special loading conditions, such as concentrated and non-uniform loads in addition to uniform loads (SJI 2005).

LH-Series Joists: With growing demand for longer spans and larger loads, SJI published the *Introduction of the LH-Series Joists* in 1962 to extend the use of joists beyond that of the K-Series. LH-Series Joists, otherwise known as longspan steel joists, have depths from 18 to 48 inches and can span distances up to 96 feet. They utilize steel whose minimum yield strength is between 36 and 50 ksi, resulting in allowable tensile stresses of 22 to 30 ksi (SJI 2005). LH-Series Joists are commonly used in engineering practice today.

DLJ- and DLH-Series Joists: The DLJ- and DLH- Series Joists, in contract to their LJ- and LH-Series counterparts, are deeper and can achieve longer spans. SJI and AISC introduced DLJ- and DLH-Series Joists (deep longspan steel joists) in 1970 to achieve greater depths and spans offered by the LJ- and LH-Series Joists. With deep longspan steel joists, it was possible to achieve depths up to 72 inches and spans through 144 feet. In 1978, the DLJ-Series Joists were eliminated due to large demand for higher strength steel joists. The DLH-Series Joists are commonly used today for roofs; they can achieve depths between 52 and 72 inches and spans

through 144 feet (SJI 2005). See Table 4.1for information about joist type by year initiated, year ceased, depth, maximum possible span, allowable tensile stresses, and minimum yield stresses.

Table 4.1 – Joist information by type.

JOIST TYPE	Year Initiated	Year Ceased	Depth (in)	Maximum Span (ft)	Allowable Tensile Stress (ksi)	Minimum Yield Stress (ksi)
SJ-Series	1929	1959	-	-	18	-
S-Series	1959	1961	24	48	20	-
J-Series	1961	1978	24	48	22	36
L-Series	1953	1961	48	96	20	-
LA-Series	1961	1966	-	-	22	-
LJ-Series	1966	1978	-	-	-	36
H-Series	1961	1986	-	-	30	50
K-Series	1986	Present	8-30	60	30	36-50
KCS-Series	1994	Present	8-30	-	30	36-50
LH-Series	1962	Present	18-48	96	22-30	36-50
DLJ-Series	1970	1978	52-72	144	-	-
DLH-Series	1970	Present	52-72	144	30	36-50

Joist Girders: SJI and AISC developed joist girders in 1978 for spans of up to 120 feet and depths between 20 to 120 inches. Joist girders serve as economical alternatives to traditional wide-flange primary framing members, and are used to support equally spaced concentrated loads along simple spans for floor and roof systems. In most cases, these concentrated loads are open web steel joists orientated perpendicular to the span of the joist girder.

In addition to K-, KCS-, LH-, DLH-Series, and Joist Girders, many other design alternatives exist, including short-span substitutes, extended span joists, extended depth joists, special profile joists, and custom joists designed to specific load profiles (Fisher 2002). Joist manufacturers have created more versatile design capacities with respect to custom-made products for cases involving non-uniform and concentrated loadings (Fisher 2002). Although type and design of specific steel joists varies per manufacturer, each product is expected to meet SJI certifications if the manufacturer is certified by the SJI. To become members of the SJI and receive certification for products, manufacturers of steel joists must submit design data for

compliance with the SJI, undergo physical design tests on K-Series Joists, undergo an initial plant inspection and subsequent biannual in-plant inspections for all products they wish to be certified, and if selected, must publish SJI specifications and load tables (SJI 2005). Six major manufacturers of steel joists across the U.S. are Canam Steel Corporation, New Millennium Building Systems, Nucor Vulcraft Group, Pacific Panel and Steel Truss, Inc., Quincy Joist Company, and Valley Joist, Inc. and steel joists are readily available around the U.S. and are easily transported. All manufacturers meet SJI design criteria for steel joists, joist girders, and other products. If joists are not certified by the SJI, they fall outside its jurisdiction.

4.1.3 Advantages of Open Web Steel Joist Roof Systems

Lightweight metal roof structures containing open web steel joists have advantages over conventional systems, including lighter members, lower construction costs, and relative ease and speed of erection. Open web steel joists are economical with high strength-to-weight ratios compared to other types of building materials because elements of steel joists are thin and require less steel. Lighter joists make the structural frame lighter overall, such that load demands on other building elements—such as foundations, columns, and walls—are reduced, along with reducing overall construction costs (Mehta 2008). An additional advantage of steel joists is their unitized construction – all elements of the joist are welded together to form a whole; they are already assembled and ready for installation upon arrival. Open web steel joists are also flexible in design with regard to depths, spans, weights, and load-carrying capacities, due to the convenience of load tables and standard specifications. For example, SJI (2010) estimates that the use of steel joists in a four-story apartment building in Buffalo, NY, led to savings of over $300,000 and provided more flexibility in the design as compared to concrete construction. They allow for the direct passageway of ventilation and mechanical systems through the web

members, which can reduce overall building heights of high rises and other tall structures. Steel joists can also span long distances, thereby reducing the use of support columns and increasing usable floor space.

4.2 Susceptibility and Failure Modes Exhibited through Literature Review and Case Studies

4.2.1 Susceptibility of Lightweight Metal Roof Systems under Snow Loads

Since the roof systems of lightweight metal buildings have small dead-to-live load ratios, unforeseen or unaccounted for loadings, such as point loads or extreme or uneven snow, may have a more dramatic effect on the structural response of the building as a whole as compared to other buildings types, which are heavier and therefore less susceptible to unanticipated roof loadings due to greater built-in reliability. Snow to dead load ratios are important in the consideration of excessive snow loads. According to Meløysund et al. (2006), lightweight structures are susceptible to snow loads due to their lesser built-in safety compared to heavier structures. This lesser factor of safety results from the fact that the percentage of snow load with respect to dead load is much greater than that of heavier buildings. For example, a lightweight metal building whose roof structure weighs 15 psf will have less overstrength to withstand a snow overload than a heavy steel building whose roof structure weighs 30 psf. As ASCE 7-05 states, "if the design snow load is exceeded, the percentage increase in total load would be greater for a lightweight structure (i.e., one with a high snow load/dead load ratio) than for a heavy structure (i.e., one with a low snow load/dead load ratio)" (2005). For example, "if a 40 psf roof snow load is exceeded by 20 psf for a roof having a 25 psf dead load, the total load increases by 31% from 65 to 85 psf. If the roof had a 60 psf dead load, the total load would increase only by 20% from 100 to 120 psf" (ASCE 2005).

A number of studies have evaluated the susceptibility of lightweight metal and steel buildings to large and nonuniform snow loads through numerical simulations. Structural reliability studies performed by Majowiecki (1998) show that 43% of all metal building failures are attributed to mistakes in design for long-span, lightweight structural systems, specifically with regard to snow drifting and wind loading. Takahashi and Ellingwood (2005) determined that simply supported structures having high snow to dead load ratios have lower reliability with respect to snow loads than heavier structures. Likewise, Holicky (2007) examined current European design procedures, concluding that lightweight roof systems fail to meet specified target reliability levels, after a number of roofs collapsed in the 2005—2006 winter, suggesting that snow loads be increased for the design of lightweight metal roofs in order to increase the reliability of such buildings. A follow-up study into the same building failures by Holicky and Sykora (2009) found that code provisions were insufficient in the sense that they underestimated actual roof snow loads, leading to the large number of lightweight metal building roof failures for the given winter. In addition to the low specific weight of lightweight buildings, the maximum span of the building can also contribute to its susceptibility to snow loading, especially in cases with large bay sizes. When buildings are loaded with nonuniform snow as opposed to uniform now, stresses will be greater. This phenomenon is especially evident in cases of snow drifting, where snow accumulates around roof obstructions (i.e. parapet walls, mechanical equipment, or multi-level roof steps as shown in Figure 2.2a, Figure 2.2b, or Figure 2.2c), or when snow is cleared from building roofs.

4.2.2 Case Studies and Failure Modes of Lightweight Metal Building Roof Systems

Past building failures help us understand collapse mechanisms and failure modes. Through building failures, patterns of design errors and failure modes are revealed, thereby allowing the continual updating and revision of building codes. The following case studies were provided by J.R. Harris & Company (2011). Although most of the buildings in these case studies do not have open-web steel joists, their failure mechanisms are significant in the general understanding of the behavior of lightweight metal buildings to snow loads. Building names and locations of these case studies have been redacted.

Case Study 1: At approximately 5:30 A.M. on January 19, 1993, the roof a building located on a college campus collapsed after four feet of snow accumulated on the roof (Associated Press 2008). Since the specific cause of failure was unknown, a forensic structural engineering firm was hired to investigate. A plan view and partial section view (section A-A) of the building are shown in Figure 4.4a and Figure 4.4b, respectively.

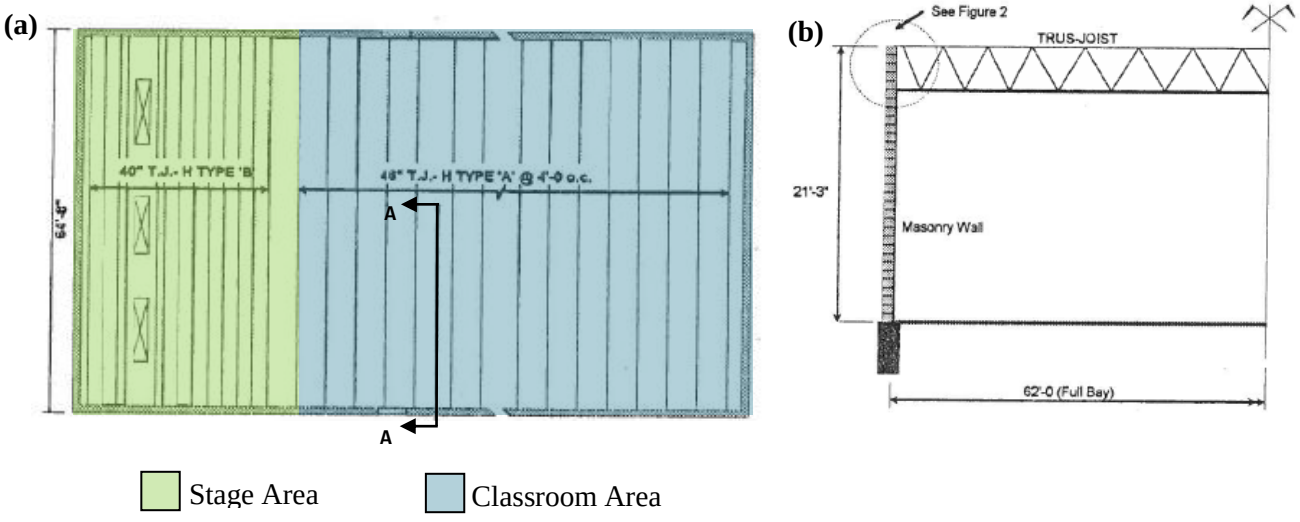

Figure 4.4 – (a) Plan view and (b) elevation view (section A-A) of the Fine Arts building. The elevation view shown in (b) continues along the entire width of the building and is mirrored on the other side (J.R. Harris & Co. 2011).

Joists used in the building were prefabricated truss joists with timber chords and tubular steel webs (see Figure 4.5a and Figure 4.6a). They spanned 62 feet between the unreinforced masonry walls, and had depths of 40 inches and 46 inches. The joists with 40-inch depths were spaced at various spacings over the stage area, while the joists with 46 inch-depths were spaced at 4'-0" on center over the classroom area, differentiated in Figure 4.4a. The top chords of the 46-inch deep joists were supported by three-inch thick timber plate as the roof structural system, and the plates were attached to a bond beam at the top of the wall. The bottom chords of the joists were attached to the inside face of the wall by nails which extended into the mortar joint. Figure 4.5a and Figure 4.5b illustrate the actual wall connection and the connection recommended by the Joist Design Manual. Note that the Design Manual shows a ½" gap between the wall and the bottom chord of the joist (Figure 4.5b), so as not to induce eccentric forces upon the wall. As built, the gap did not exist (Figure 4.6a).

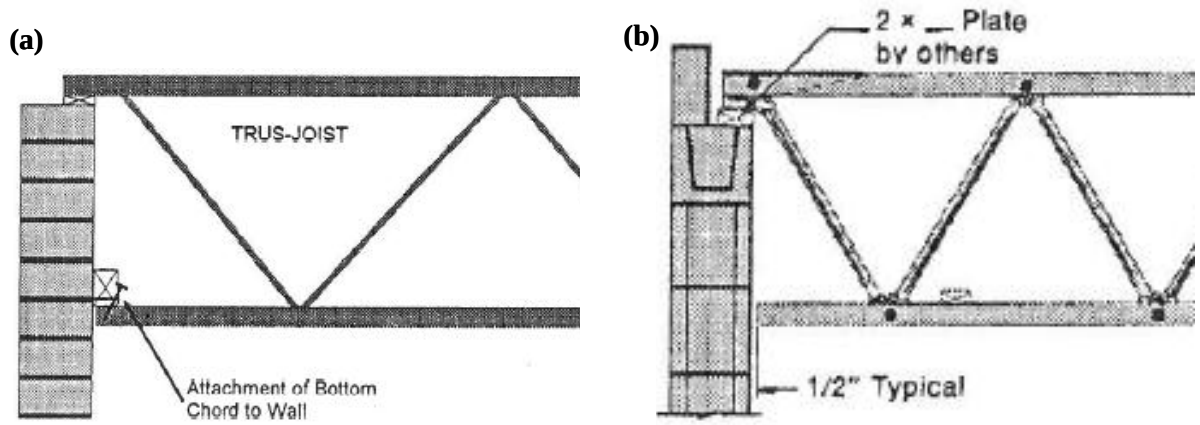

Figure 4.5 – (a) Wall-joist detail as constructed and (b) bearing detail from TRUS-JOIST Design Manual (J.R. Harris & Co. 2011).

Three possible failure scenarios of the building roof were identified: failure of the joists; failure of the masonry walls; or failure of a combination of these structural elements. In the first scenario, the failure of one or more joist could have initiated a propagation of failure along the entire length of the building, beginning with the failure of the joist(s) due to a loss of tensile

capacity in the bottom chord(s), causing the top chord(s) of the joist(s) to pull the masonry wall inward and resulting in failure of a part of the masonry wall and remaining joists. A second possible failure scenario could have been the masonry wall failing before the joists. In this scenario, snow loading on the roof could have caused the joists to deform, initiating high tension forces in the bottom chord of the joist and high compressive forces in the top chord. Forces induced by the snow action would have then been transferred to the masonry wall via the top and bottom chord at their attachment points, as shown in Figure 4.5a, resulting in moment on the wall. Rotation in the joist would increase to such an extent as to cause the mortar joints on the outside wall to lift. The ever-growing eccentric bearing force would create a moment on the wall, eventually resulting in its instability and leading to failure of the joists along the length of the classroom. A third failure scenario is the combined failure of the joist joists and masonry wall. Figure 4.6a and Figure 4.6b show the joists and unreinforced masonry wall after failure, respectively.

(a)  **(b)** 

Figure 4.6 – (a) Open-web joists and (b) masonry wall after failure (J.R. Harris & Co. 2011).

Considering the connection between the bottom chord of the truss and the masonry wall, the investigative firm found the second scenario the most likely cause of failure. Through finite element analysis, which simulated nonlinear material behavior, it was concluded that failure occurred as depicted by Figure 4.7a, Figure 4.7b, and Figure 4.7c. Snow loading built up on the

roof until a gap in the mortar occurred on the external wall face, causing a destabilizing force in the top chord and causing the mortar to crush on the internal face, resulting in ultimate collapse of the wall and joists (J.R. Harris & Co. 2011).

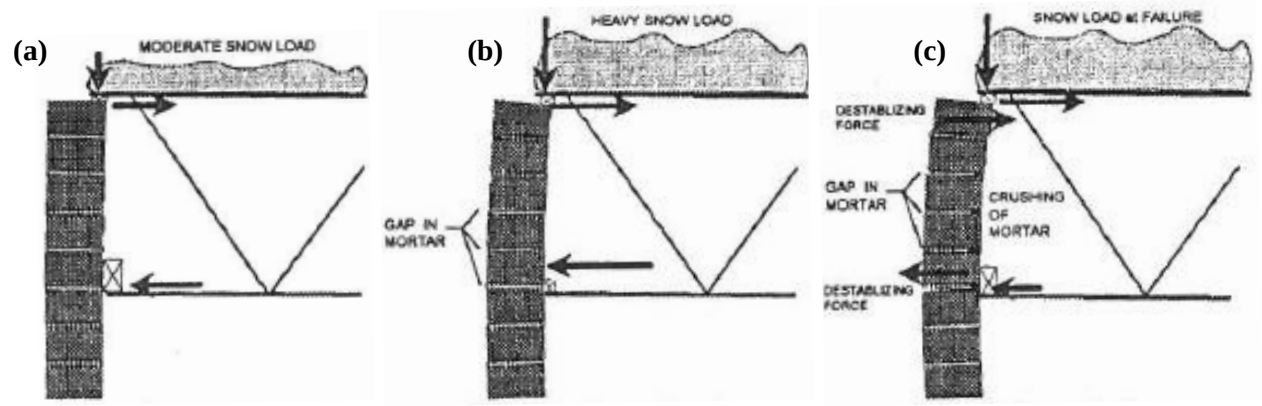

Figure 4.7 – Masonry wall behavior under (a) moderate snow load, (b) heavy snow load, and (c) just prior to failure (J.R. Harris & Co. 2011).

Case Study 2: On January 27, 2007, a portion of a metal roof of a large industrial facility collapsed under approximately 6.5 feet of dense, drifted snow. Snow density tests revealed the actual snow load on the roof to be 171 psf at the time of failure, which was about eight times higher than the uniform roof design snow load of 21 psf. Information about how and when the test was conducted was not included in engineering report. See Figure 4.8a and Figure 4.8b for the drifted snow profile and roof profile at the location of failure, respectively.

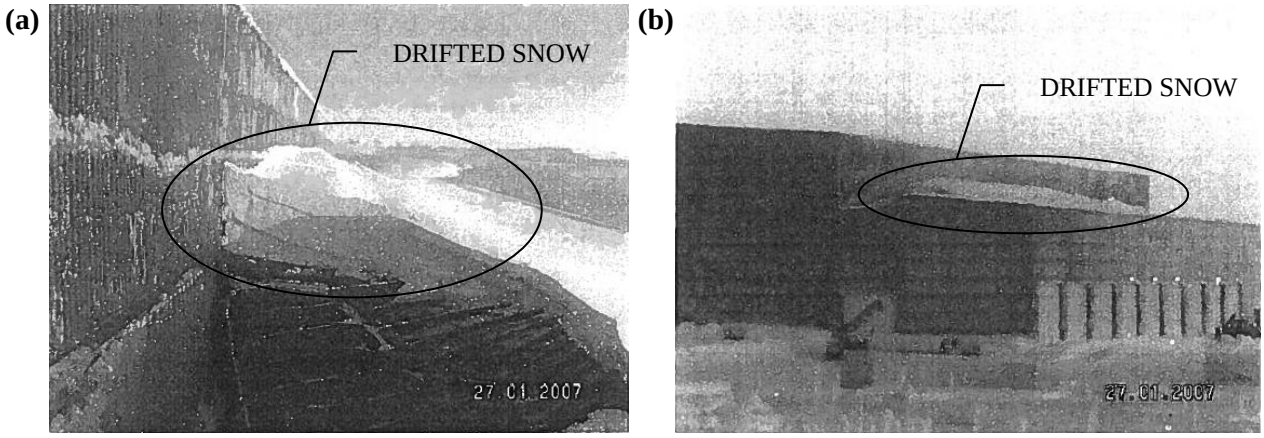

Figure 4.8 – (a) Drifted snow profile and (b) roof profile at location of failure (J.R. Harris & Co. 2011).

Investigation revealed that the failure of the roof purlins was due to improper design. The building was mistakenly designed without taking into account the effects of drifting snow on the roof, which caused the roof purlins and supporting wide-flange to buckle. See Figure 4.9 for a picture of the failure. More details about the failure and structural behavior at the element level were not included with the report.

Figure 4.9 – Roof failure (J.R. Harris & Co. 2011).

Case Study 3: On January 19, 2006, the roof of a manufactured metal building collapsed under a roof snow load (41 psf) that was 68% of the design roof snow load. After investigation of the site wreckage, review of building plans and calculations, and performance of the structural analysis, the most likely causes of collapse were found to be defects in the design and construction of the foundation and defects in the installation of the metal building.

The manufactured metal building was built in 2001 and was initially used as a horse riding arena. The superstructure was a single story, rigid steel framed structure, spanning 110 feet and spaced at 25 feet on center with overall building dimensions of 134 feet by 300 feet. The roof system consisted of 10 inch deep cold-formed steel Z-shaped purlins spanning 25 feet on center between the rigid frames, with 8 inch deep cold-formed Z-shaped sections spanning 25 feet on center at the two ends of the building. The lateral force resisting system included steel cable cross-bracing in both the roof and walls, and the foundation consisted of reinforced concrete spread footings with no slab-on-grade.

Investigations revealed that the roof failure began when incorrectly installed purlins on one side of the roof yielded at their supports, forming a catenary suspension system between the main frames. Once yielding occurred, the incomplete lateral force system failed to support the horizontal forces caused by the roof purlins. This failure caused the building to collapse from the exterior walls inward (J.R. Harris & Company 2011). See Figure 4.10a and Figure 4.10b for pictures of a deformed purlin and the displaced foundation, respectively.

(a)

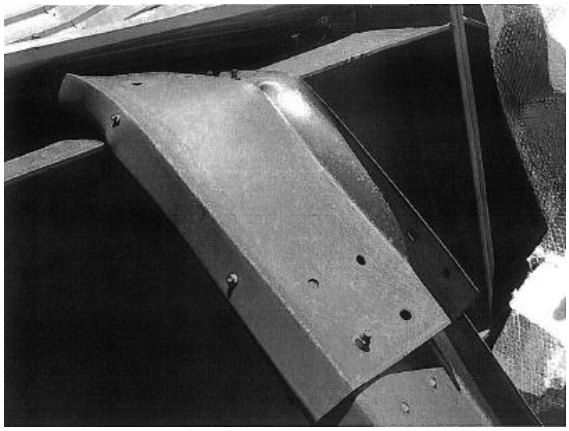

(b)

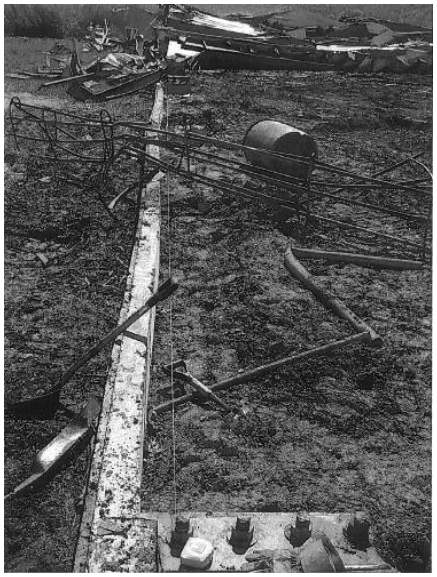

Figure 4.10 – (a) Rollover of purlin with missing splice bolt and (b) lateral displacement of foundation (J.R. Harris & Co. 2011).

Many design errors contributed to the total and catastrophic failure of the building roof. The roof Z purlins on one side of the roof were installed incorrectly oriented with respect to the roof slope and the concrete foundation was inadequately reinforced to resist lateral loads imposed by the system at the time of failure. The building was built without a building permit and the foundation was not designed by a structural engineer. Other design and construction errors included missing splice bolts, omitted cable braces, incorrectly installed anchor bolts, inadequate depth and reinforcement of foundation, and omitted eave struts. Although the

structure was mistakenly designed for 60 psf design snow load when it should have been designed for an 80 psf design load, the actual roof snow at the time of failure was substantially less than the design snow load. If the structure was designed to resist 60 psf design snow load and was properly constructed, the structure would have been expected to failure at snow loads between 30 and 60 psf. As built, the structure was expected to fail at 40 psf of roof snow load.

Case Study 4: On February 22, 1996, the roof of a horse barn collapsed due to insufficient strength of the central columns. The building was built in 1994 and was designed for a ground snow load of 70 psf, resulting in a design roof snow load of approximately 40 to 45 psf. Given the slope of the building and metal roof, the roof was found to be designed adequately to resist drifting snow.

The horse barn was attached to a much larger riding arena, and is approximately 25 feet by 150 feet in plan view, divided into a series of stalls about twelve feet square along the exterior face of the barn and a 15 foot wide walkway along the interior of the barn. See Figure 4.11a and Figure 4.11b for an elevation view of the barn and interior view of the stalls and walkway, respectively. The roof system consisted of cold-formed metal decking on C-shaped steel purlins, which spanned 12'-4" on center to the wide-flange rafters. The rafters were supported at three points, each spanning approximately 12 feet: the wall of the arena, the inside edge of the stalls, and the outside edge of the stalls. Given the 1:6 slope of the roof, the roof was about one foot higher than the stalls on the outside edge and about three feet higher than the stalls on the inside edge. The roof of the arena was approximately seven feet higher than the barn roof at the intersection, shown in Figure 4.11a.

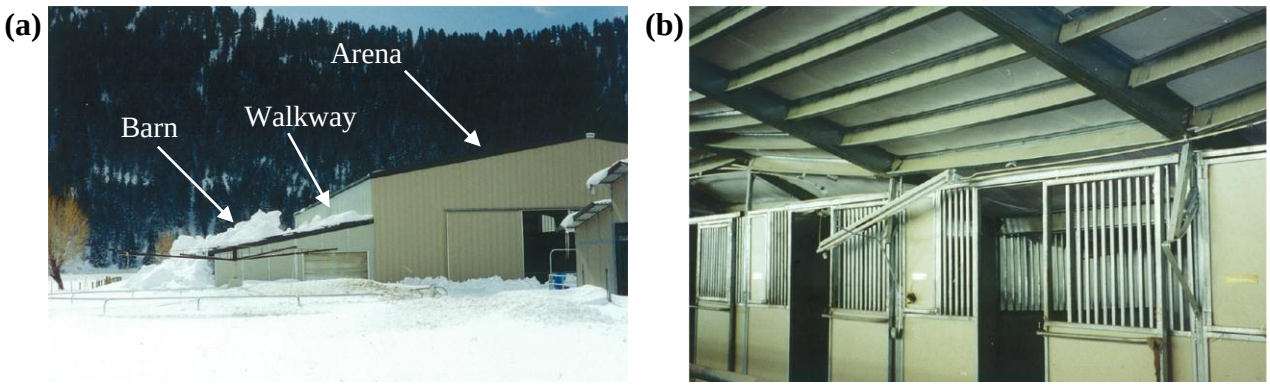

Figure 4.11 – (a) Roof and snow drifting profile and (b) roof after failure (J.R. Harris & Co. 2011).

'Connector columns' were used at the inside and outside edges of the stalls; they served to connect the wall panels of the horse stalls together while supporting the roof. The columns were made up of two sections, a C-shape formed from sheet steel with a depth of 2 inches and flange widths of 1 ½ inches and a 2 inch square tube nested inside the C-shape and welded together (see Figure 4.12 and Figure 4.13).

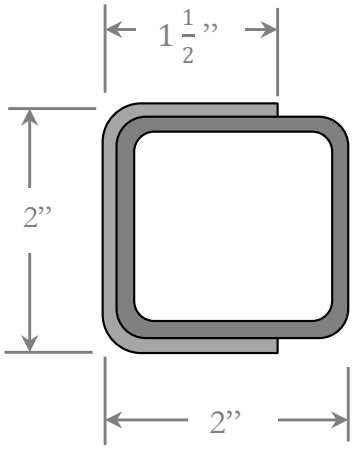

Figure 4.12 – Connector column.

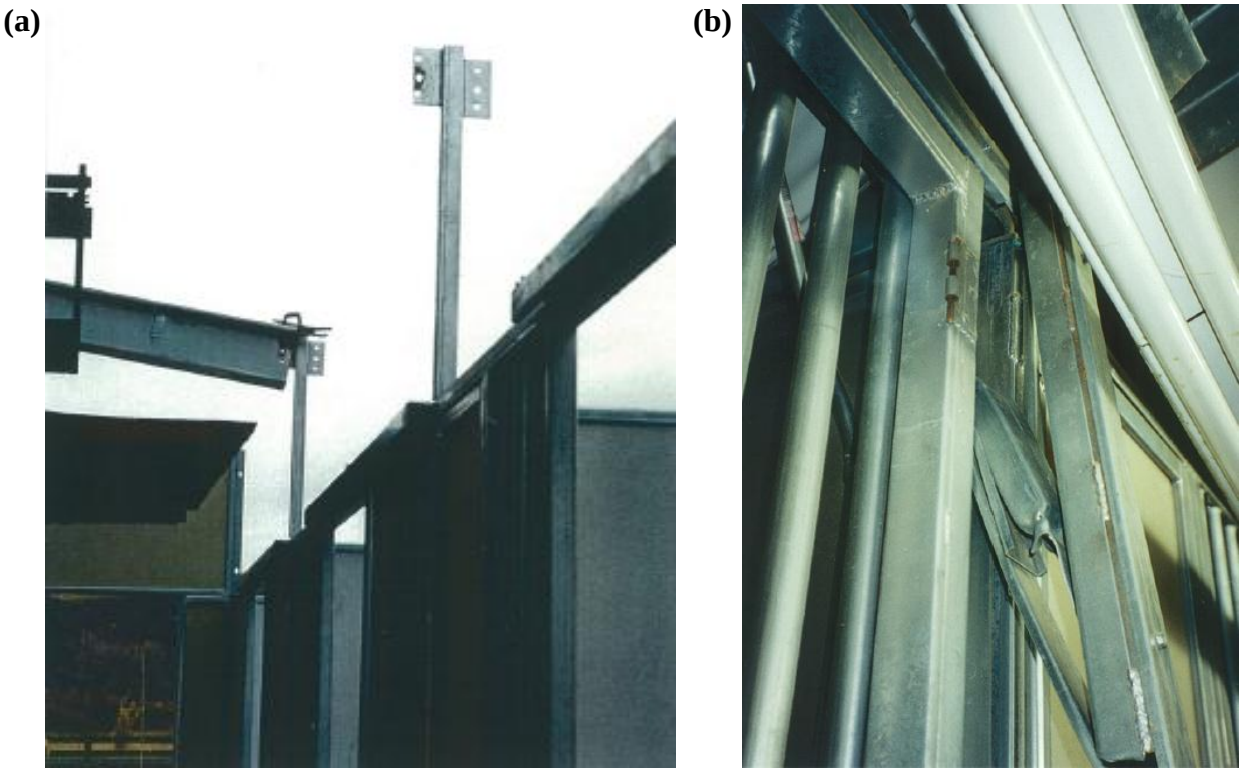

Figure 4.13 – Connector column (a) during erection and (b) after failure (J.R. Harris & Co. 2011).

The failure of this structure did not occur due to the roof elements, but rather due to the columns. As snow slid from the upper arena roof onto the lower barn roof, seven of the thirteen interior columns buckled, causing the roof to collapse in on itself. During the incident, four outer columns and one pair of inner columns remained intact. It is likely that the buckling of the columns caused a sudden drop of the beams, which impacted the stall walls, and caused the purlins to fracture. Since a beam failure would result in a slower yielding-type failure, the purlins would most likely not have broken. Therefore, evidence of the specific failure modes of the beams and purlins revealed that the column failures preempted the beam failures.

The roof failure was caused by the buckling of the central columns; evidence shows that these columns were not properly designed for demand loads. Drawings by the fabricator were incomplete and contained several internal contradictions, making construction extremely difficult if the contractor was not familiar with this style of column construction. Miscalculations in the

design of the columns resulted in an overestimation of the slenderness ratio and column strength. The calculated demand of the column load was over 13 kips, while the allowable column load was only 5.2 kips.

Case Study 5: On December 9, 1978, a portion of the auditorium roof (Figure 4.14) of a high school collapsed under drifted snow. Design deficiencies and unanticipated additional loads from leaks in the roof resulted in the failure of this roof.

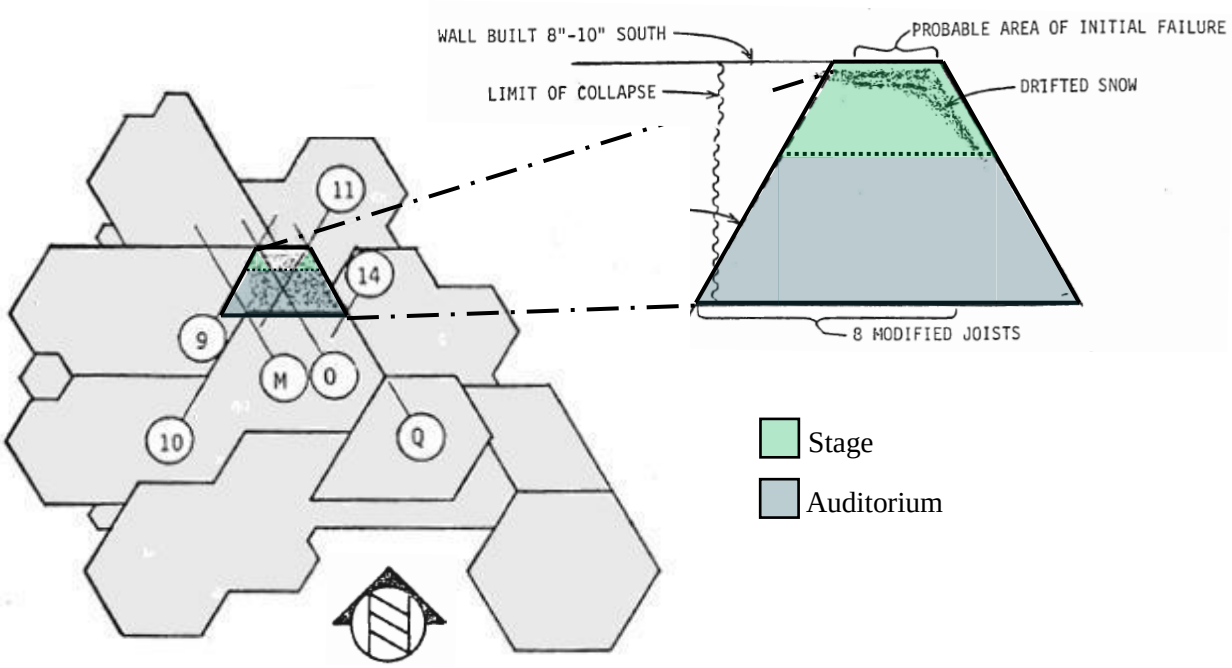

Figure 4.14 – Plan view of building with enlarged view of collapsed area (J.R. Harris & Co. 2011).

The roof system failed after one joist, located over the auditorium (see Figure 4.14), severely deformed under drifted snow and ponded water. The deformation of the joist caused the roof to leak, as nonstructural elements, including roofing materials and insulation, failed and released water into the structure. The water and melted snow caused the joist to deflect even more, which transferred additional load to adjacent joists. This action caused the joists to deform in a similar manner, until progressive failure of the entire roof system took place. The north end of the roof fell first, ultimately pulling the south end from its bearing or tearing it away from the

supporting wall. After investigation, it was found that one significant construction flaw contributed to the ultimate collapse of this roof system. The bar joists intended for the stage area were installed over the auditorium (see Figure 4.14), and the auditorium joists were installed over the stage area, which resulted in understrength of the joists over the stage and overstrength of the joists over the auditorium. The joists over the stage were designed to handle additional loads from equipment and scenery, while the auditorium joists were not. After installation, the incorrectly installed joists over the stage were deficient with respect to snow and dead loads since they could not carry the weight of the stage equipment and scenery. Of the 527 bar joists located in the auditorium roof, 370 were found to be incapable of supporting the required roof snow load of 30 psf. The 11 beams and 30 columns supporting these joists were also found to be incapable of carrying the 30 psf snow load. Due to a leak in the roof, an additional 4 to 5 psf of ponding water was present in the roof at the time of failure. Considering that the structural roof system was insufficiently designed for ponding requirements altogether, this additional load only contributed the roof's failure. Specific details about the structural behavior at the element level were not included with the report.

Table 4.2 compares actual loads experienced by various auditorium and stage structural components at the time of failure to their ultimate respective design load capacities. Overloaded by 25 to 35 psf, the weakest link was the stage joists when carrying equipment and scenery. Without equipment or scenery, the maximum snow load the roof was able to support as built was about 10 psf, which was only a third required by the building codes.

Table 4.2 – Actual and theoretical load capacities for various auditorium and stage structural components (J.R. Harris & Co. 2011).

STRUCTURAL COMPONENTS	Design Load (psf)		Actual Load (psf)		Capacity Load (psf)		Snow Load (psf)
	Min	Max	Min	Max	Min	Max	Max
Auditorium Joists	20	50	40	75	50	50	10
Stage Joists w/out Equip.	20	50	40	75	45	54	14
Stage Joists w/ Equip.	20	50	80	115	45	54	-26
Trusses	20	50	40	95	50	50	10
Columns	20	50	45	75	50	55	10

Design and construction errors were the main causes of roof failure for the buildings described above. In one case, the connection of the bottom chord of the steel joists to the outer unreinforced masonry wall caused a significant overturning moment, leading to instability and ultimate collapse of the masonry wall and dependent joists. In the other case, joists with lower design capacities were mistakenly installed in place of ones with higher design capacities, leading to severe overloading and ultimate failure of these joists after drifted snow accumulated on the roof. Although these case studies have revealed patterns of design and construction errors, the following studies will focus on buildings designed according to modern code provisions and without design and construction errors.

Studies into building failures can reveal patterns of collapse mechanisms and failure modes, which are important factors in determining what makes certain types of buildings more susceptible to snow overloading than other types of buildings. The case studies in this chapter revealed patterns of design and construction errors as the main cause of failure under drifted snow loads for many different types of building constructions. Although we cannot state directly that design errors and construction errors also contribute to the susceptibility of open-web steel joist roof systems to snow-induced failure based on these case studies, we can theorize that these errors would have the same effect on buildings with open-web steel joists, ultimately contributing to their failure. It is unclear from the case studies what the typical failure

mechanisms are for buildings with open-web steel joist roof systems. The purpose of the next chapters is to shed more light on this subject by studying how specific design elements, building characteristics, and loading conditions contribute to the susceptibility of lightweight metal buildings when loaded with snow. Buildings included in the study will be designed according to modern code provisions and will be considered free of design and construction errors.

4.3 Archetypical Buildings

4.3.1 Typical Building Characteristics for Roof Systems with Open-Web Steel Joists

In order to obtain a representative set of design characteristics for roof systems of lightweight metal buildings, several local buildings containing lightweight metal roof systems were examined. The building set was selected from various local retailers whose buildings have roof systems containing open-web steel joists, metal decking, and wide-flange beams. Although building geometries and design characteristics were estimated through visual inspection rather than exact measurements, these estimates give a good sense of typical overall building design characteristics.

Typical roof, wall, joist, girder, and column characteristics are tabulated in Table 4.3. Nearly all structural systems have wide-flange girder roof supports and masonry or concrete block walls along the perimeter. Typical interior columns consist of 6- or 8-inch round or square HSS sections and roof height varies from 25 to 35 feet. When spaced at 3-foot intervals, open-web steel joists are typically 12 inches deep. However, when spacing increases to 6-foot intervals, joist depth varies from 14 and 20 inches. From the design set, it seems that wide-flange girders are used when shorter spans are required, while joist girders are used for longer spans.

Table 4.3 – Building characteristics of seven buildings in Boulder, CO having lightweight roof systems.

Building No.	Roof Height	Ext. Walls	K-Series Joists		Girders			Columns
		Type	Depth	Spacing	Depth	Type	Spacing	Size and Type
1	30'	Masonry	20"	6’ o.c.	12”	I-beam	15’ o.c.	6x6 square HSS & 6" round HSS
2	25'	Masonry?	14-16"	6’ o.c.	14-16"	I-beam	30’ o.c.	?
3	30-35'	Concrete Block	16-20"	6’ o.c.	24-26"	Joist Girder	45’ o.c.	8x8 HSS
4	35'	Masonry	12"	3’ o.c.	20-24"	I-beam	40’ o.c.	8" round HSS
5	20'	Masonry	12"	3’ o.c.	24"	I-beam	40’ o.c.	6" round HSS
6	30'	Masonry	20"	6’ o.c.	12"	I-beam	15’ o.c.	6x6 square HSS & 6" round HSS
7	25'	Masonry	14"	5’ o.c.	16"	I-beam	30’ o.c.	6x6 HSS

The building set contained many different types and styles of open-web steel joists, as shown in Figure 4.15 through Figure 4.19. Joists were made up of rods, angles, double angles, and combinations of these elements. Double angles were commonly used for upper and lower chords, while rods were commonly used for interior web members. There seemed to be some correlation between building age and the type of joists used in the roof system. Older buildings more commonly used joists with rods and single angle members (Figure 4.15 and Figure 4.16), while newer buildings more commonly involved joists with double angle and single angle elements (Figure 4.17 through Figure 4.20).

Figure 4.15 – Open web steel joist consisting of rods for web and chord members (Building 4).

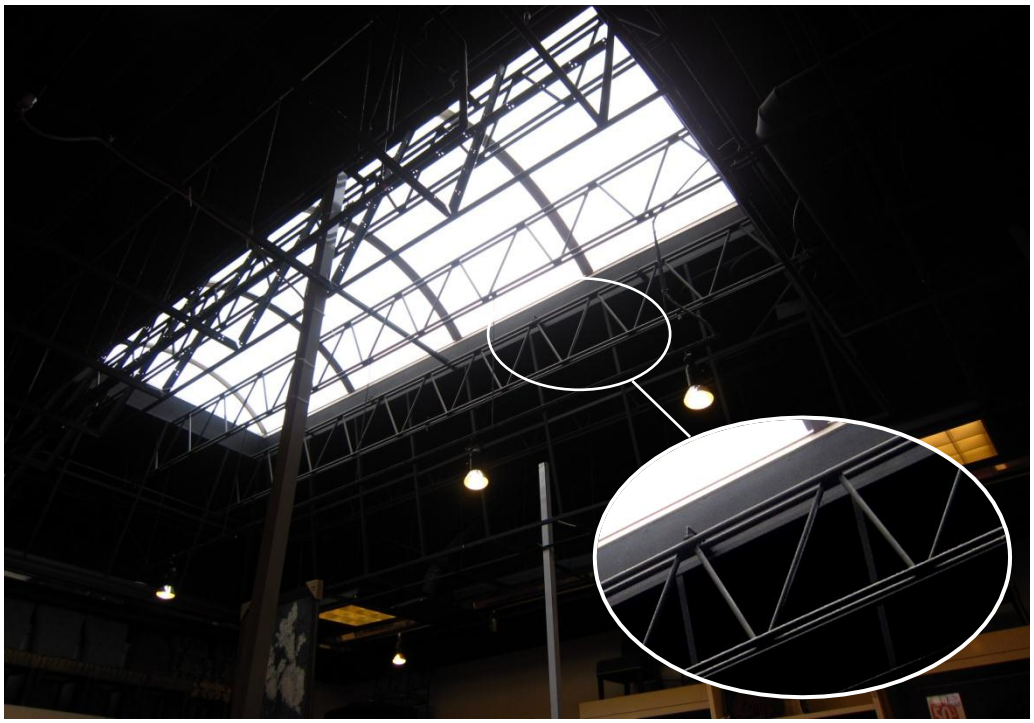

Figure 4.16 – Open web steel joist consisting of rods for web and chord members (Building 5).

Figure 4.17 – Open web steel joist consisting of double angled chord members with rod web members (Building 1).

Figure 4.18 – Open web steel joist consisting of double angled chord members with alternating rod and double angled web members (Building 2).

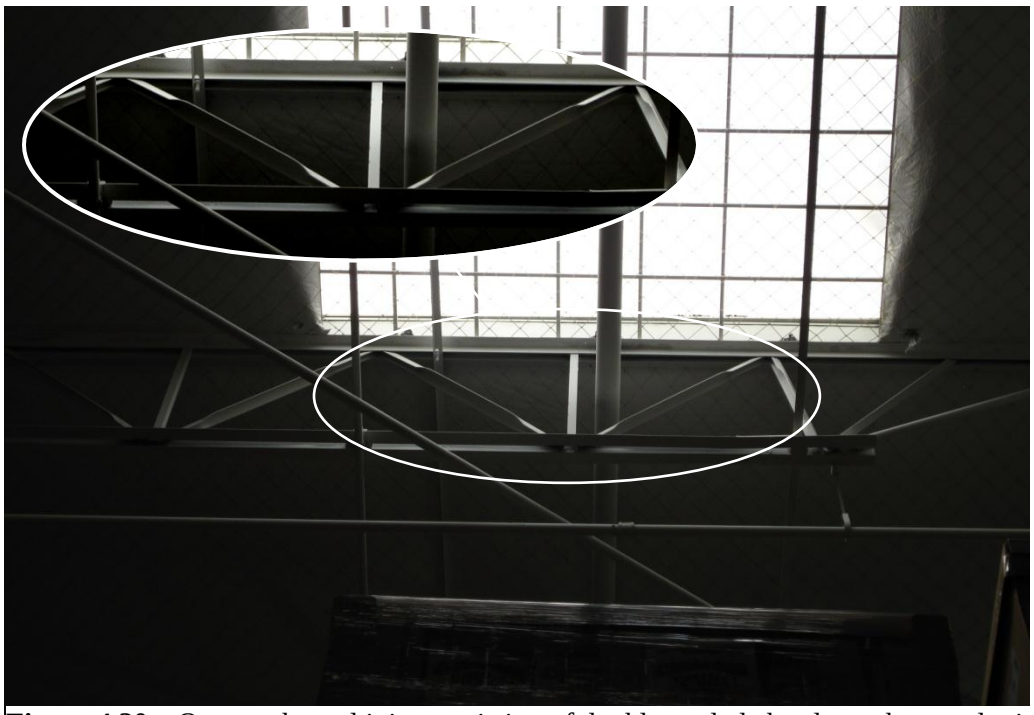

Figure 4.20 – Open web steel joist consisting of double angled chord members and crimped single angled web members with vertical elements (Building 6).

Figure 4.19 – Open web steel joist consisting of double angled chord members and crimped single angled web members with vertical elements (Building 3).

4.3.2 Archetypical Lightweight Metal Building Matrix

Based on typical design characteristics of representative buildings and failure modes exhibited through case studies, a set of archetypical lightweight metal buildings was created in order to determine which properties effect structural response to snow loads. Factors influencing building response are separated into four main categories: building geometry, building elements, nonuniform snow loading, and extreme snow loading. Building geometry factors include specific roof weight, joist span, girder span, length-to-width ratio, column height, joist spacing, connection type, diaphragm type, joist depth, and girder depth. Building elements include inner column type, outer wall and/or column type, joist type, and roof material type. Nonuniform snow loading factors include wind, exposure, parapet height, and roof slope. Extreme snow loading factors include geographical location, concentrated loadings, rain-on-snow effects, melting snow effects, drainage considerations, and structure thermal conditions. Design and construction effects (errors) were not considered for our archetypical building set.

The archetypical lightweight metal building set selected for this study consists of 71 unique buildings—each with unique design characteristics, shown in Table 4.4. Depending on the type of factor, each category is varied incrementally or by type. Joist span, for example, varies in increments of five feet from 20 to 40 feet, while outer wall type varies from HSS sections to masonry. This archetypical building matrix is the first step in allowing us to model each building independently and compare building responses (such as forces and deflections) in order to determine the factors that contribute to the susceptibility of lightweight metal buildings with open-web steel joist roof systems. This matrix provides the basis for the analysis in the subsequent chapters.

Table 4.4 –Archetypical Lightweight Metal Building Matrix.

ARCHETYPICAL BUILDING MATRIX																			
Bldg No.	D/S Load Ratio	GSL (psf)	RSL (psf)	Joist Span (ft)	Gird. Span (ft)	L (ft)	W (ft)	W/L Ratio	Joist Spacing (ft)	Joist Type	Joist Depth (in)	Girder Depth (in)	Column Height (ft)	Inner Column Type	Outer Wall Type	Conn-ections	Dia-phragm	Roof Type	Parapet Height (ft)
FIND MOST SUSCEPTIBLE DEAD/SNOW LOAD RATIO																			
1	0.80	31.7	20.0	30	40	240	120	2.0	5	D18-1	18	8	30	HSS6 R	HSS6 R	Simple	-	Gravel	-
2	0.57	45	28.4	30	40	240	120	2.0	5	D18-2	18	8	30	HSS6 R	HSS6 R	Simple	-	Gravel	-
3	0.43	60	37.8	30	40	240	120	2.0	5	D22-2	22	8	30	HSS6 R	HSS6 R	Simple	-	Gravel	-
4	0.34	75	47.3	30	40	240	120	2.0	5	D24-2	24	8	30	HSS6 R	HSS6 R	Simple	-	Gravel	-
5	0.29	90	56.7	30	40	240	120	2.0	5	D24-4	24	8	30	HSS6 R	HSS6 R	Simple	-	Gravel	-
6	0.22	120	75.6	30	40	240	120	2.0	5	D26-5	26	8	30	HSS6 R	HSS6 R	Simple	-	Gravel	-
FIND MOST SUSCEPTIBLE JOIST SPAN																			
7	0.5	45	28.4	20	40	360	120	3.0	5	D18-2	18	22	30	HSS6 R	8" R.M.	Simple	Rigid	Gravel	1.5
8	0.5	45	28.4	25	40	360	120	3.0	5	D18-2	18	22	30	HSS6 R	8" R.M.	Simple	Rigid	Gravel	1.5
9	0.5	45	28.4	30	40	360	120	3.0	5	D18-2	18	22	30	HSS6 R	8" R.M.	Simple	Rigid	Gravel	1.5
10	0.5	45	28.4	35	40	360	120	3.0	5	D18-2	18	22	30	HSS6 R	8" R.M.	Simple	Rigid	Gravel	1.5
11	0.5	45	28.4	40	40	360	120	3.0	5	D18-2	18	22	30	HSS6 R	8" R.M.	Simple	Rigid	Gravel	1.5
FIND MOST SUSCEPTIBLE GIRDER SPAN																			
12	0.5	45	28.4	30	30	360	120	3.0	5	D18-2	18	22	30	HSS6 R	8" R.M.	Simple	Rigid	Gravel	1.5
13	0.5	45	28.4	30	35	360	120	3.0	5	D18-2	18	22	30	HSS6 R	8" R.M.	Simple	Rigid	Gravel	1.5
14	0.5	45	28.4	30	40	360	120	3.0	5	D18-2	18	22	30	HSS6 R	8" R.M.	Simple	Rigid	Gravel	1.5
15	0.5	45	28.4	30	45	360	120	3.0	5	D18-2	18	22	30	HSS6 R	8" R.M.	Simple	Rigid	Gravel	1.5
16	0.5	45	28.4	30	50	360	120	3.0	5	D18-2	18	22	30	HSS6 R	8" R.M.	Simple	Rigid	Gravel	1.5
FIND MOST SUSCEPTIBLE LENGTH/WIDTH RATIO																			
17	0.5	45	28.4	30	40	120	120	1.0	5	D18-2	18	22	30	HSS6 R	8" R.M.	Simple	Rigid	Gravel	1.5
18	0.5	45	28.4	30	40	240	120	2.0	5	D18-2	18	22	30	HSS6 R	8" R.M.	Simple	Rigid	Gravel	1.5
19	0.5	45	28.4	30	40	360	120	3.0	5	D18-2	18	22	30	HSS6 R	8" R.M.	Simple	Rigid	Gravel	1.5
20	0.5	45	28.4	30	40	480	120	4.0	5	D18-2	18	22	30	HSS6 R	8" R.M.	Simple	Rigid	Gravel	1.5
21	0.5	45	28.4	30	40	600	120	5.0	5	D18-2	18	22	30	HSS6 R	8" R.M.	Simple	Rigid	Gravel	1.5
FIND MOST SUSCEPTIBLE JOIST SPACING																			
22	0.5	45	28.4	30	40	360	120	3	3	D18-2	18	22	30	HSS6 R	8" R.M.	Simple	Rigid	Gravel	1.5
23	0.5	45	28.4	30	40	360	120	3	5	D18-2	18	22	30	HSS6 R	8" R.M.	Simple	Rigid	Gravel	1.5
24	0.5	45	28.4	30	40	360	120	3	7	D18-2	18	22	30	HSS6 R	8" R.M.	Simple	Rigid	Gravel	1.5
FIND MOST SUSCEPTIBLE JOIST DEPTH																			
25	0.5	45	28.4	30	40	360	120	3.0	3	D18-2	14	22	30	HSS6 R	8" R.M.	Simple	Rigid	Gravel	1.5
26	0.5	45	28.4	30	40	360	120	3.0	3.5	D18-2	16	22	30	HSS6 R	8" R.M.	Simple	Rigid	Gravel	1.5
27	0.5	45	28.4	30	40	360	120	3.0	4	D18-2	18	22	30	HSS6 R	8" R.M.	Simple	Rigid	Gravel	1.5
28	0.5	45	28.4	30	40	360	120	3.0	4.5	D18-2	20	22	30	HSS6 R	8" R.M.	Simple	Rigid	Gravel	1.5
29	0.5	45	28.4	30	40	360	120	3.0	5	D18-2	22	22	30	HSS6 R	8" R.M.	Simple	Rigid	Gravel	1.5

ARCHETYPICAL BUILDING MATRIX																			
Bldg No.	D/S Load Ratio	GSL (psf)	RSL (psf)	Joist Span (ft)	Gird. Span (ft)	L (ft)	W (ft)	W/L Ratio	Joist Spacing (ft)	Joist Type	Joist Depth (in)	Girder Depth (in)	Column Height (ft)	Inner Column Type	Outer Wall Type	Conn-ections	Dia-phragm	Roof Type	Parapet Height (ft)
FIND MOST SUSCEPTIBLE GIRDER DEPTH																			
30	0.5	45	28.4	30	40	360	120	3.0	3	D18-2	14	18	30	HSS6 R	8" R.M.	Simple	Rigid	Gravel	1.5
31	0.5	45	28.4	30	40	360	120	3.0	3.5	D18-2	16	20	30	HSS6 R	8" R.M.	Simple	Rigid	Gravel	1.5
32	0.5	45	28.4	30	40	360	120	3.0	4	D18-2	18	22	30	HSS6 R	8" R.M.	Simple	Rigid	Gravel	1.5
33	0.5	45	28.4	30	40	360	120	3.0	4.5	D18-2	20	24	30	HSS6 R	8" R.M.	Simple	Rigid	Gravel	1.5
34	0.5	45	28.4	30	40	360	120	3.0	5	D18-2	22	26	30	HSS6 R	8" R.M.	Simple	Rigid	Gravel	1.5
FIND MOST SUSCEPTIBLE COLUMN HEIGHT																			
35	0.5	45	28.4	30	40	360	120	3.0	5	D18-2	18	22	15	HSS6 R	8" R.M.	Simple	Rigid	Gravel	1.5
36	0.5	45	28.4	30	40	360	120	3.0	5	D18-2	18	22	25	HSS6 R	8" R.M.	Simple	Rigid	Gravel	1.5
37	0.5	45	28.4	30	40	360	120	3.0	5	D18-2	18	22	35	HSS6 R	8" R.M.	Simple	Rigid	Gravel	1.5
FIND MOST SUSCEPTIBLE INNER COLUMNS																			
38	0.5	45	28.4	30	40	360	120	3.0	5	D18-2	18	22	30	HSS6 SQ	8" R.M.	Simple	Rigid	Gravel	1.5
39	0.5	45	28.4	30	40	360	120	3.0	5	D18-2	18	22	30	HSS8 SQ	8" R.M.	Simple	Rigid	Gravel	1.5
40	0.5	45	28.4	30	40	360	120	3.0	5	D18-2	18	22	30	HSS6 R	8" R.M.	Simple	Rigid	Gravel	1.5
41	0.5	45	28.4	30	40	360	120	3.0	5	D18-2	18	22	30	HSS8 R	8" R.M.	Simple	Rigid	Gravel	1.5
42	0.5	45	28.4	30	40	360	120	3.0	5	D18-2	18	22	30	#1 W	8" R.M.	Simple	Rigid	Gravel	1.5
43	0.5	45	28.4	30	40	360	120	3.0	5	D18-2	18	22	30	#2 W	8" R.M.	Simple	Rigid	Gravel	1.5
FIND MOST SUSCEPTIBLE OUTER WALLS																			
44	0.5	45	28.4	30	40	360	120	3.0	5	D18-2	18	22	30	HSS6 R	HSS R	Simple	Rigid	Gravel	1.5
45	0.5	45	28.4	30	40	360	120	3.0	5	D18-2	18	22	30	HSS6 R	HSS8 SQ	Simple	Rigid	Gravel	1.5
46	0.5	45	28.4	30	40	360	120	3.0	5	D18-2	18	22	30	HSS6 R	W-shape	Simple	Rigid	Gravel	1.5
47	0.5	45	28.4	30	40	360	120	3.0	5	D18-2	18	22	30	HSS6 R	8" U.M.	Simple	Rigid	Gravel	1.5
48	0.5	45	28.4	30	40	360	120	3.0	5	D18-2	18	22	30	HSS6 R	12" U.M.	Simple	Rigid	Gravel	1.5
49	0.5	45	28.4	30	40	360	120	3.0	5	D18-2	18	22	30	HSS6 R	8" R.M.	Simple	Rigid	Gravel	1.5
50	0.5	45	28.4	30	40	360	120	3.0	5	D18-2	18	22	30	HSS6 R	12" R.M.	Simple	Rigid	Gravel	1.5
FIND MOST SUSCEPTIBLE CONNECTIONS																			
51	0.5	45	28.4	30	40	360	120	3.0	5	D18-2	18	22	30	HSS6 R	8" R.M.	#1 Simple	Rigid	Gravel	1.5
52	0.5	45	28.4	30	40	360	120	3.0	5	D18-2	18	22	30	HSS6 R	8" R.M.	#2 Simple	Rigid	Gravel	1.5
53	0.5	45	28.4	30	40	360	120	3.0	5	D18-2	18	22	30	HSS6 R	8" R.M.	#3 Simple	Rigid	Gravel	1.5
54	0.5	45	28.4	30	40	360	120	3.0	5	D18-2	18	22	30	HSS6 R	8" R.M.	#1 SR	Rigid	Gravel	1.5
55	0.5	45	28.4	30	40	360	120	3.0	5	D18-2	18	22	30	HSS6 R	8" R.M.	#2 SR	Rigid	Gravel	1.5
56	0.5	45	28.4	30	40	360	120	3.0	5	D18-2	18	22	30	HSS6 R	8" R.M.	#3 SR	Rigid	Gravel	1.5
57	0.5	45	28.4	30	40	360	120	3.0	5	D18-2	18	22	30	HSS6 R	8" R.M.	#1 Fixed	Rigid	Gravel	1.5
58	0.5	45	28.4	30	40	360	120	3.0	5	D18-2	18	22	30	HSS6 R	8" R.M.	#2 Fixed	Rigid	Gravel	1.5
59	0.5	45	28.4	30	40	360	120	3.0	5	D18-2	18	22	30	HSS6 R	8" R.M.	#3 Fixed	Rigid	Gravel	1.5

ARCHETYPICAL BUILDING MATRIX																		
Bldg No.	D/S Load Ratio	GSL (psf)	RSL (psf)	Joist Span (ft)	Gird. Span (ft)	L (ft)	W (ft)	W/L Ratio	Joist Spacing (ft)	Joist Type	Joist Depth (in)	Girder Depth (in)	Column Height (ft)	Inner Column Type	Outer Wall Type	Conn-ections	Dia-phragm	Roof Type	Parapet Height (ft)
FIND MOST SUSCEPTIBLE DIAPHRAGM																			
60	0.5	45	28.4	30	40	360	120	3.0	5	D18-2	18	22	30	HSS6 R	8" R.M.	Simple	#1 Flex	Gravel	1.5
61	0.5	45	28.4	30	40	360	120	3.0	5	D18-2	18	22	30	HSS6 R	8" R.M.	Simple	#2 Flex	Gravel	1.5
62	0.5	45	28.4	30	40	360	120	3.0	5	D18-2	18	22	30	HSS6 R	8" R.M.	Simple	#3 Rigid	Gravel	1.5
63	0.5	45	28.4	30	40	360	120	3.0	5	D18-2	18	22	30	HSS6 R	8" R.M.	Simple	#4 Rigid	Gravel	1.5
FIND MOST SUSCEPTIBLE PARAPET HEIGHT																			
64	0.5	45	28.4	30	40	360	120	3.0	5	D18-2	18	22	30	HSS6 R	8" R.M.	Simple	Rigid	Gravel	1
65	0.5	45	28.4	30	40	360	120	3.0	5	D18-2	18	22	30	HSS6 R	8" R.M.	Simple	Rigid	Gravel	1.5
66	0.5	45	28.4	30	40	360	120	3.0	5	D18-2	18	22	30	HSS6 R	8" R.M.	Simple	Rigid	Gravel	2
67	0.5	45	28.4	30	40	360	120	3.0	5	D18-2	18	22	30	HSS6 R	8" R.M.	Simple	Rigid	Gravel	2.5
68	0.5	45	28.4	30	40	360	120	3.0	5	D18-2	18	22	30	HSS6 R	8" R.M.	Simple	Rigid	Gravel	3
69	0.5	45	28.4	30	40	360	120	3.0	5	D18-2	18	22	30	HSS6 R	8" R.M.	Simple	Rigid	Gravel	3.5
70	0.5	45	28.4	30	40	360	120	3.0	5	D18-2	18	22	30	HSS6 R	8" R.M.	Simple	Rigid	Gravel	4
71	0.5	45	28.4	30	40	360	120	3.0	5	D18-2	18	22	30	HSS6 R	8" R.M.	Simple	Rigid	Gravel	4.5

Chapter 5

Design and Modeling of Lightweight Metal Roof Structures with Open-Web Steel Joists under Snow Loads

5.1 Introduction

To determine the factors that contribute to the susceptibility of lightweight metal buildings with open-web steel joist roof systems to snow-induced failure, building response under snow loading is simulated using nonlinear models in the OpenSees software package. Roof systems of these types of buildings have some unique features that may potentially make them susceptible to snow-induced failure compared to heavy steel or concrete buildings. As such, they may experience excessive deflections, local member buckling, and member yielding. To adequately account for failure characteristics experienced by these systems, robust building models are developed and adapted for factors determined to influence structural response, including building geometry, material type, and extreme snow loading. Advancement and development of these building models leads to a broad and representative set of models aimed with the intention of furthering our understanding of open-web steel joist roof systems. The following section includes a detailed methodology of the design and analysis for the nonlinear building models.

5.2 Joist Design for Modern Code Requirements

Before models of lightweight metal buildings are created, structural elements of representative joist systems must be designed according to modern code provisions. It is important for these elements to exhibit actual behavior demonstrated by open-web steel joists and to be representative of today's practice.

SJI design specifications state that required stresses be calculated according to the load combinations in Table 5.1, where *D* is the dead load due to the weight of the structural elements and the permanent features of the structure, *L* is the live load due to occupancy and movable equipment, *Lr* is the roof live load, *S* is the snow load, and *R* is the load due to initial rainwater or ice exclusive of the ponding contribution (SJI 2005). Allowable Strength Design (ASD) was used throughout this project, implying that loads did not need to be factored. For our building set, load case (2) of ASD designation is used throughout the analysis since it governs over dead load only (load case (1)) in all design cases, considering that roof live load, snow load, or rain load will always be present on roofs of this construction type. Wind and other types of lateral loads were not considered in the design.

Table 5.1 – ASD and LRFD Load Combinations (SJI 2005).

ASD		LRFD	
(1)	D	(1)	$1.4D$
(2)	D + (L or Lr or S or R)	(2)	$1.2D$ + 1.6 (L or Lr or S or R)

5.2.1 Basic Joist Design

Due to time constraints, only the first six buildings from the archetypical building matrix are selected for analysis (shown below in Table 5.2). These buildings all have the same overall length, width, height, and other characteristics, but different dead-to-snow load ratios. The dead-to-snow load ratios for each building are selected based on the roof snow load and dead load of the building roof.

The roof snow load is calculated using the methods discussed in Chapter 2 with ASCE 7-05, where C_e = 0.9 (fully exposed, terrain category B), C_t = 1.0 (heated structure), and I = 1.0 (normal occupancy and function). The first building is assumed to be located in a region where the design roof snow load is equal to 20 psf. This roof snow load is selected so that roof live load does not govern design. The design roof snow loads of Buildings 2-5 were selected based on 15 psf ground snow load increments. Building 6 is designed for a ground snow load of 120 psf, which is selected to represent a very large snow load case, common in some parts of the more mountainous regions of the U.S. (like the Rocky Mountains, Cascade Mountains, etc.).

The dead load includes the self-weight of the joists and girders themselves plus any additional dead load imposed on the roof system. Additional dead loads for these types of buildings are calculated as 12 psf from Table 17-13 of the AISC Steel Design Manual (2005), accounting for 5 psf of suspended ceiling materials, 1 psf of 3-ply ready roofing, and 6 psf for 5-ply felt and gravel roofing. In this project, the weight of metal decking was assumed to be constant. However, in reality metal decking increases in weight and thickness as transient loads increase, which causes dead loads of the system to increase. Any future research will need to incorporate the thickness of the metal decking into design. The additional weight of thicker metal decking would need to be incorporated into the all of the buildings. Since the total dead load of the roofs of every building are about the same (16 psf), the additional dead load from the metal decking would have about the same impact in terms of dead-to-snow load ratio for every building. Since the governing design feature of the first six buildings in the archetypical building matrix is the dead-to-snow load ratio, only uniform snow loads were considered in design. Drifted snow and non-uniform snow loads were not included in the design. However, future

research will need to incorporate these into design for the remaining buildings of the archetypical building matrix.

Table 5.2 – Buildings selected for analysis (SJI 2005).

Building Number	D/S Load Ratio	GSL (psf)	RSL (psf)	Joist Span (ft)	Girder Span (ft)	Length (ft)	Width (ft)	Joist Spacing (ft)	Joist Type	Joist Depth (in)	Column Height (ft)	Column Type
1	0.80	31.7	20.0	30	40	240	120	5	D18-1	18	30	HSS6 R
2	0.57	45	28.4	30	40	240	120	5	D18-2	18	30	HSS6 R
3	0.43	60	37.8	30	40	240	120	5	D22-2	22	30	HSS6 R
4	0.34	75	47.3	30	40	240	120	5	D24-2	24	30	HSS6 R
5	0.29	90	56.7	30	40	240	120	5	D24-4	24	30	HSS6 R
6	0.22	120	75.6	30	40	240	120	5	D26-5	26	30	HSS6 R

Joists are selected and designed for these six buildings based on the roof snow load and the overall joist length (30 ft) shown in Table 5.2. Figure 5.1 and Figure 5.2 show 3D plots and plan views for the building to be modeled for all six building cases, while Figure 5.3 and Figure 5.4 show front and side elevation views, respectively.

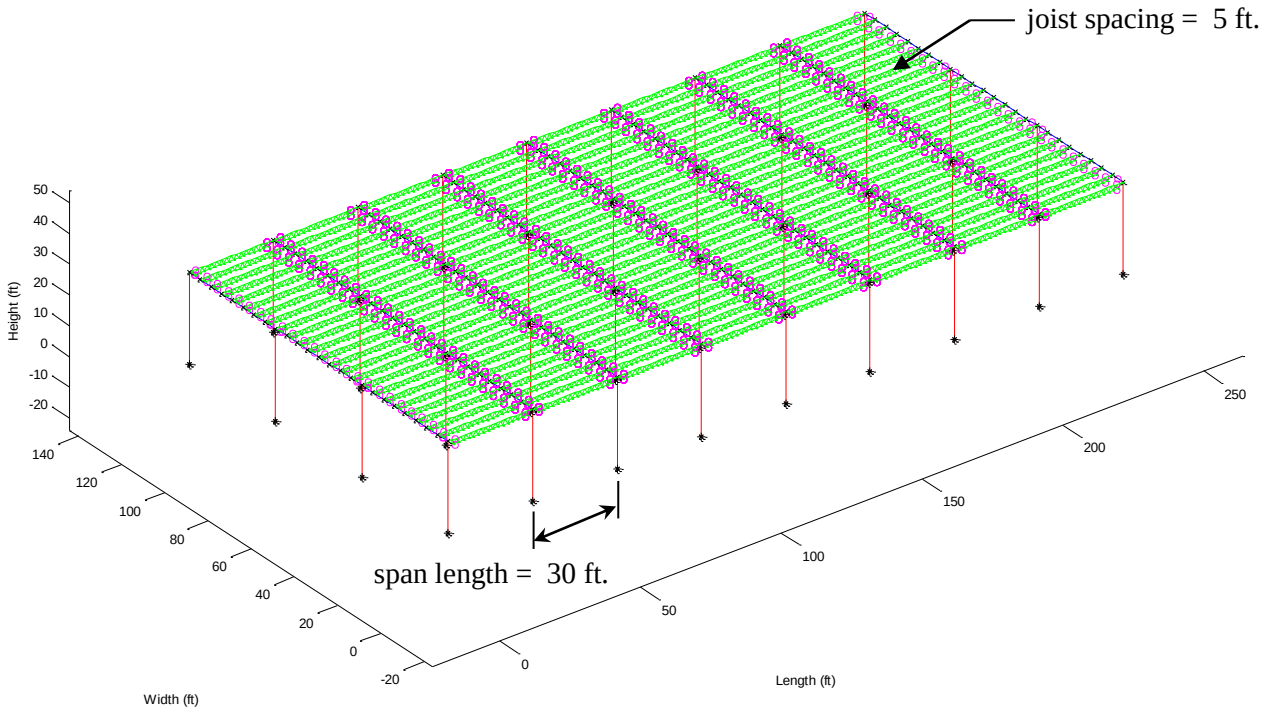

Figure 5.1 – 3D view of building models with overall length equal to 240 ft. and overall width equal to 120 ft.

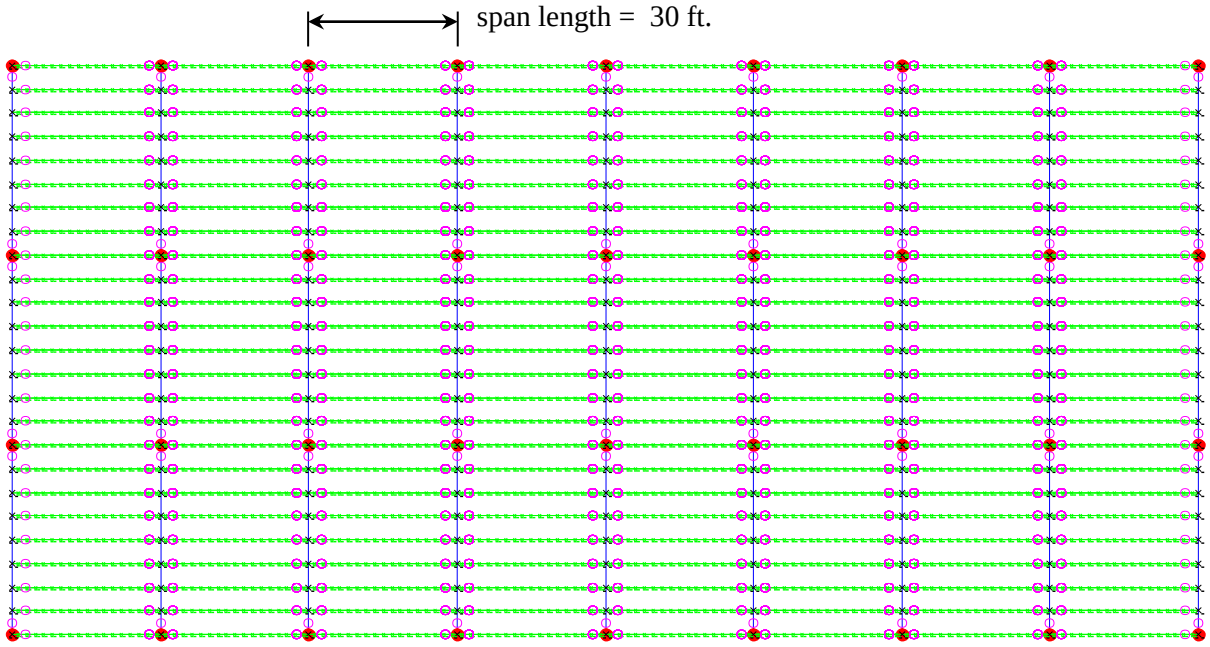

Figure 5.2 – Plan view of building models with 3 bays along the width and 8 bays along the length.

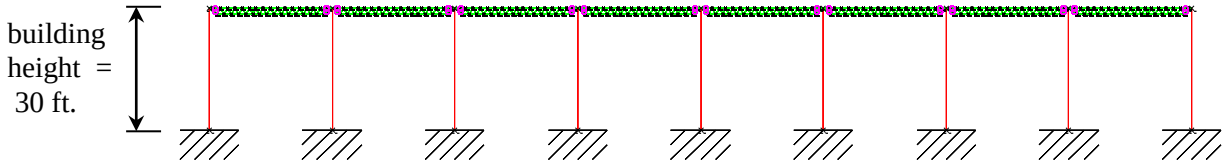

Figure 5.3 – Front elevation view of building models with 8 bays along the length (total length = 240 ft.).

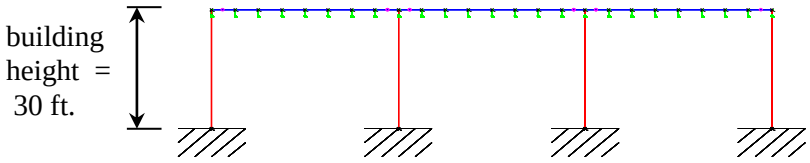

Figure 5.4 – Side elevation view of building models with 3 bays along the width (total width = 120 ft.).

Like SJI (2005), Vulcraft (2005) and Canam (2010), every major joist manufacturer has a joist catalog with load tables for use in selecting the type of joist to be used for given span dimensions and loading cases. A standard load table for K-Series Joists with ASD designation is shown below in Figure 5.5. The numbers shown in black are the total safe uniformly distributed

load-carrying capacities, while the numbers shown in red are the nominal live loads per linear foot of the joist which will produce an approximate deflection of 1/360 of the span (SJI 2005). For deflections of 1/240 of the span, the numbers in red can be multiplied by 1.5. These deflection limits are discussed in more detail later.

STANDARD LOAD TABLE FOR OPEN WEB STEEL JOISTS, K-SERIES
Based on a 50 ksi Maximum Yield Strength - Loads Shown in Pounds per Linear Foot (plf)

Joist Designation	18K3	18K4	18K5	18K6	18K7	18K9	18K10	20K3	20K4	20K5	20K6	20K7	20K9	20K10	22K4	22K5	22K6	22K7	22K9	22K10	22K11
Depth (In.)	18	18	18	18	18	18	18	20	20	20	20	20	20	20	22	22	22	22	22	22	22
Approx. Wt. (lbs./ft.)	6.6	7.2	7.7	8.5	9	10.2	11.7	6.7	7.6	8.2	8.9	9.3	10.8	12.2	8	8.8	9.2	9.7	11.3	12.6	13.8
Span (ft.) ↓																					
18	550	550	550	550	550	550	550														
	550	550	550	550	550	550	550														
19	514	550	550	550	550	550	550														
	494	523	523	523	523	523	523														
20	463	550	550	550	550	550	550	517	550	550	550	550	550	550							
	423	490	490	490	490	490	490	517	550	550	550	550	550	550							
21	420	506	550	550	550	550	550	468	550	550	550	550	550	550							
	364	426	460	460	460	460	460	453	520	520	520	520	520	520							
22	382	460	518	550	550	550	550	426	514	550	550	550	550	550	550	550	550	550	550	550	550
	316	370	414	438	438	438	438	393	461	490	490	490	490	490	548	548	548	548	548	548	548
23	349	420	473	516	550	550	550	389	469	529	550	550	550	550	518	550	550	550	550	550	550
	276	323	362	393	418	418	418	344	402	451	468	468	468	468	491	518	518	518	518	518	518
24	320	385	434	473	526	550	550	357	430	485	528	550	550	550	475	536	550	550	550	550	550
	242	294	318	345	382	396	396	302	353	396	430	448	448	448	431	483	495	495	495	495	495
25	294	355	400	435	485	550	550	329	396	446	486	541	550	550	438	493	537	550	550	550	550
	214	250	281	305	337	377	377	266	312	350	380	421	426	426	381	427	464	474	474	474	474
26	272	328	369	402	448	538	550	304	366	412	449	500	550	550	404	455	496	550	550	550	550
	190	222	249	271	299	354	361	236	277	310	337	373	405	405	338	379	411	454	454	454	454
27	252	303	342	372	415	498	550	281	339	382	416	463	550	550	374	422	459	512	550	550	550
	169	198	222	241	267	315	347	211	247	277	301	333	389	389	301	337	367	406	432	432	432
28	234	282	318	346	385	463	548	261	315	355	386	430	517	550	348	392	427	475	550	550	550
	151	177	199	216	239	282	331	189	221	248	269	298	353	375	270	302	328	364	413	413	413
29	218	263	296	322	359	431	511	243	293	330	360	401	482	550	324	365	398	443	532	550	550
	136	159	179	194	215	254	298	170	199	223	242	268	317	359	242	272	295	327	387	399	399
30	203	245	276	301	335	402	477	227	274	308	336	374	450	533	302	341	371	413	497	550	550
	123	144	161	175	194	229	269	153	179	201	218	242	286	336	219	245	266	295	349	385	385

Figure 5.5 – Open-web steel joist standard load table in ASD designation for K-Series Joists based on a 50 ksi maximum yield strength (Nucor 2005).

For ASD design, a joist is selected such that the joist capacity from the table exceeds the design loads of the joist. The joist chosen for Building 1 is similar to an 18K3 joist (30 feet long), which has a total design capacity of 203 plf and is about 20 plf greater than the total design load. The 18K3 was selected as the design basis for Building 1 because it is the lightest joist meeting the design criteria for the given span of 30 feet. Although joist nomenclatures vary depending on the manufacturer, the majority of joists are specified by a three-part code; the first set of digits refers to the depth, the second refers to the series, and the third refers to the cross-

sectional make-up of the joist (Management Computer Controls, Inc. 2010). The 18K3 joist therefore refers to an 18-inch deep K-Series Joist with the third type of section in the series. Since our joists are not particular to any joist manufacturer, the joist designations for the joists used in our buildings takes on the form DX-X, where D and the first number refer to the depth of the joist and the second number refers to the cross-sectional make-up of the joist within its depth category. For example, the joist in Building 1 (D18-1) has a depth of 18 inches and is the first cross-sectional make-up within its depth category.

Designs for open-web steel joists are proprietary. Information about the structural make-up of joists, including element type, size, geometry, etc., is not publicly available. Therefore, the joists used in these building models are designed so that they conform to modern joist designs without being specific to any manufacturer. This goal is accomplished by designing the joists to meet strength and serviceability requirements of the SJI, while ensuring that the joists developed in this study weigh approximately the same as other joists on the market with similar depths and spans, and have the same moment of inertias and basic geometry. Each joist is constructed to a basic geometry similar to that shown below in Figure 5.6, which is typical for most joists on the market (Nucor 2005).

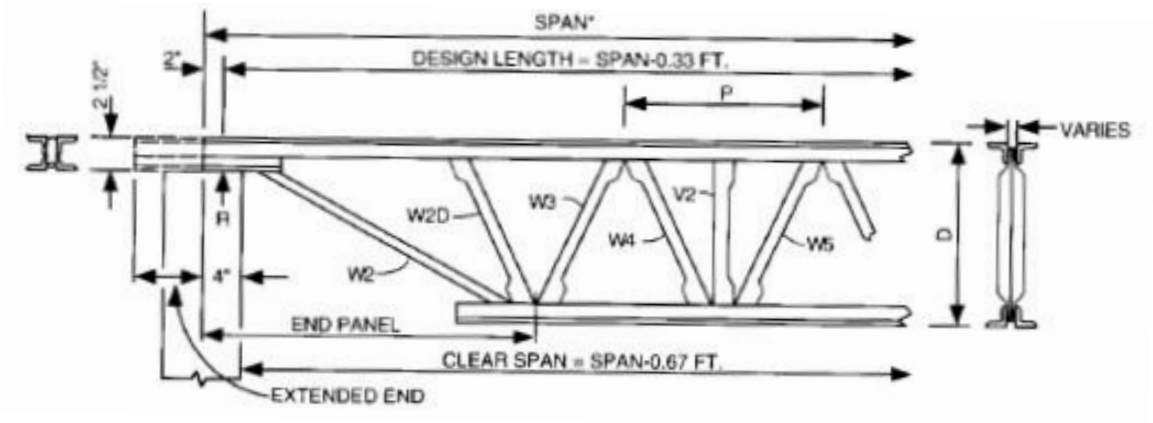

Figure 5.6 – Basic geometry for open-web steel joist design (Nucor 2005).

5.2.2 Strength Design for Joists

SAP2000 is used to build and analyze the joists to ensure that they meet design strength requirements. Each joist is built up from individual elements based on the arrangement in Figure 5.6 and based on the depths of the joist selected from the load tables for the specified design dead and snow loads. Double angles are selected for upper and lower chord joist elements. Rods are selected for the web members in Buildings 1 and 2; single angles are selected for the web members in Buildings 3 through 6. These elements are commonly used in open-web steel joists in practice. Theoretically, angles could have been used for the web members in all the buildings, but joists of both types were created in order to compare the differences in key behavior between joists with angled web members and joists with rod web members. Since the joists of Buildings 1 and 2 were designed for the smallest roof snow loads and since rods are usually used for web members in joists with lighter and smaller sections, rod web members were used in Buildings 1 and 2. Also, as shown by site visits (Chapter 4), both are commonly used for joist design in practice. The back-to-back distance between the double angles is taken as zero. In the model, all joist elements are rigidly connected, while end connections are pinned. In practice, all joist connections are performed by arc or resistance welding, acting as more or less fixed (Nucor 2005). The connections at the ends of the joists are usually pinned. The joists were constructed in SAP2000 from the elements detailed in Table 5.3. Figure 5.7 shows a visual representation of a joist in SAP2000.

Table 5.3 – Final joist selection for Joists 1 - 6 by element type, including the service deflection, dead load, and moment of inertia compared to a traditional joist of the same selection.

Upper Chord	Lower Chord	Web Member	End Rod dia. (in)	Δ (in)	w_{design} (plf)	$w_{catalog}$ (plf)	I_{design} (in^4)	$I_{catalog}$ (in^4)
2L2x2x1/16	2L2x2x1/16	13/16	13/16	-1.50	6.67	6.6	80.0	86.0
2L2x2x1/16	2L2x2x1/16	7/8	7/8	-1.49	7.23	7.2	81.4	100.7
2L2x2x1/8	2L2x2x1/16	L2x2x1/8	5/8	-1.43	7.99	8	172.9	153.1
2L2x2x1/16	2L2x1-1/2x1/8 LLBB	L2x2x3/16	5/8	-1.50	8.74	8.4	198.4	183.2
2L2x2x1/8	2L1-1/2x1-1/2x1/8	L1-1/2x1-1/2x1/4	3/4	-1.45	9.92	9.7	198.4	223.0
2L2x2x1/8	2L2x1-1/2x1/8 LLBB	L2x2x3/16	15/16	-1.40	10.71	10.9	307.9	291.5

*LLBB stands for 'long legs back-to-back' – the long legs in these cases are vertical, while the short legs are horizontal.

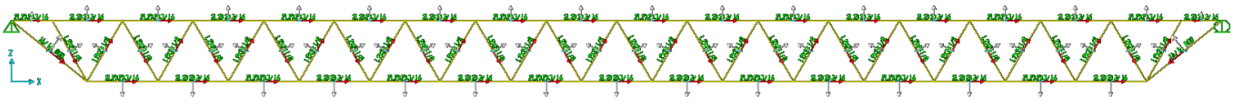

Figure 5.7 – Constructed open-web steel joist in SAP2000.

The depths of the sections are determined from their corresponding joist in the design catalog. After initial section sizes were determined, elements in each joist are altered until the moments of inertia of the joist are within 20% of the moment of inertia of a similar joist in the joist design catalog. The moment of inertia of the joists in the joist catalogs is calculated by Equation (5-1), where W_{LL} is the red figure in the load table and L is the span length minus 0.33 ft. This moment of inertia equation is the same per every joist manufacturer certified by SJI.

$$I_{catalog} = 26.767(W_{LL})(L^3)(10^{-6}) \quad (5\text{-}1)$$

The moment of inertia of the joists designed in this study is calculated by determining the average moment of inertia of the composite section by the parallel axis theorem (Equation (5-2)) at every location of the web member along the height of the joist.

$$Ix = \sum (I_{local} + y^2 A) \quad (5\text{-}2)$$

The element selection also considered the deflection limitations in the building code, as described in the next section.

5.2.3 Serviceability Design for Joists

For K-Series Joists, SJI requires that the deflections due to live load shall not exceed 1/360 of the span for roofs with plaster ceilings attached or suspended and 1/240 of the span for all other roof types (SJI 2005). Our building set is assumed not to have attached or suspended ceilings, so the second serviceability requirement is used ((30 ft x 12 inches)/240 = 1.5 inch deflection limit).

In contrast to SJI, IBC appears to present more stringent deflection criteria when considering total load requirements for serviceability as per Section 1604.3. Table 1604.3 in this section requires a total load deflection limit (dead plus live load) in addition to a live load deflection limit (IBC 2006), while SJI has no requirement for a total load deflection limit. An exception to the IBC table does exist, however – "For steel structural members, the dead load shall be taken as zero" (IBC 2006). This allows the engineer to discount the effects of dead load and only consider live load for serviceability requirements for roofs with open-web steel joists. In this regard, the deflection limits by SJI specifications meet IBC limits and in some cases are more stringent (Holtermann et al. 2009).

Only the live load was applied to the top chord of the joist when analyzing the joist for the 1.5 inch deflection limit consideration. For the first iteration in meeting the live load deflection criteria, trial element sizes were selected. For every iteration thereafter, larger or smaller elements were used in the section, depending on whether higher or smaller stiffnesses were required to meet the moment of inertia requirements. Elements forming the composite cross-section and meeting the deflection limit and strength requirement were selected for the joist, so long as the joist weight was about the same as the similar joist the load tables. The iteration process for each joist required selective care in order to balance stiffness, deflection,

and weight requirements. Final joist elements were selected for each building, which are tabulated in Table 5.3. The design values in the table are from the joist designs we created, while the catalog values are from the standard K-Series joist load tables based upon the catalog designs. The moments of inertia of the joists we created vary, at the most, by 20% from the moments of inertia of the joists in the design catalogs.

5.3 Modeling Buildings with Lightweight Metal Roof Systems

5.3.1 Modeling Software

The modeling software used in the creation of the six building models includes MATLAB®, OpenSees, and SAP2000. MATLAB is a programming language used for algorithm development, data analysis, data visualization, and numerical computation (Mathworks 2011). OpenSees is an open-source software that can be used to evaluate the performance of structural and geotechnical systems under critical external loading conditions. It has been primarily used for seismic response. Developed by the Pacific Earthquake Engineering Research Center (PEER), OpenSees is a community-oriented software, continually updated by users and developers, with advanced computational capabilities for nonlinear response and material selection (PEER 2006). In this study, OpenSees is used to develop nonlinear models of the joists, using MATLAB as a driver. SAP2000®, developed by Computers & Structures, Inc. (CSi), is a fully-integrated, general purpose structural analysis program with complex built-in graphical user interfaces, analysis engines, and design tools. SAP2000 is used here for the joist design, as described previously.

5.3.2 Methodology

The archetypical buildings are created and analyzed through interdependent MATLAB and OpenSees files. Initially, three Matlab codes are developed: 1) *Inputs and Knowns*, 2)

Building Geometries for OpenSees, and 3) *Plot Building Geometries*. The purpose of these files is to compute and plot basic building characteristics of any type of one-story, lightweight metal building as specified in the Archetypical Building Matrix described in Chapter 4. The first file holds all basic inputs and knowns, including building characteristics (length, width, height, number of bays in each direction, and joist spacing), roof snow loading conditions (uniform or non-uniform), and member properties (geometric and material characteristics for joists, girders, and columns). Output information, such as nodal location, nodal connectivity, member properties, loading conditions, and connectivity, is calculated through *Building Geometries* for OpenSees for any building geometry specified in the input file. *Plot Building Geometries* plots two- and three-dimensional views of the building, labels elements and nodes, distinguishes between joist, girder, and column elements by color, and shows fixity conditions. See Figure 5.1, Figure 5.2, Figure 5.3, and Figure 5.4 for plots of the building. Columns are distinguished by the color red, girders are distinguished by the color blue, joists are distinguished by the color green, springs are distinguished by the color magenta, and fixities are distinguished by the color black. More information about building elements and nodes is found in Section 5.3.4.

Another MATLAB file, *Write File to OpenSees*, converts building information from *Building Geometries for OpenSees* to a .tcl file for OpenSees to read. OpenSees then gathers the information included in this file, builds the models, runs the analysis, and records output parameters specified by the user. For ease and simplification, one MATLAB file (*Max Forces*) is created to summarize the maximum force(s) and/or displacement(s) of the respective element(s) and/or node(s) experienced during the analysis, while another (*Run Analysis*) is created to run all MATLAB and OpenSees files in sequence.

5.3.3 Modeling Details

The OpenSees .tcl files define a collection of elements, nodes, constraints, load patterns, analysis specifications, and recorders (PEER 2006). The following section discusses basic characteristics of the elements, loads, and analyses included in the models, as well as general characteristics of the model itself.

General Characteristics: The models in this study have three dimensions (global X, Y, and Z) and six degrees of freedom per node (translations and rotations in the X, Y, Z directions). It is assumed that the columns are rigidly attached to the foundation, therefore translations and rotations of the nodes at the base of the columns are constrained in all dimensions, as shown in Figure 5.3 and Figure 5.4. Output files of displacements, forces, stresses, and strains are created during the analysis.

Element Characteristics: All elements in our building set are made up of structural steel with an Elastic Modulus of 2.9×10^6 psi and a yield strength capacity of 50 ksi. Each top chord, bottom chord and web element in the models is composed of nonlinear beam-column elements. In OpenSees, these elements are force-based and consider the spread of plasticity along the element. To account for localized response, elements of the joist are decomposed into smaller fibers, each having its own stress-strain and deflection-force response. The number of fibers selected for each section was chosen to adequately represent the response of the section without slowing down the analysis and varies from 40 to 100. Each fiber is assigned the Giuffré-Menegotto-Pinto steel material in OpenSees. The transition between linear and nonlinear behavior of the steel is controlled by isotropic strain hardening curve relationship, as shown in Figure 5.8 (PEER 2006). The yield strength capacity of steel is not 70 ksi, as show in Figure 5.8, but follows the same strain hardening relationship. The strain-hardening ratio is specified as 0.3.

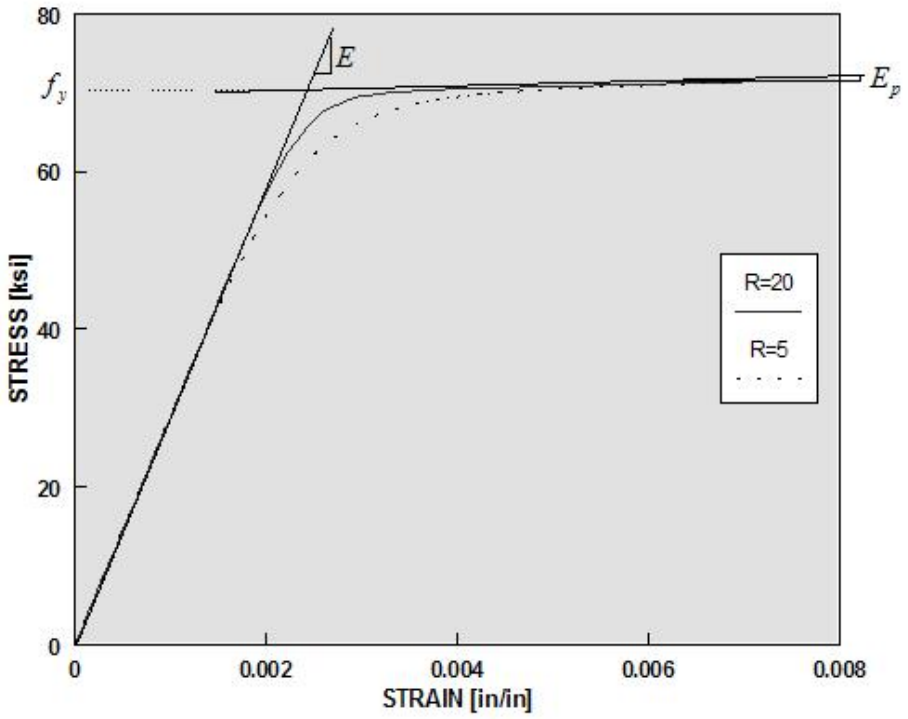

Figure 5.8 – Stress-strain relationship for steel material used in OpenSees (PEER 2006).

The purpose of geometric transformations is to transform beam stiffness and resisting force from the local coordinate system to the global coordinate system based on the element coordinate system. P-delta geometric transformations are used in OpenSees to account for geometric nonlinearities resulting from the changing orientation of the members in space as loads or displacements are applied. More specific details about the definition of 3D geometric transformations are included in Appendix 5.1.

Fixities and Connectivity Between Internal Joist Elements: As in the SAP models, nodes in the joist connecting internal joist members without any specified connectivity are assumed to have rigid connections, i.e. the angle between the members remains unchanged throughout the analysis.

In practice, joists and girders in building roofs are connected to other building elements by bolts or welds. While most connections from the joists to other members involve either

pinned or fixed connections, some connections are semi-rigid. A semi-rigid connection behaves somewhere in between a fixed or pinned connection by controlling the transfer of forces and moments between the structural roof members. To model connections between joists, girders and columns (as shown in Figure 5.1 through Figure 5.3), zero-length springs are created in the model at the end of every girder and joist. The spring stiffness is assumed to be large in the directions of translation (ten times the Elastic Modulus of steel = $2.9x10^{10}$ psi), but is assumed to be small in the directions of rotations (one-tenth the amount of the Elastic Modulus of steel = $2.9x10^{8}$ psi) in all degrees of freedom. In this regard, only minimal moments are transferred from the joists to the girders and columns, while complete forces transfer.

Since web members of the joists are welded to the top and bottom chords in practice, no releases in the bending moments are applied to the web members in the OpenSees models. As a result, the web members are designed to resist small bending moments due to their self weight, which is representative of real-life conditions.

Analysis Characteristics: In this study, we are conducting static nonlinear analysis. No masses or damping effects are assigned to the nodes in these models since no dynamic analyses are completed. OpenSees settings related to analysis options include constraint handlers, degree of freedom numberers, integrators, tolerance levels, definition of solution algorithms, system of equations, and convergence tests. These parameters impact the computational time needed to obtain a solution, as well as ease of convergence.

Loading Characteristics: For the building set, the self weights of the elements are applied as a uniformly distributed load along the length of the element in the direction of gravity. Additional dead loads are applied along the top chord of the joists. For snow loading, two loading techniques were used: load-controlled and displacement-controlled analysis. In a load-

controlled analysis, forces are applied and system response is monitored; in a displacement-controlled analysis, displacements are imposed on the system, and the system is monitored. The displacement-controlled analysis is used to simulate post-peak (negative) stiffness behavior after elements have buckled.

Out-of-Plane Joist Behavior: If the upper chords of the joists are not constrained laterally, the joists may undergo significant horizontal movement, leading to lateral torsional buckling. In terms of primary lateral load effects, such as wind or earthquakes, and secondary lateral load effects, such as non-uniform or drifted snow loads, adequate bracing is crucial in providing lateral stability of the joists. Since only uniform snow loads are applied in this project and no lateral deformity exists initially, forces remain vertical throughout the analysis and no lateral bracing is required. Metal decking is not directly attached to the joists in the model; rather, the load is applied as a uniformly distributed dead load along the upper chord of the joists. As future research implements lateral load effects, restraints will be incorporated into the models to account for adequate decking attachment and initial lateral imperfections will be introduced.

5.4 Pushdown Analysis

The goal of these building models is to predict how these buildings respond to any given value of roof snow load. We seek to understand the load level under which the roof begins to fail and what specifically causes the elements fail to (buckling, yielding, etc.), as well as which elements in the joists are most likely to fail as the snow load on the building roof increases. A good method to achieve this understanding is by means of pushdown analyses, which can be implemented using a displacement-controlled procedure. Instead of analyzing building response at every value of roof snow load, a pushdown analyses imposes a specified displacement on the system in a number of increments, and analyzes building response at each time increment. From

data gathered at each increment, we can analyze the behavior in each joist element and see at which value of imposed displacement causes yielding and/or failure in the system. Once we know the maximum deflection value the building can resist, we are able to back-calculate for the roof snow load expected to cause this deflection. In short, we are able to load the buildings until failure and find the value of roof snow load that would cause this deflection. The next chapter addresses how the pushdown analysis is implemented for the buildings of interest, the joist responses when imparted with the deflections, and the expected displacements and responses of these joists for any value of roof snow load.

Chapter 6

Analysis of Lightweight Metal Roof Structures with Open-Web Steel Joists under Snow Loads

6.1 Overview

This chapter presents the results of the pushdown analyses for the first six buildings in the archetypical building matrix. By means of a static pushdown analysis, joists in all six buildings are induced with specified deflections at mid-span, and building forces and displacements are recorded up to the point where the analysis would not converge. A static pushdown is chosen for the analysis, as opposed to force-controlled analysis, in order to understand building response for all increments of imposed displacement. A force-controlled analysis would capture building response for a given value of roof snow load, but would fail to capture building response after the peak load is applied. Building 2 is selected and induced with displacements beyond its initial convergence limit so as to provide a greater in-depth study of the structural response and failure modes of lightweight metal buildings with open-web steel joists.

6.2 Loading for Pushdown Analysis

The original 120 ft. x 240 ft. buildings are simplified to one-by-one bay models with three joists spaced at 5 ft. on center. In all building models, only the interior joists are studied. The joists in the one-bay building models are identical to those in the full size buildings. Therefore, the simplified models should exhibit the same deflection and force trends as the full size building models. The ability to simplify the full-scale buildings to one-by-one bays

significantly reduces computation and analysis time, resulting in a solution that is obtained more quickly, without compromising accuracy. Figure 6.1 and Figure 6.2 show the one-bay buildings modeled in this chapter in three-dimensional space and two-dimensional cross-sectional space, respectively.

For the static pushdown analysis, displacements are imposed on the building at the middle node of each joist. Depending on the geometry of the joist, the middle node can be in the top or bottom chord. The magnitude of displacements imposed on each joist is based on the relative amount of snow that joist is expected to carry. Since the interior joist carries twice as much snow as the exterior joists, due to the tributary width of 5.0 ft., as compared to 2.5 ft., displacements imposed on the interior joist are twice as large as the exterior joists, shown in Figure 6.1.

The joist dead load is applied to each structure as a uniformly distributed load along each element in the joist, applied in the direction of gravity (global Z). Dead loads of the individual joist elements are calculated by multiplying the density of structural steel (490 pcf) by the cross-sectional area of the element. To account for ceiling weight, roof materials, etc., additional dead loads of 12 psf, or 60 plf along the interior joist and 30 plf along the exterior joists, are applied as uniformly distributed loads along the top chords.

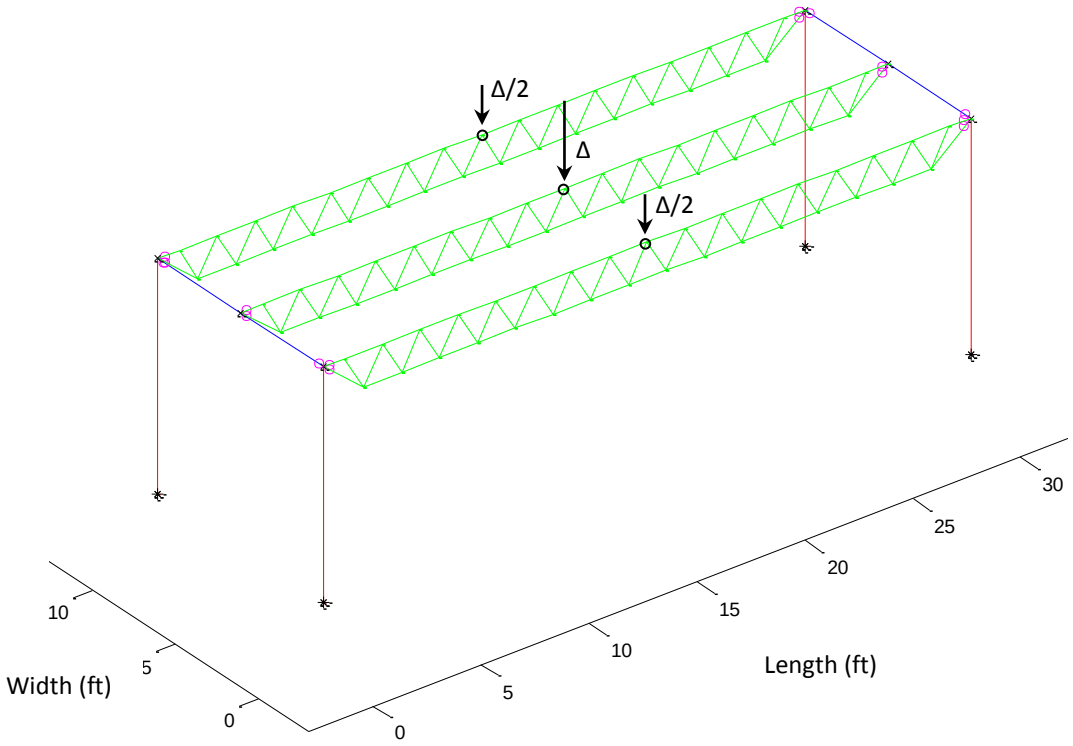

Figure 6.1 – 3D view of the buildings as modeled in static pushover analysis, showing imposed deflection locations and magnitudes.

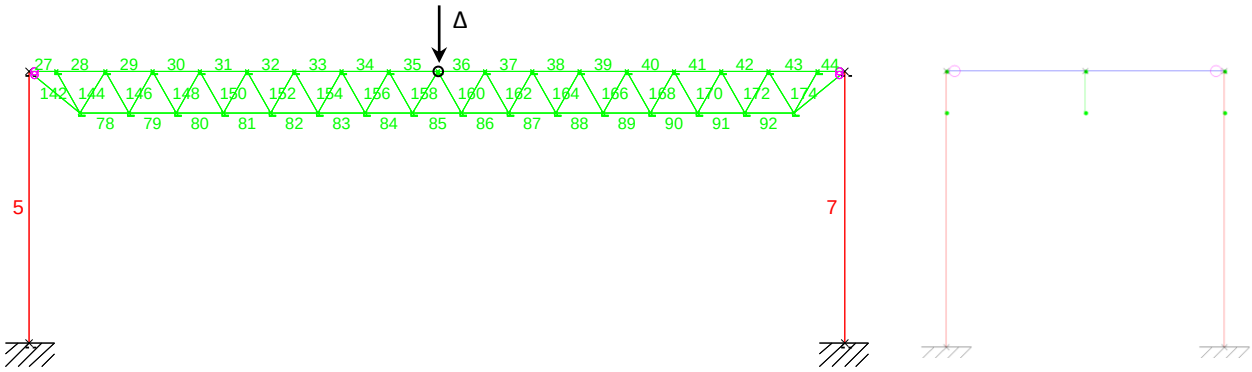

Figure 6.2 – Elevation views of the interior joist of the simple buildings used in static pushover analysis, showing imposed deflection locations and magnitudes.

6.3 Differences in Response for all Six Buildings

The pushdown analyses performed on the six lightweight metal buildings in this project represent the impacts of increasing amounts of snow on the building roofs. In the discussion below, results of pushover analyses are used to quantify the shear in the joists, the maximum

equivalent uniform snow load on the roof before failure, the ratio of the ultimate snow load to the design snow load, and the deformation capacity at yielding. The calculation of the design snow load capacity, based on approximations for deflection, shear, and moment is also included.

6.3.1 Design Snow Load Capacity Based on Approximations for Deflection, Shear, and Moment

The snow load capacity of the buildings is calculated from the pushover analysis by taking the reactions at the ends of the joists and subtracting the total dead load. Because the pushdown is applied to the joist as an imposed displacement at a single point, the moments and displacements will be larger and more concentrated in the middle portion of the joist than if a distributed load had been applied along the length of the joist. Therefore, to represent an equivalent uniformly distributed load, the snow load capacity is scaled by a factor based on Equation (6-1), where the maximum deflection in a beam with a point load is set to equal the maximum deflection in a beam with a uniformly distributed load:

$$\frac{PL^3}{48EI} = \Delta = \frac{5wL^4}{384EI} \tag{6-1}$$

Simplifying, the equation becomes Equation (6-2), where *w* is the uniformly distributed load.

$$w = 0.0533P \tag{6-2}$$

As calculated, the scale factor for deflection is 0.0533. This scale factor is intended to approximate the equivalent deflection would be of a joist with a uniformly distributed load.

Although not used in this thesis, other conversion factors are possible for approximations of shear and moment in a beam loaded with a uniformly distributed load, based on the maximum shear and moment of a beam loaded with a point load. For example, instead of assuming the deflections in the center of the beam are equal, shear forces can be assumed to be equal between

the uniformly distributed and point load cases. The scale factor based on the shear conversion equation (Equation (6-3)) is:

$$\frac{P}{2} = V = \frac{wL}{2} \tag{6-3}$$

Simplifying, the equation becomes Equation (6-4), where the scale factor of 0.0333 is determined from shear equivalency. It is important to note that this conversion for maximum shear was not used in Figure 6.3. Future study shall incorporate this conversion in analysis.

$$w = 0.0333P \tag{6-4}$$

Similarly, the scale factor for determining moment based on assuming equal moments in the point and distributed load cases is based on the scale factor in Equation (6-5):

$$\frac{PL}{4} = M = \frac{wL^2}{8} \tag{6-5}$$

The equation becomes Equation (6-6) after simplifying, where the scale factor for moment is 0.0666:

$$w = 0.0666P \tag{6-6}$$

The scale factors for deflection, shear, and moment vary since each point-to-distributed load relationship is different with regard to deflection, shear, and moment. The scale factors calculated above should only be used for their respective deflection, shear, or moment conversion. For example, a 0.0666 scale factor should only be used when converting the maximum moment in a beam loaded with a point load to the maximum moment in a beam loaded with a uniformly distributed load. A 0.0533 scale factor should be used when converting deflections and a 0.0333 scale factor should be used when converting shear.

6.3.2 Discussion of Results and How the Results are Obtained

This section presents the results of the pushdown analyses for all six buildings. The results of the pushdown analyses allow us to find the maximum equivalent uniformly distributed snow load that is expected to cause failure. The maximum roof snow load taken by each building is a measure of how susceptible that building is to failure, based upon its strength. The strength of the buildings can be quantified by studying the maximum shear experienced in the joists as displacements are imposed on the system. The higher the shear, the higher the roof snow load. The total shear force in the joists is determined by adding the reaction force at one end of the joist to the reaction force at the other end of the joist and dividing this value by two for the average shear force. Due to asymmetric deformations in the joists at the last increment of imposed displacement, reactions at both ends of the joists differ slightly. Although it is unclear why asymmetric deformations occur, it is possible that as the joists deflect under uniform loading, stresses increase in the joist symmetrically about its middle node until one side reaches yield just before its symmetric counterpoint. After one side deforms, stresses and forces redistribute in the joist, leading to asymmetric deformations.

Figure 6.3 shows the maximum shear in the interior joists in each building as a function of the imposed displacement at the midspan of the interior joist. During the analysis, each building follows the same force displacement pattern. Before the joist reaches yielding, the shear in the joist is linearly related to joist displacement; after yielding, the stiffness of the buildings is reduced, leading to decreased shear as displacements are imposed, as shown below in Figure 6.3. As explained in Chapter 5, Buildings 1 and 2 are designed for the lowest snow load cases, so the joists in their roof systems yield under the smallest snow loads, while Building 6 is designed for the highest snow load case and is capable of carrying higher snow-induced shear loads. From a

stiffness perspective, the lighter buildings are more flexible, while the heavier buildings are more rigid, shown by the fact that the stiffer buildings yield at higher values of shear.

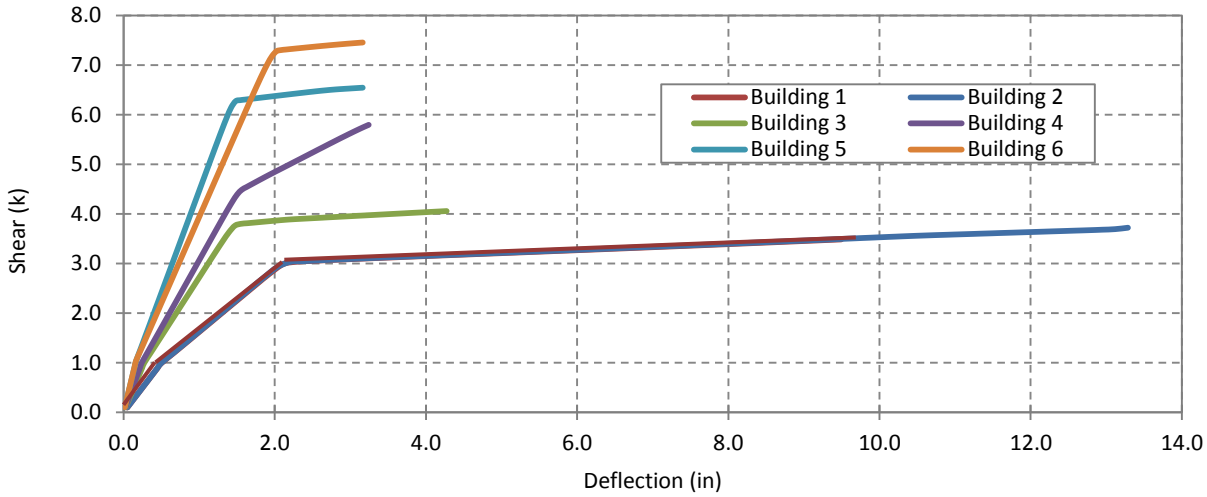

Figure 6.3 – Total shear force in the joists vs. imposed deflection for all six buildings.

Responses in shear for Buildings 1 and 2 are nearly identical because the only difference between the two is in the size of the end web rod member in the joists; Building 1 has 13/16-inch diameter rod members while Building 2 has 7/8-inch diameter rod members, as shown in Table 5.3. Elements in the joists of Buildings 1, 2, and 6 yield around 2 inches, while element in the joists of the other buildings yield at joist displacements of 1.5 inches. As Figure 6.3 shows, the joists in Buildings 1 and 2 are able to displace the most (9 inches and 13 inches) before failing to converge, while the joists in Buildings 4, 5, and 6 fail to converge around imposed displacements of 3 inches. The joists in Building 3 reach an imposed displacement of about 4.3 inches before failing to converge.

With regard to design snow load values, the buildings are able to carry a snow load well above their intended design snow load values. For example, Buildings 1 and 2 are designed for roof snow loads of 20.0 psf and 28.4 psf, respectively; each can carry up to 55 psf of snow before yielding. Building 3 is designed for a uniformly distributed roof snow load of 37.8 psf, but can

carry up to 66 psf. Building 4 is designed to carry 47.0 psf of snow, but can carry 83 psf. Buildings 5 and 6 (designed for roof snow loads of 56.7 psf and 75.6 psf, respectively) can carry 121 psf and 143 psf. See Figure 6.4 for more information. When dead loads are applied to the buildings at the beginning of the analysis, imposed deflections are zero, indicated by the flat portions of the curves in Figure 6.4.

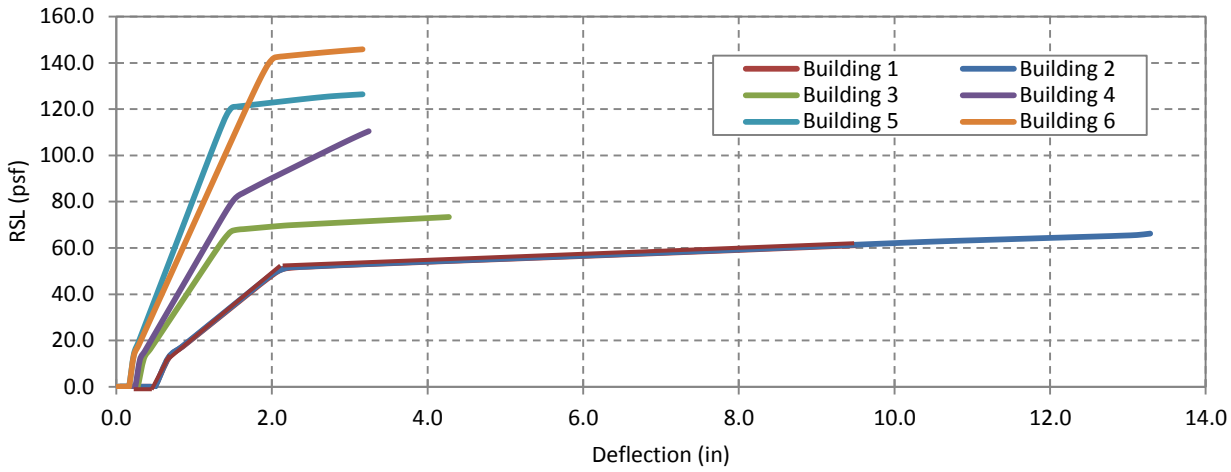

Figure 6.4 – Roof snow load vs. imposed deflection for all six buildings.

As expected, the lighter buildings (Buildings 1, 2 and 3) are weaker, while the heavier buildings (Buildings 4, 5, and 6) are stronger. Buildings 1 through 6 have strength-to-design load ratios of 2.8, 1.9, 1.8, 1.8, 2.1, and 1.9, respectively, when roof snow loads at yielding are divided by the design roof snow load capacity. In other words, at the minimum, the buildings can withstand 80% greater roof snow loads than their design loads. Building 1 has the maximum capacity to design load ratio and can withstand about triple its design roof snow load capacity.

Dead-to-snow load ratios give an indication of the amount of built-in resiliency a building has towards resisting snow overloading. They are calculated by dividing the dead load of the roof structure by the design roof snow load for each building. A building is considered to be overloaded with snow when the amount of snow present on the roof exceeds the design

capacity. In this study, the buildings with smaller dead-to-snow load ratios are designed for larger design roof snow loads (Buildings 4 through 6), while the buildings with larger dead-to-snow load ratios are designed for smaller design roof snow loads (Buildings 1 through 3). The dead load of the roof systems in each building is about the same – around 16 psf. Therefore, the buildings with greater design snow loads should be less resilient toward snow overloading than buildings with smaller design snow loads.

When building response is analyzed according to dead-to-snow load ratios, the buildings behave as expected. The lighter buildings yield at greater dead-to-snow ratios and undergo larger deflections than the heavier buildings, which yield at smaller dead-to-snow load ratios and undergo smaller deflections. Therefore, the results show that heavier buildings with smaller dead-to-snow load ratios (Buildings 4, 5, and 6) are less resilient toward snow overloading than lighter buildings with larger dead-to-snow load ratios (Buildings 1, 2, and 3).

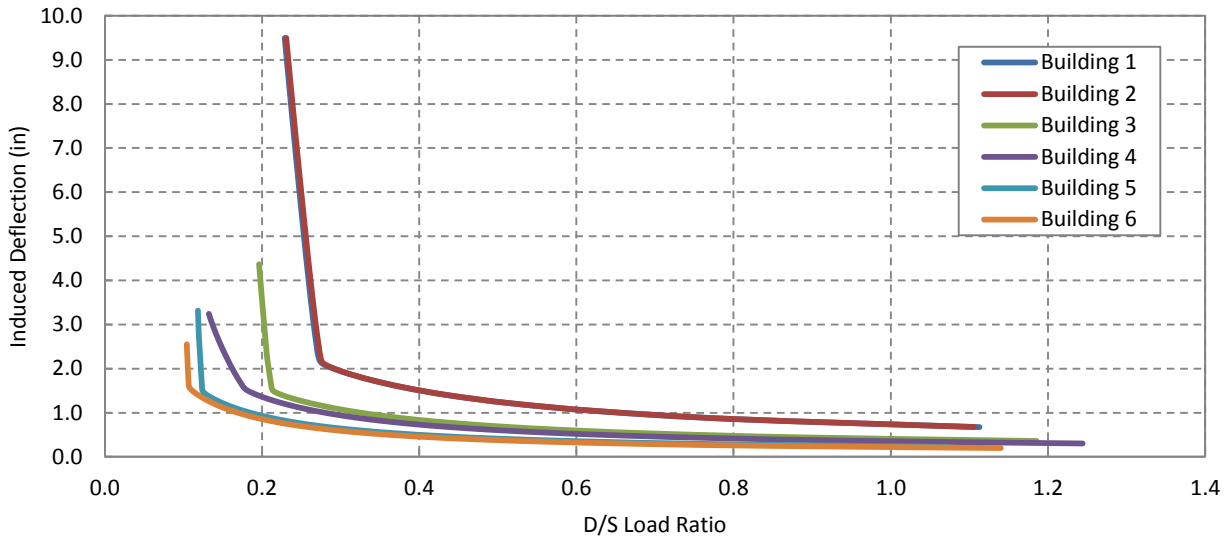

Figure 6.5 – Dead-to-snow load ratios vs. induced deflections for all six buildings.

To achieve a normalized measure of the strength of these buildings, the ratio of yield-to-design roof snow load is calculated for each building and plotted according to dead-to-snow load ratio. The yield-to-design roof snow load ratio is a measure of building strength. As mentioned earlier, other researchers have observed that buildings with higher dead-to-design roof snow load ratios are more resistant to overload than buildings with lower ones. As Figure 6.6 illustrates, a slight downward trend exists between Buildings 1 and 5, indicating that the buildings with larger dead-to-design roof snow loads are more resistant to overloading than buildings with lower ones. However, there is not a significant difference in building responses with different ratios of yield-to-design roof snow load except Buildings 1 and 5. This might be attributed to the fact that Building 1 is slightly overdesigned (its joists are designed according to the lightest joist which meets the loading criteria in the joist catalogs, whose design load capacity is slightly larger than necessary), and Building 5 has joists with much larger moment of inertias (223 in^4) than the joists in the joist manuals (198 in^4). Moment of inertias of joists used in other buildings are somewhat smaller than those from the catalogs.

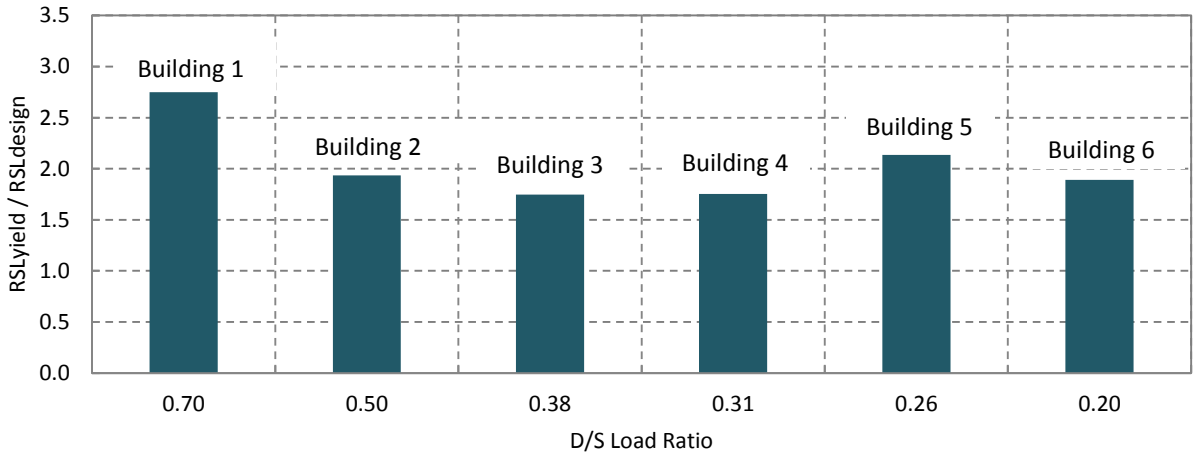

Figure 6.6 – Ratio of yield-to-design roof snow load vs. dead-to-snow load ratio for all six buildings.

In depth studies are not performed to determine the failure modes of these buildings, with the exception of Building 2, the analysis of which is described in detail in the next section.

6.4 Pushdown Analysis for Building 2

6.4.1 Summary

Building 2 is selected for greater in-depth study of the pushdown analysis due to the fact that it converged under larger imposed displacement as compared to the other buildings. To achieve a greater imposed displacement in Building 2, the solution algorithm, the number of analysis steps, and the tolerance are adjusted until the analysis converges. As shown in Figure 6.7, three revised analysis cases push the displacement beyond the 9 inches at which the initial model failed to converge. In Case 1, the number of analysis steps are increased; in Case 2, the solution algorithm is altered to a Newton-Raphson with line search method from the Newton-Raphson method used originally (PEER 2006); and in Case 3, the tolerance (allowable force-based error) is decreased by a factor of ten (1.0e-6 to 1.0e-5). Although Case 3 fails to converge 0.2 inches later than Case 2, Case 3 exhibits more instability at the end of its solution compared to Case 2. Therefore, Case 2 is used for the analysis with a maximum displacement of 13.5 inches.

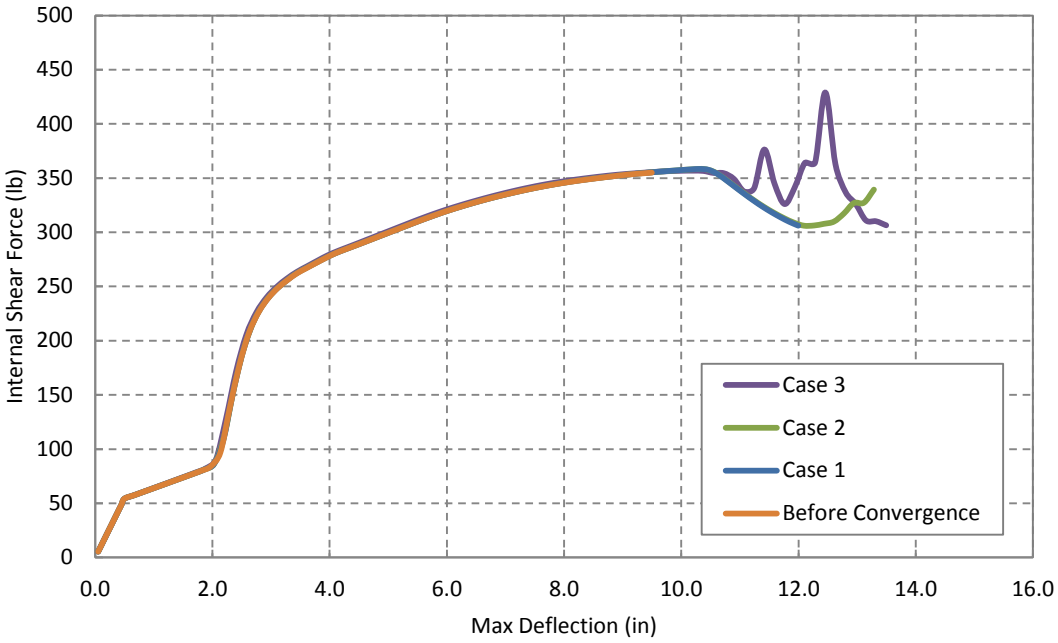

Figure 6.7 – Deflection vs. internal shear force in the top chord for Building 2, illustrating three different convergence scenarios.

6.4.2 Deflected Shapes due to Dead Load vs. Snow Load

For analysis purposes, the dead load is applied to the structure in even force increments over ten time steps. Subsequently, displacements due to snow loads are applied. Under dead load only (uniform load), the deflected shape of the joist takes on a different form than the deflected shape under snow load by pushdown techniques (point load for this analysis). Under dead load, the deflected shape takes on the form shown in Figure 6.8, with a maximum deflection of 0.5 inches. Although the figure appears to have a sudden distortion due to the plotting function used in Matlab, the deflected shape is, in fact, parabolic. If the dead loads were larger, the deflected shape would be more pronounced, and the plotted curve would take on the appearance of a more gradual and less distorted shape. Under the pushdown, the deflected shape takes on the form shown in Figure 6.9, with a maximum deflection of 13.5 inches. In the case of the pushdown, stresses, forces, and moments are more heavily concentrated in the middle of the

joist. The horizontal displacements were multiplied by a factor of 2.0 so that they could be more easily seen in the figures.

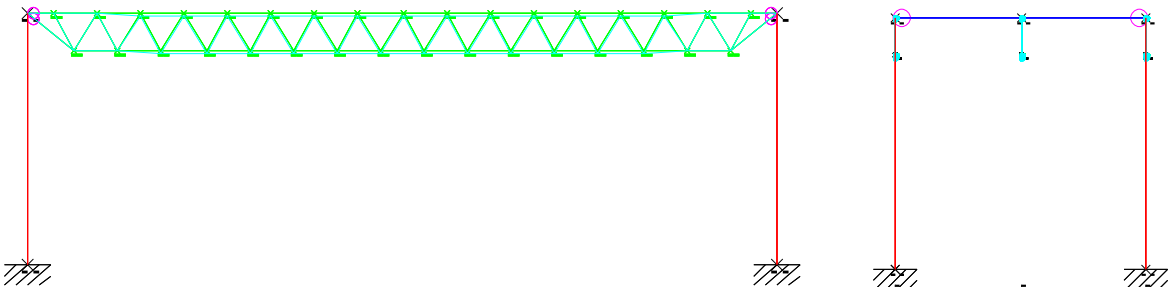

Figure 6.8 – Elevation views showing the displaced shape of the interior joist in Building 2 due to dead loads only: max deflection = 0.5 inches.

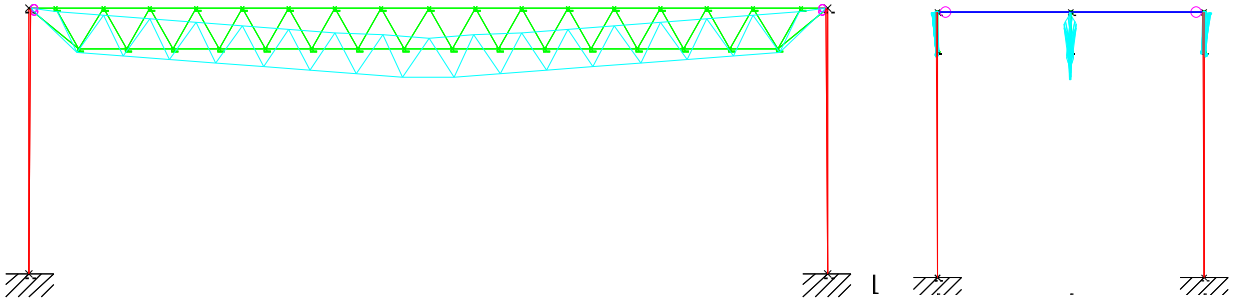

Figure 6.9 – Elevation views showing the displaced shape of the interior joist in Building 2 due to dead loads and the maximum pushdown displacement: max deflection = 13.5 inches.

6.4.3 Maximum Stresses and Strains in Joist

For upper and lower chord elements, stresses and strains are measured at the fiber in the outermost corner of the section (Fiber 1 in Figure 6.12 and Figure 6.13). For the interior web members and exterior rod web elements (elements at outermost ends of joists), maximum stresses and strains are measured at the outermost fibers of the circular cross-sections. The stress and strain responses are symmetric in those members. Throughout the analysis, the maximum stresses and strains in the lower chord occur in Element 85, the middlemost member (this

element is labeled in Figure 6.2). Figure 6.10 shows the stress in the fiber at the outmost corner of the lower chord along joist length for 11 displacement increments. Displacements 0.05 and 0.5 inches are the result of dead load only. As seen in the graph, the maximum stresses occur in the middle element for every increment step. Stresses are measured at the midspan location of each upper or lower chord segment. Since the lower chord is shorter than the upper chord of the joist, Figure 6.10 shows stresses along the length of the lower chord, from 3 ft. to 27 ft. along the total joist span.

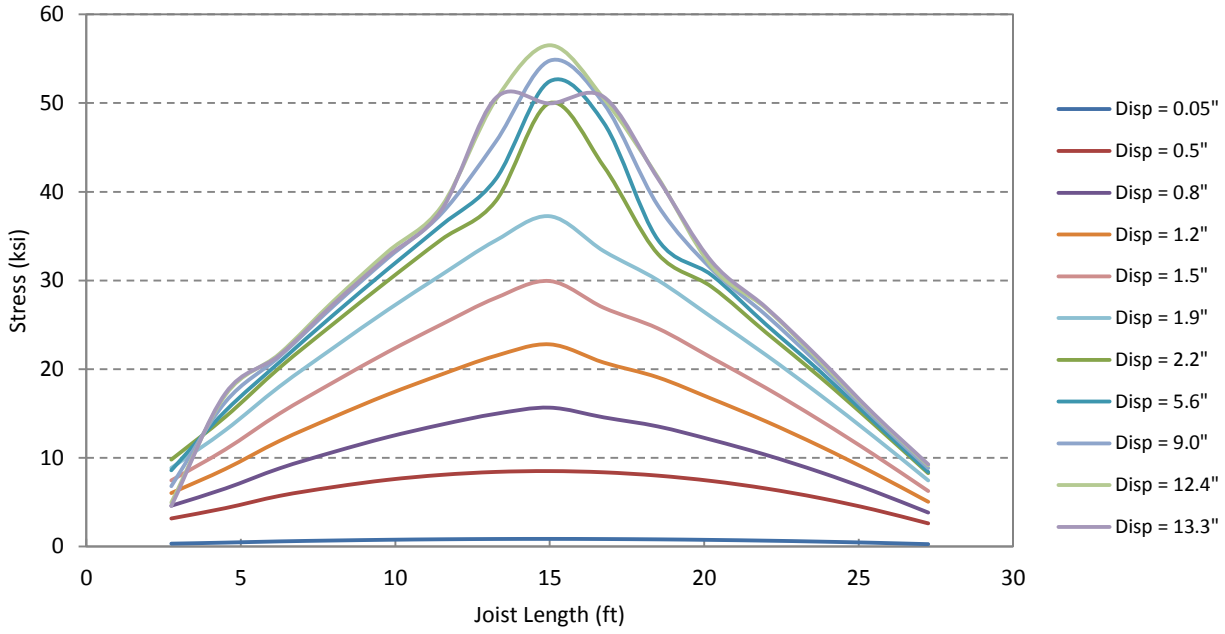

Figure 6.10 – Maximum stresses in each lower chord element along the length of the joist.

For the top chord of the joist, the maximum stresses and strains occur in Element 36 before the displacement reaches 13.3 inches; after which, they occur in Element 35 (see Figure 6.2 and Figure 6.11). Elements 35 and 36 meet in the middle of the chord and, due to symmetry, have essentially the same loading condition. Figure 6.11 shows the stress in the fiber at the outmost corner of the upper chord as function along joist length for 11 displacement increments.

The maximum stresses and strains in the web members occur in Elements 158 and 159 (see Figure 6.2) throughout the analysis.

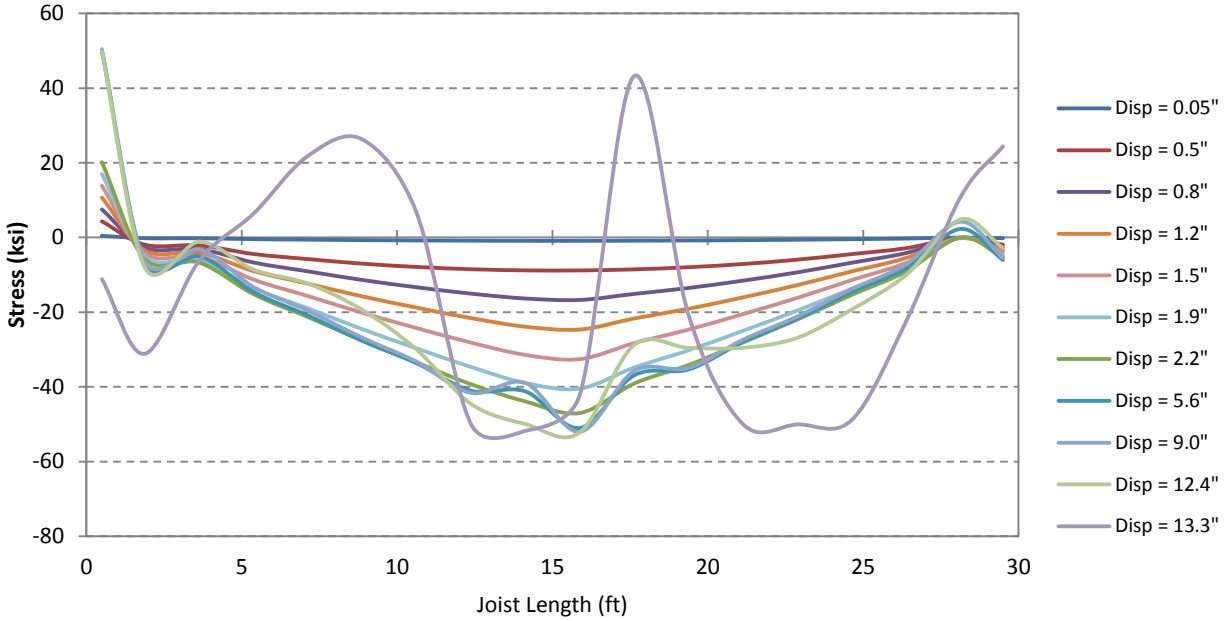

Figure 6.11 – Maximum stresses in each upper chord element along length of the joist.

6.4.4 Sequence of Failures

Since the maximum stresses occur in Element 85 of the bottom chord throughout the pushdown, the stresses in the cross-section are analyzed to determine local elemental response as snow loads increase. Maximum stresses are determined at each fiber location (Points 1 – 13 in Figure 6.12). Recall that the bottom chord cross-section consists of two angles; since the cross section is symmetric and loads are applied along the centroid of the section, only the right angle is analyzed. Although analysis was not performed on the left angle, it most likely has the same stress distribution as the right angle, considering that the joist is symmetric about its cross-section and is loaded symmetrically.

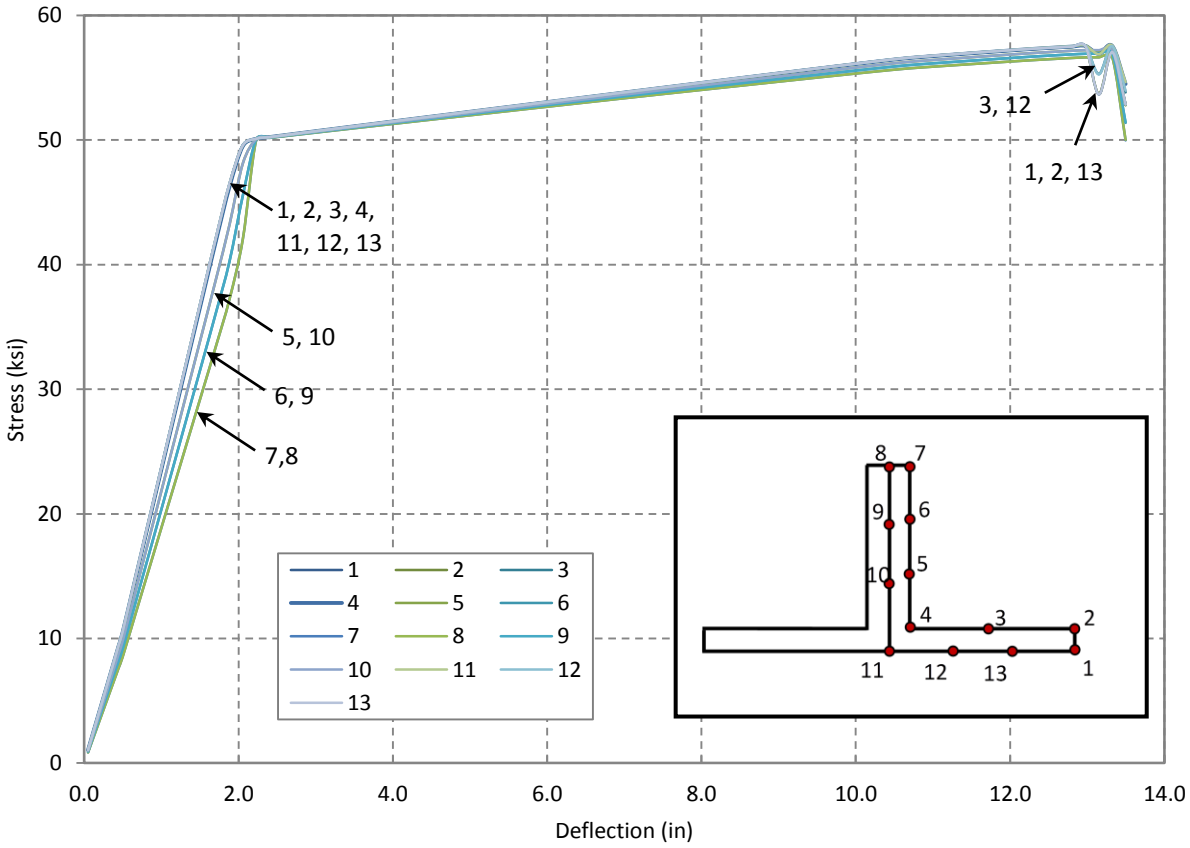

Figure 6.12 – Maximum stresses at points along the cross-section of the lower chord in Building 2.

As shown in Figure 6.12, the cross-section undergoes fairly linear behavior until the section bottommost fibers of the lower chord yield at around 2.1 inches. If the joist was simply modeled with truss elements, the bottom chord would be in tension and the stresses would be the same in the entire cross-section. However, it can be seen that the lower portion of the double angle (Fibers 1, 2, 3, 4, 11, 12, and 13) undergoes a higher stress than the upper portion of the double angle (Fibers 7 and 8) at the same value of induced deflection. For example, when induced deflections are 2.0 inches, the stress in Fibers 7 and 8 is 40 ksi and the stress in Fibers 1, 2, 3, 4, 11, 12, and 13 is 49 ksi. Therefore, the lower portion of the double angle yields before the upper portion because the bottom chord is in tension and, in addition, it is bending under its own self weight, increasing the tension in the bottom fiber of the bottom chord. The full section

yields in tension at a deflection of a little over 2.1 inches. The bottom chord undergoes significant in-plane deformations between induced deflections of 2.1 inches and 13 inches, and the section continues to yield and undergoes strain hardening throughout the remainder of the pushdown. From Figure 6.12, the stress in Fibers 1, 2, and 13 decreases from 57.5 ksi to 53.7 ksi when the joist deflection is 13.2 inches, and the stress in Points 3 and 12 decreases from 57.5 ksi to 55.3 ksi. Most likely, the steel reaches its fully plasticized strength at this point.

For the upper chord, a stress analysis over the cross-section of Element 36 is performed to determine if and when local buckling occurs. Although maximum stresses also occur in Element 35 in the top chord, due to symmetry, this discussion focuses on Element 36. For Element 36, maximum stresses are determined at each fiber location the same way as discussed above for the bottom chord (Points 1 – 13 in Figure 6.13). As shown this figure, the cross-section undergoes fairly linear behavior until the section yields at a joist deflection of 2.1 inches. Since the stress values are negative, the section is in compression, due to the overall configuration of the joist truss such that Element 36 is a top chord element.

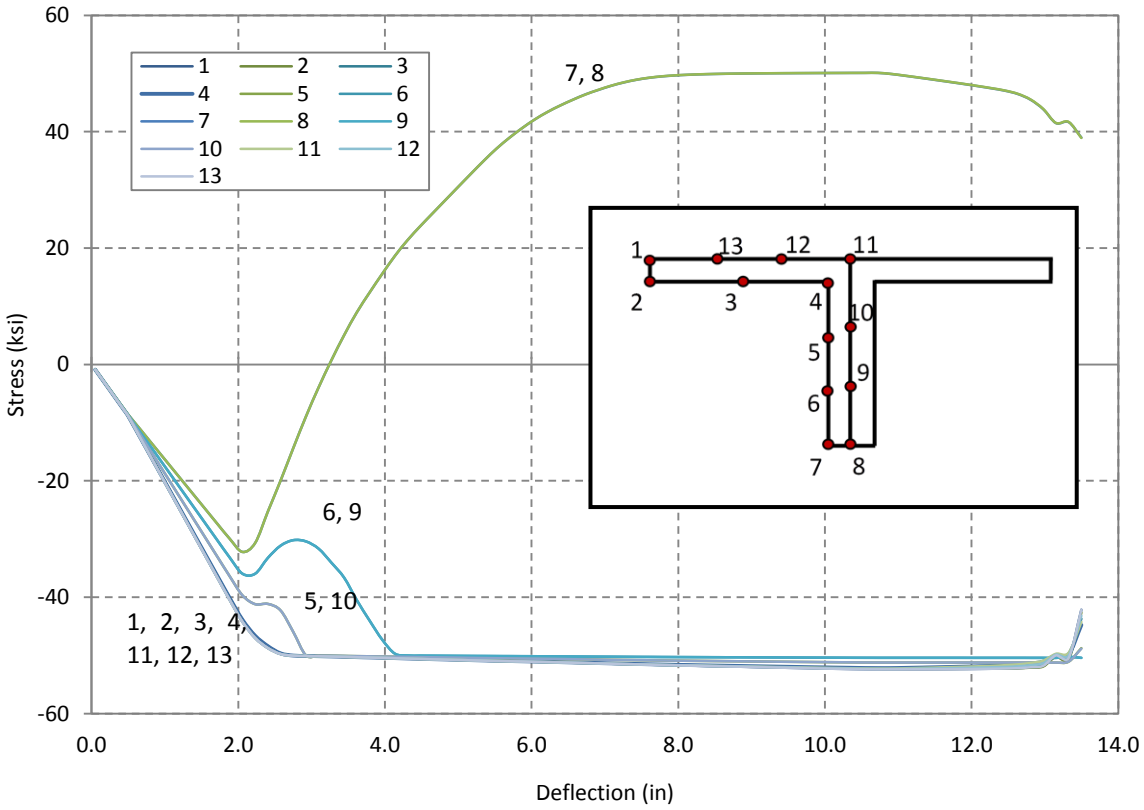

Figure 6.13 – Maximum stresses at points along the cross-section of the upper chord in Building 2.

The upper portion of the double angle (Fibers 1, 2, 3, 4, 11, 12, and 13) undergoes a higher stress than the lower portion of the double angle (Fibers 7 and 8) at the same value of induced deflection due to the fact that the upper chord is supporting its own self weight, increasing the compression in the top fibers induced by the overall joist configuration. For example, when induced deflections are 2.0 inches, the stress in Points 7 and 8 (bottom of section) is 32 ksi and the stress in Fibers 1, 2, 3, 4, 11, 12, and 13 is 43 ksi (top of section). At 2.1 inches, the stress in Fibers 7 and 8 begins to decrease and at 3.3 inches, the stress reaches zero and transitions from tension to compression, continuing to increase. This phenomenon can be attributed to the fact that, as the joist deflects, the bottom chord yields and becomes less stiff, causing the neutral axis of the entire joist section to move up. At an induced deflection of 3.3 inches, the stiffness in the bottom chord has decreased so much that it causes the neutral axis of

the section to enter into the top chord. From this point onward, fibers in the upper chord begin to change from compression to tension from the bottom of the section (Fibers 7 and 8) upward. However, as shown by in Figure 6.13, since the stresses in Fibers 6 and 9 remain negative from 3.3 inches onward, the neutral axis of the section lies somewhere between Points 6 and 9 and Points 7 and 8. Strain hardening takes place in the compressive fibers of the section after 2.7 inches and in the tensile fibers of the section after 8 inches. When the induced deflection reaches 13.5 inches, the stresses at Points 1, 2, 3, 12, and 13 decreases from approximately -50.4 ksi to -42.6 ksi. As mentioned above for the bottom chord, the strains of the fibers in the cross-section reveal no dramatic change during the analysis. It can be hypothesized that the extreme compression and extreme tension fibers begin to lose their strength at this point, perhaps due to some form of buckling.

The top and bottom chords both reach their yield capacity, while the interior web members do not. Throughout the analysis, stresses remain fairly constant in the interior web members. It is not until around a 9-inch deflection of the joist that the stresses in the middle interior web members increase. Up to this point, the stresses are the highest in web elements closest to the ends of the joists.

6.4.5 Out-of-Plane Behavior

At different stages of displacement loading, the top and bottom chords of the joists deflect somewhat out-of-plane, as shown below in Figure 6.14. These increments are very small, and are in order of magnitude of one-hundredth of an inch. The stresses shown in Figure 6.14 are the measured at the outermost corners of the top and bottom chords; they are not the average stresses of the cross-section. Therefore, between 5 and 11 feet and 17 and 19 feet along the length of the joist (Figure 6.14), the outermost corners of the top and bottom chords are in

tension, most likely due to the combination of slight out-of-plane movement and bending under joist self weight.

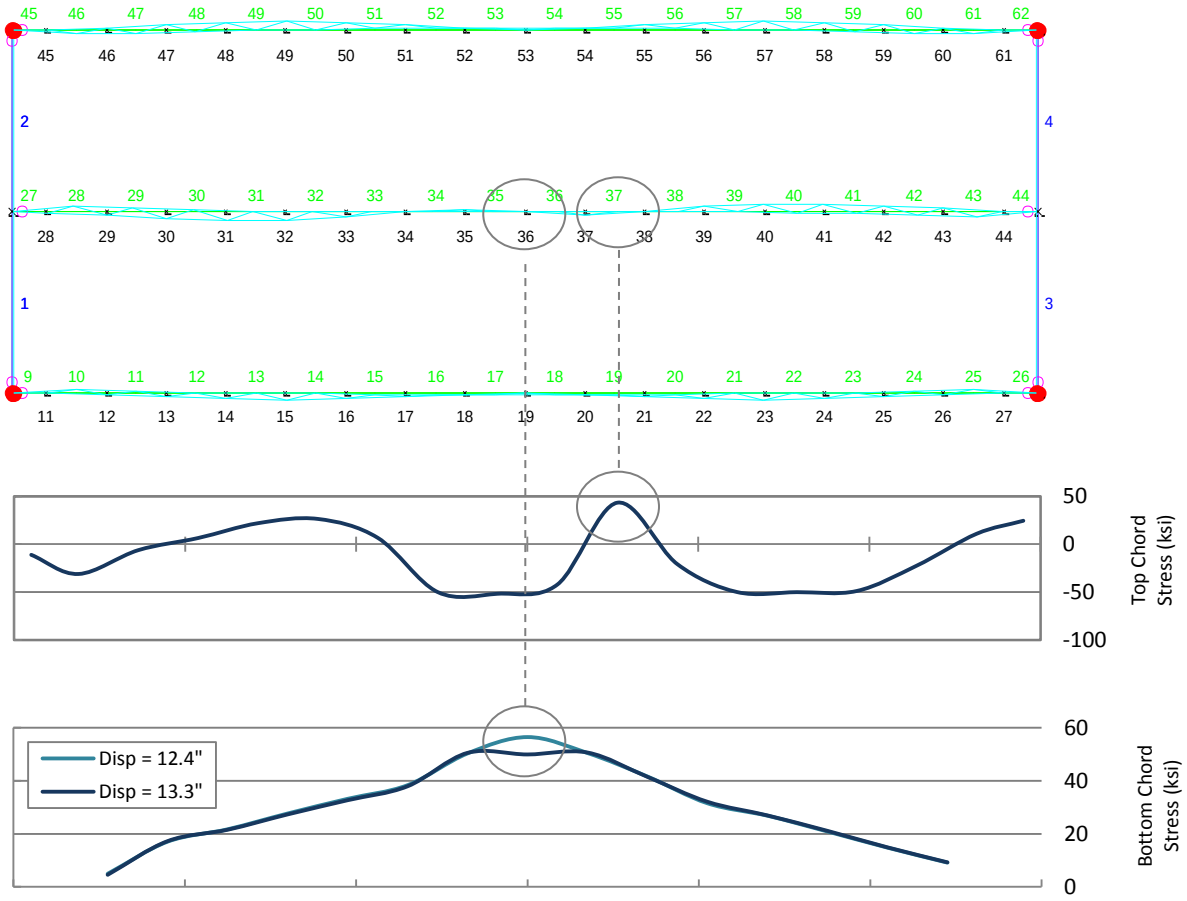

Figure 6.14 – Plan view showing the displaced shape and stress in the top and bottom chords when loaded to maximum deflections.

The top and bottom chords do not deflect much in the out of plane direction until displacements reach about 8 inches, as shown in Figure 6.15. At this point, the bottom chord begins displacing out-of-plane. The bottom chord continues to displace to about -0.011 inches at the last time step, while the top chord displaces to about -0.0005 inches. These out-of-plane deflections are very small in magnitude (one-hundredth of an inch) and, in all reality, are not significant due to the reasons discussed above. The joists are not expected to displace laterally

very much given that the dead loads and pushdown for the snow loads was directed along the in-plane axis.

Although lateral restraints are not directly incorporated into the building models, the sinusoidal behavior of the out-of-plane displacements in Figure 6.14 seem to indicate some type of lateral restraint at mid-span. One possible explanation for this behavior is the application of the imposed displacement. The displacement was imposed on the joist at mid-span, which may cause an indirect out-of-plane constraint during the pushdown analysis. Instead of allowing the joist to move freely out-of-plane, the mid-point of the joist is constrained to the reference location so that the incremental displacement can be imposed at that point. To prevent this behavior in future work, and to analyze future out of plane behavior of the structure, these nodes should be offset by extremely small out-of-plane displacements.

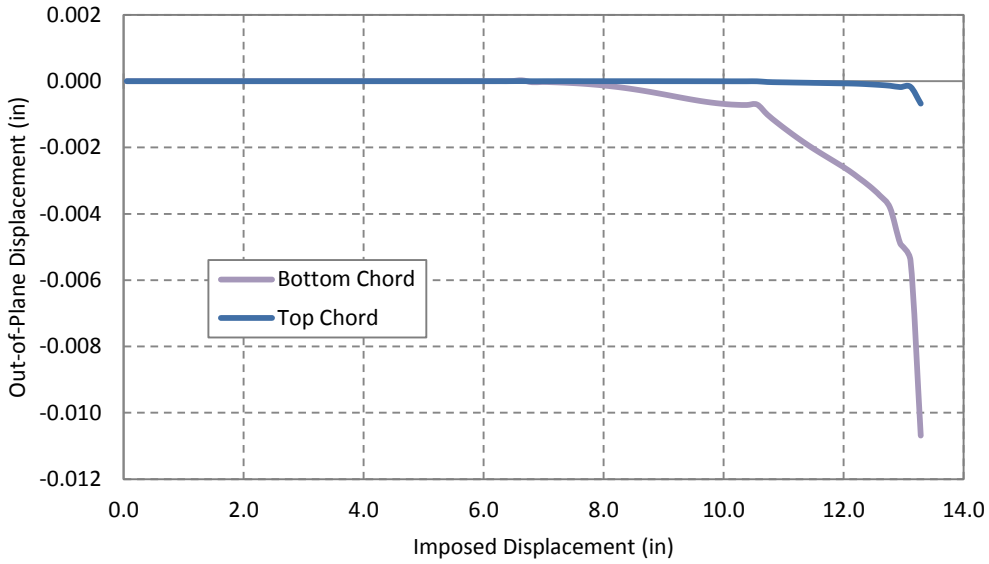

Figure 6.15 – Out-of-plane displacements at the middle of the upper and lower chords at induced displacements.

6.4.6 Probabilistic Analysis

In order to determine the frequency of occurrence of roof snow loads on our building set, previously developed Monte Carlo simulations by Jackson (2010) are used for given ground snow loads. The Monte Carlo simulations in this study generate 10,000 realizations for the probability distributions of given design ground snow loads. For a ground snow load of 10.0 psf, for example, the probability of the occurrence of a certain value of roof snow load is represented by the histogram below (Figure 6.16). Roof snow loads are based on the ground snow load and other factors shown to affect the amount of snow that will accumulate on roof, including exposure, thermal, and slope. For a given ground snow load, there is a level of uncertainty associated with the conversion to roof snow load, based on the uncertainty involved in the exposure, thermal, and slope factors. At any given time, the roof snow load may be greater than or less than expected due to these inherent uncertainties. Monte Carlo simulations allow us to quantify the uncertainty associated with the variability in roof snow loads that may be present on building roofs (Jackson 2010). The roof snow load values used in design are usually greater than roof snow load values obtained through probabilistic methods since prescriptive procedures conservatively estimate roof snow loads based on average ground snow load conversions and factors and do not take into account the uncertainties involved. Once the uncertainties are quantified and measured in probabilistic assessments, the roof snow loads are altered to values generally smaller than those of prescriptive design procedures.

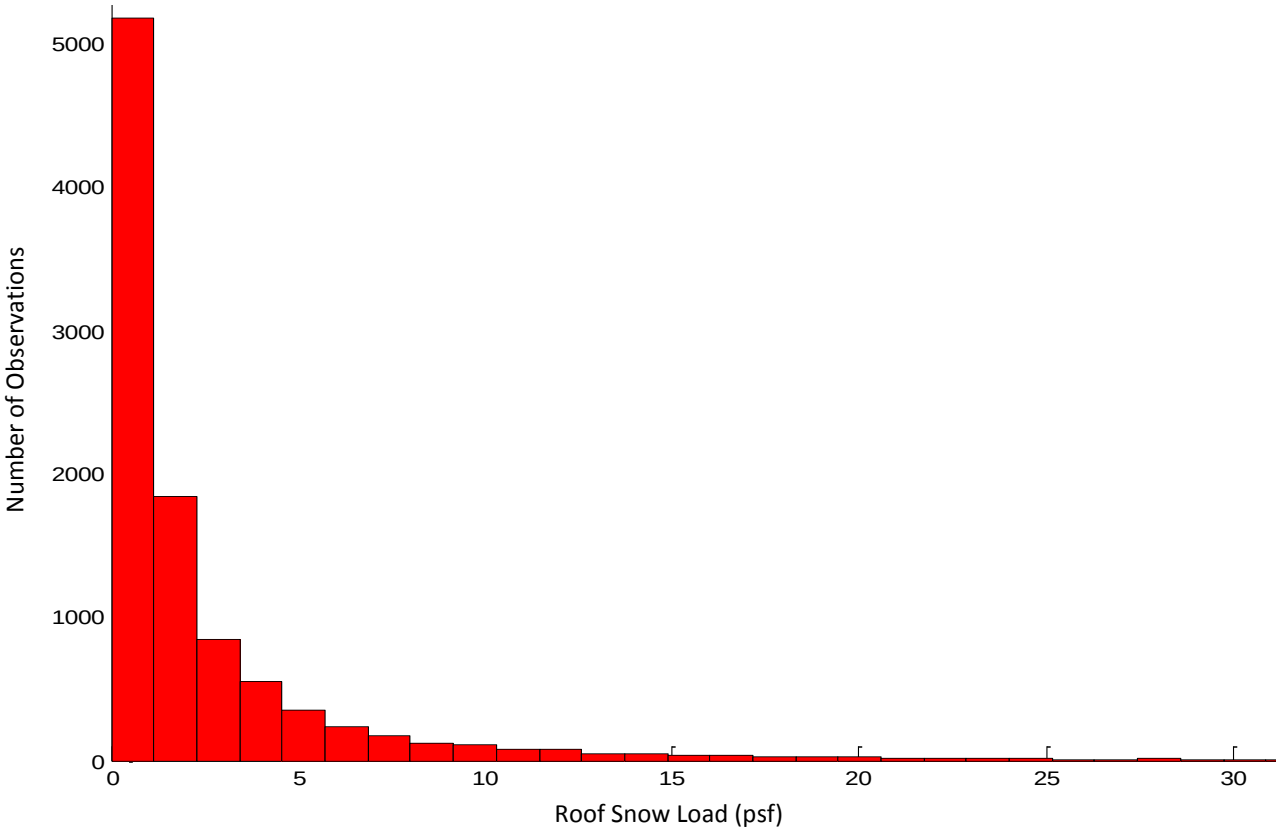

Figure 6.16 – Histogram of the likelihood of roof snow load, given a ground snow load of 10 psf.

In order to determine for our buildings how structural response varies with ground snow loads, ten different values of ground snow loads are considered and shown in Table 6.1. Each of the ground snow loads are inputted into the Monte Carlo simulations to generate 10,000 realizations of the roof snow load, which represent the uncertainty in roof snow loading for a particular ground snow load. For the Monte Carlo simulations, the building is assumed to be fully-exposed with typical insulation and a flat roof. Therefore, the exposure factor C_e is 1.0, the temperature factor C_t is 1.0, the slope factor is C_s is 1.0, and the importance factor is 1.0. The mean roof snow loads for the different ground snow load values are also shown in Table 6.1, and compared to the roof snow load used in design for a building with the same exposure and other parameters.

Table 6.1 – Predicted roof snow loads and deflections, which incorporate the variability of roof snow loads that may be present on building roofs, based on given ground snow loads.

GSL (psf)	RSL_{design} (psf)	mean RSL (psf)	mean Deflection (in.)
10	6.3	3.89	0.639
20	12.6	5.63	0.703
30	18.9	7.07	0.756
40	25.2	9.00	0.828
50	31.5	11.7	0.929
60	37.8	13.9	1.009
70	44.1	15.4	1.066
85	53.6	18.7	1.186
100	63.0	20.2	1.243
120	75.6	22.6	1.331

For each value of ground snow load, ten different roof snow loads are applied to Building 2 and the response (maximum displacement) is recorded. Since each roof snow load has a different likelihood of occurring (i.e. lower roof snow loads are likely to occur more frequently than higher roof snow loads), each roof snow load is weighted according to the Monte Carlo simulations histogram to compute the average maximum roof deflection for a particular ground snow load value (Figure 6.17 and Figure 6.18), accounting for the uncertainty in the roof snow load values (Jackson 2010). These deflections are reported in Table 6.1. In Figure 6.18, the data points represent individual load realizations of roof deflection, while the solid line represents the weighted average of roof deflections for given ground snow loads. The results are expected: as ground snow loads increase, maximum mean deflections increase.

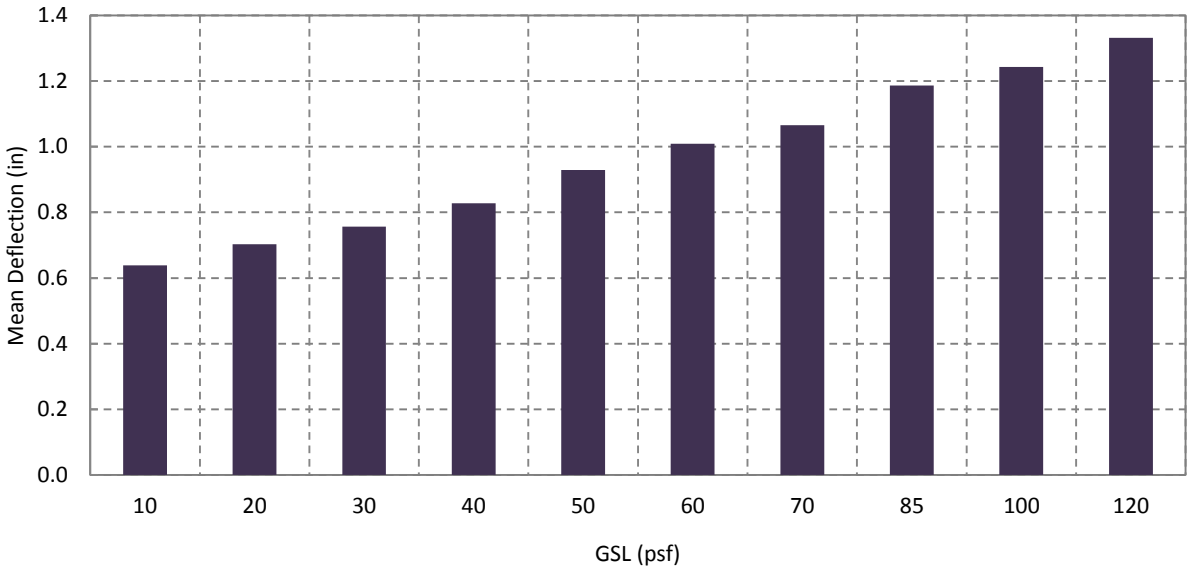

Figure 6.17 – Design ground snow load versus the mean deflection for Building 2.

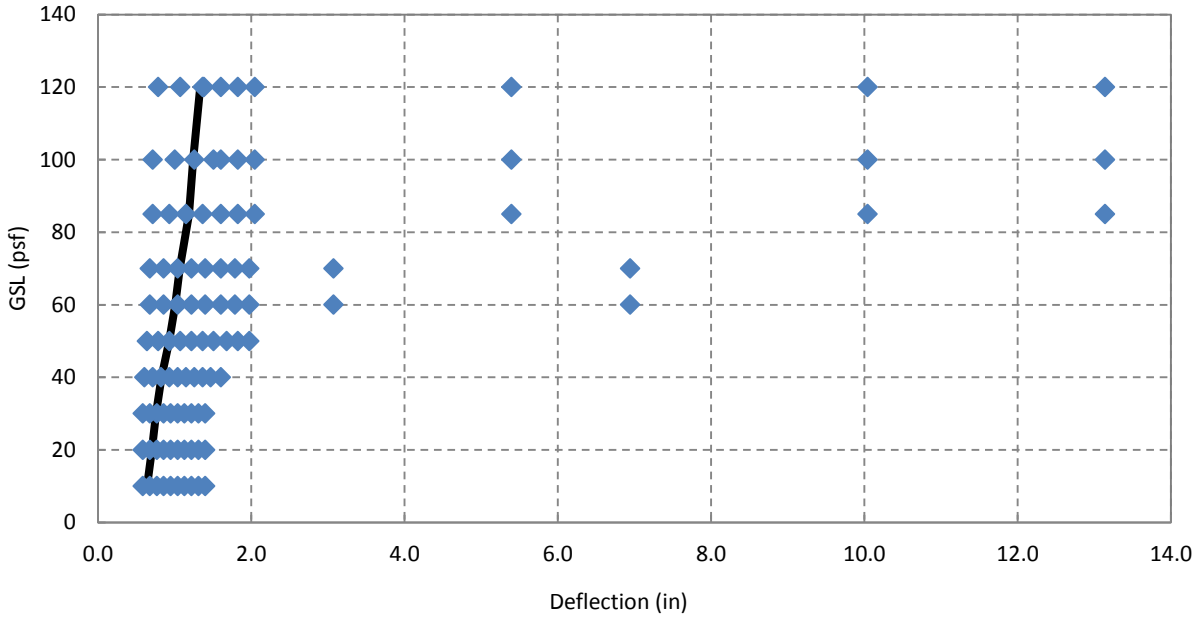

Figure 6.18 – Predicted maximum roof deflection as a function of ground snow load for Building 2.

The results of the probabilistic analysis are important because they use performance-based techniques to specifically take into account the levels of uncertainty associated with the building characteristics (thermal, slope, and exposure factors) and the uncertainty associated with the variability in roof snow loads that may be present on building roofs. The probabilistic and deflection-controlled methods exhibit the same general trends for expected deflections, based on ground snow loads. With larger ground snow loads, deflections in the buildings are expected to increase. Joist deflections are much smaller in the probabilistic methods than in the pushdown methods for any particular value of roof snow load. The Monte Carlo simulation in this chapter serves as an important example of how probabilistic design methods can be implemented in the design of buildings to resist snow.

6.5 Conclusions

All buildings included in this analysis are able to resist about twice as much snow load than their design snow load capacity, which implies that there is built-in safety when considering snow overload due to extreme or unanticipated snow events, such as rain-on-snow or drifted snow. Buildings with lighter structural roof systems yield at lower levels of roof snow loads, while buildings with heavier structural roof systems yield at higher levels. All exhibit the same type of response trend, with an elastic linear response up to the point of yielding, and an inelastic strain hardening response after the point of yielding. Generally, buildings with smaller dead-to-snow load ratios are shown to be less resilient toward snow overloading than buildings with larger dead-to-snow load ratios. However, in this study, buildings show similar ratios of yield-to-design roof snow load (normalized measure of building strength) except buildings that are overdesigned or have joists with high stiffnesses.

The results of the deflection-controlled static pushover analysis for Building 2 give a general sense of the types of failure exhibited by lightweight metal buildings with open-web steel joists with overloaded with snow. When subjected to incremental deflections at mid-span, the top and bottom chords of open-web steel joists are most likely to yield first in tension and compression, respectively. Once both chords yield, the joists undergo strain hardening and increased deformations. As the bottom chord of the joist looses stiffness, the bottom fibers in the top chord change from compression to tension, signifying movement of the neutral axis of the section into the top chord. Although the cause of failure is not clear through strain analyses, rupture is a likely cause of failure. No significant out-of-plane behavior occurs, as all loads are applied in the direction of gravity. From a probabilistic standpoint, average maximum deflections are expected to increase as ground snow load increase. We determined the mean average roof snow load value that was expected for the design ground snow load of Building 2 (45 psf), given the likelihood of occurrence and uncertainty associated with different values of roof snow load for one particular ground snow load value. For the design ground snow load of Building 2, the average maximum roof deflection is expected to be 0.878 inches.

Chapter 7

Conclusions and Implications

7.1 Summary

This research sought to quantify the risks associated with snow-induced damage and collapse in order to better understand the implications on life safety, building downtime, and economic losses. In order to accomplish this goal, the effects and consequences of snow-induced building failure were quantified by means of probabilistic analyses using nonlinear simulation models. First, in Chapter 3, national and worldwide building failure trends were investigated in order to identify key failure modes and building types that experienced snow-induced damage or failure. Then, in Chapters 4, 5, and 6, nonlinear structural models were developed to determine the design factors that contribute to the susceptibility of lightweight metal buildings with open-web steel joists to snow-induced failure. In particular, the behavior, performance, and potential vulnerability of these types of buildings with different design snow to dead load ratios to snow overloading were investigated. The following section describes the building failure trends and results of the nonlinear building simulation models to snow loading.

In Chapter 3, national and worldwide building failure trends were quantified using content analysis of newspaper articles in order to identify key failure modes and building types that underwent snow-induced damage or failure. The U.S. data included incidents from 1989—2009, while the international data included incidents from 1979—2009.

In terms of the number of snow-induced building damage or failure incidents observed in the database, 1,029 national and 91 international building failures revealed categories of industrial, government and public, retail and commercial, and minor structures such as garages that experienced the greatest number of incident classifications. In terms of construction type, metal/steel, timber, and masonry buildings were particularly susceptible in the U.S., while metal/steel and concrete buildings showed up most frequently in the international database. The impacts of these failures have included casualties, business interruptions, and repair costs. The high number of incidents reported for new buildings in both the U.S. and international data sets indicates that a risk of snow-related failure can occur even in modern buildings designed according to current codes. The data also shows that snow-related building incidents increase with increased snowfall. Besides the amount of snow being reported as the main cause of incidents, rain-on-snow mixes and building problems were commonly attributed as causes in the U.S. and building problems and melting snow were commonly reported as causes internationally.

In the United States, New York, New Hampshire, and Massachusetts had the highest number of snow-related building failure incidents; if the number of incidents in each state was normalized by population and building stock, New Hampshire, Maine, and North Dakota were identified as the most susceptible to building-related snow incidents. On average, more than one out of 3.0 million buildings nationwide suffered a snow-failure collapse each year. The collapse

rate of non-residential buildings was much higher than that of residential buildings in the U.S., with at least one out of 145,000 non-residential buildings suffering collapse each year.

In Chapter 4, case studies of structural building collapses were investigated, focusing in particular on lightweight metal buildings. These collapses revealed design and construction errors as the most common causes of failure. For example, joists were mistakenly attached to the outer unreinforced masonry wall at the bottom chords in one case study building. Since no attachment was required in the design, significant overturning moments took place at the wall connections, which led to instability and ultimate collapse of the masonry wall and dependent joists. In another case, open-web steel joists with lower design capacities were mistakenly installed in the place of ones with higher design capacities, leading to severe overloading and failure of the joists under drifted snow.

Site visits to seven different lightweight metal buildings with open-web steel joist roof systems revealed critical design characteristics that provided the basis for further analysis. In particular these open-web steel joist roof systems typically consist of wide-flange girders or joist girders, exterior masonry walls, and 6- or 8-inch round or square HSS interior columns. Roof height varied from 25 to 35 feet, and joist spacing varied between three and six-foot intervals, while joist depth varied between 14 and 20 inches. The open-web steel joists in the buildings were designed in different truss arrangements and were composed of combinations of rods, angles, and double angles. Rods and single angles were more commonly used in joists the older buildings, while single and double angles were more commonly used in joists in the newer buildings.

Chapters 5 and 6 centered on the analysis of open-web steel joist roof systems, which may be particularly vulnerable to snow-related failures. Seventy-one archetypical lightweight metal buildings were identified, each with different design characteristics that may have an influence on structural response. These characteristics included building geometry, structural type, and design roof snow loads. Nonlinear simulation models for the first seven archetypical buildings were developed and subjected to pushdown analyses under uniform snow loads. The joists in these buildings were constructed and designed for roof snow load values of 20, 28.4, 37.8, 47.3, 56.7, and 75.6 psf (corresponding to ground snow loads of 31.7, 45, 60, 75, 90, and 120 psf) based upon strength and serviceability requirements of modern code provisions. For simplicity, simple one-by-one bays were analyzed for snow loads, rather than the full-scale buildings. By means of static pushdown analyses, joists in all six buildings were imposed with a specified deflection at mid-span in order to study building response. An in-depth analysis into the behavior of one building to snow loading was selected to provide insight into structural response and failure modes of lightweight metal buildings with open-web steel joists.

In Chapter 7, the buildings responded to snow loads as expected. All exhibited the same type of response trend, with an elastic linear response up to the point of yielding, and an inelastic strain hardening response after the point of yielding. Buildings with lighter structural roof systems yielded at lower levels of roof snow loads, while buildings with heavier structural roof systems yielded at higher levels. Buildings designed for roof snow loads of 20 and 28.4 psf yielded at roof snow loads of 52 psf, while buildings designed for roof snow loads of 37.8, 47.3, 56.7, and 75.6 psf yielded at roof snow load values of 67, 83, 121, and 142 psf, respectively. In all cases, the buildings began to fail at roof snow loads about twice the design roof snow load, corresponding to an approximate overstrength of a factor of 2.0. As far as vulnerability is

concerned, lighter buildings did not prove to be more vulnerable than heavier buildings, although there was a slight trend. Strength-to-design load ratios indicate that the buildings have, at the minimum, an overstrength factor of 1.8. In other words, the buildings can carry 80% greater roof snow loads than their design roof snow load capacities indicate. There did not seem to be a trend between lighter or heavier buildings with regard to overstrength. Building 1 has a strength-to-design load ratio of 2.8, while the other buildings have strength-to-design load ratios of about 2.0.

Through a deflection-controlled static pushover analysis, one building was analyzed with increasing incremental deflections at mid-span until the interior joist's maximum deflection of 13.3 inches was achieved. Tensile yielding occurred in the bottom chord and compressive yielding occurred in the top chord of the joist at a deflection of 2.1 inches. As the bottom chord of the joist lost stiffness, the bottom fibers in the top chord changed from compression to tension, signifying movement of the neutral axis of the section into the top chord. Both the top and bottom chord underwent major in-plane yielding until a deflection of 13.3 inches. At that point, the top and chord chords lost strength in their extreme fibers. Although the cause of failure was not clear through strain analyses, it is likely that the steel reached its full plastic strength. No significant out-of-plane behavior occurred, as all loads were applied in the direction of gravity.

A probabilistic assessment was performed on one building to determine the frequency of occurrence of roof snow loads on that building. Since each roof snow load had a different likelihood of occurring, roof snow loads were weighted according to the Monte Carlo simulations to compute average maximum roof deflections for particular ground snow load values. For given ground snow load values, the maximum roof deflection was predicted. The

results were as expected: as ground snow loads increased, maximum mean deflections increased, as shown in Chapter 7.

7.2 Implications

This study attempts to enhance our understanding of snow-related failure and damage trends, particularly structural design issues that may contribute to snow-induced building failures. The data gathered here indicates that buildings may be at risk of failure due to large snow loads, and that this susceptibility is particularly apparent in certain types of building construction, as well as those structures that are poorly maintained or designed. The susceptibility associated with different building systems disproportionately impacts economic and social activities that tend to concentrate in these buildings, for example retail and industrial activities in metal or steel buildings. These observations lead to a variety of possible risk mitigation strategies. Building owners, especially those with high-value structures, contents, or those sensitive to business closure, may be able to use data on the impacts of failures to value preventative maintenance. Quantitative differences in risk associated with different types of building construction motivates further examination of the consistency of reliability provided by current building code snow load provisions. In addition, the large number of failures attributed to rain-on-snow may also indicate the need for more carefully considering this phenomenon in design procedures.

Results from nonlinear static pushover analyses show that the open-web steel joist roof systems yield when loaded with roof snow loads of about double their design roof snow load capacities. This overload capacity implies that there is a built-in level of safety when considering snow overload due to extreme or unanticipated snow events, such as rain-on-snow. With regard to susceptibility, the data gathered in this study does not conclusively indicate that

these types of buildings are more susceptible to failure when overloaded with snow compared to other types of buildings. However, it does indicate a slight downward trend between the buildings with larger and smaller dead-to-snow load ratios. The buildings with larger dead-to-design roof snow loads may offer more resistance to snow overloading than buildings with smaller ones. Investigations into case studies have revealed a likelihood of snow-induced failure when lightweight metal buildings are poorly maintained or designed, however, no conclusions can be drawn because the buildings in this study were not modeled with design imperfections. Advancement and development of the building models in this study will lead to a broad and representative set of models aimed with the intention of furthering our understanding of open-web steel joist roof systems.

7.3 Limitations and Future Research

Although the building models developed in this research gave a general sense of how lightweight metal buildings with open-web steel joist roof systems respond to snow overloading, they lacked important characteristics from a design perspective. For instance, the building models were not designed for lateral loads. Subjecting the buildings to gravity and snow loads only is unrealistic and does not capture the true nature of these types of structural systems. It limits the design and excludes possibly important behavior and interactions between the gravitational and lateral structural systems. In addition, lightweight metal buildings are required to resist unbalanced snow, drifting effects, and wind and seismic forces in practice. The models in this study lacked horizontal bridging and extra joists along the perimeter where drifting could occur. Since drift loads were also not applied in the analysis models, it is not clear what the impacts of this limitation might be. Another design deficiency was the application of connections in the building models, which were modeled by inelastic springs. Springs may not be truly

representative of real connections because they might not effectively capture their true behavior with regard to the adequate transferring of forces and moments to the columns. The spring stiffness specified in this study may not provide the exact resistance found in practice for the transfer of forces and moments. The last significant design deficiency is the out-of-plane restrictions of the joists in the models. The joists were imposed with initial deflections at midspan in the direction of gravity, which indirectly caused out-of-plane constraints at those points during the pushdown analysis. To prevent this, an extremely small out-of-plane displacement should be imposed at the midspan nodes such that lateral buckling could be observed. Future research should adapt building models to account for drifted snow, lateral loads, indirect out-of-plane constraints, and adequate connections, as these are critical in building design.

From a modeling perspective, one main deficiency exists in this research: the proprietary nature of the open-web steel joist industry. Information about the specific structural make-up of joists, including element type, size, geometry, etc., is not publicly available, which served as a challenge when designing joists for the building models. Software programs for joist design are owned by the joist manufacturing industry. Design professionals can use other programs, such as SAP2000 and RISA, to design buildings with open-web steel joists. However, these programs fail to account for localized failure criteria exhibited by these types of buildings, such as yielding and buckling. Although the joists in these building models were designed to meet strength and serviceability requirements of modern code provisions, they may not be completely representative of the geometry, element selection, etc. as those used by joist manufacturers. Therefore, future collaboration with joist manufacturers is recommended to address this deficiency.

For future research, the remainder of the archetypical building matrix should be analyzed after the modeling and design deficiencies previously mentioned are addressed. Pushdown analyses should be performed to determine the buildings' yield capacities. After the value of design roof snow load for which the building yields is determined, the sources of failure should be investigated to determine if local buckling occurred. After all analyses are completed, building response should be compared for the building set to categorize the vulnerability of these types of buildings to extreme snow loads. Lastly, probabilistic assessments should be continued to assess the risks of these types of buildings to snow-induced failure, integrating these types of structural analyses with a hazard analysis of how likely different roof snow loads are to occur.

Notation List

ASCE	American Society of Civil Engineers
ASD	allowable strength design
C_e	exposure factor
C_s	slope factor
C_t	thermal factor
D	dead load due to the weight of the structural elements and the permanent features of the structure
E	modulus of elasticity of steel (Chapter 6)
h_b	height of balanced snow load determined by dividing p_s by γ
h_c	clear height from top of balanced snow load to (1) closest point on adjacent upper roof, (2) top of parapet, or (3) top of a projection on the roof
h_d	height of snow drift
I	importance factor
I	moment of inertia of joist (Chapter 6)
IBC	International Building Code
l_u	length of the roof upwind of the drift
L	live load due to occupancy and movable equipment
L	length of joist (Chapter 6)

LRFD	load resistance factor design
Lr	roof live load
NWS	National Weather Service
OpenSees	Open System for Earthquake Engineering Simulation
PEER	Pacific Earthquake Engineering Research Center
P	point load (Chapter 6)
p_d	maximum intensity of drift surcharge load
p_f	flat roof snow load (roof slope ≤ 5°)
p_g	ground snow load
p_s	sloped roof snow load
R	load due to initial rainwater or ice exclusive of the ponding contribution
SCS	Soil Classification Service
SJI	Steel Joist Institute
S	snow load
w	drift width
w	scale factor for deflection, shear, and moment (Chapter 6)
W	horizontal distance from ridge to eave of upper sloped roof
γ	snow density

References

[1] AISC. *Steel Construction Manual*. Chicago, IL: American Institute of Steel Construction, Inc., 2005.

[2] ASCE. *Minimum Design Loads for Buildings and Other Structures (ASCE 7-05).* Reston, VA: ASCE Structural Engineering Institute, 2005.

[3] Associated Press. "Mounds of Snow in Durango Raise Roof Collapse Concerns." *DenverPost.com* Feb. 5, 2008.

[4] Biegus, A., and K. Rykaluk. "Collapse of Katowice Fair Building." *Engineering Failure Analysis* 16 (2009): 1643-54.

[5] Boon, G. "Truss Design" Model Bridge Design, 2011. <http://www.garrettsbridges.com/design/trussdesign/>.

[6] Burns, N. "Westford Bible Church Hopes to be in New Home by Summer's End." *Lowell Sun* May 24, 2002.

[7] Canam Group Inc. *Joist Catalog*. Point of Rocks, MD: Canam Group, Nov. 2010.

[8] Canam Group Inc. "Open-Web Joists: Using ASD and LRFD to Design Your Project." Jan. 19, 2011. <http://www.canam-steeljoists.ws/www/v4/ecanams.nsf/steeljoists/asd-lrfd?open>.

[9] Cella, M., and J.H. Prince. "Roof Collapses at Toys R Us; Lanham Accident Injures Nine as the Weight of Rain and Snow is Too Much for the Building." *The Washington Times* Feb. 23, 2003: A01.

[10] Clem, W. "Wen Visits Hebei After Disastrous Snowfall; Cloud Seeding May Be to Blame for Chaos." *South China Morning Post* Nov. 13, 2009: 7.

[11] Comerio, M.C. "Estimating Downtime in Loss Modeling." *Earthquake Spectra* 22.2 (2006): 349-65.

[12] CSi. SAP2000; 2011. < http://www.csiberkeley.com/sap2000>.

[13] deFiebre, C., and K. Duchschere. "Warehouse and Traffic Succumb to the Snow." *Star Tribune* Dec. 6, 1991: 1B.

[14] DeGaetano, A.T., T.W. Schmidlin, and D.S. Wilks. “Evaluation of East Coast Snow Loads Following January 1996 Storms.” *Journal of Performance of Construction Facilities* 11.2 (1997): 90-4.

[15] DeGaetano. A.T., and D.S. Wilks. “Mitigating Snow-Induced Roof Collapses Using Climate Data and Weather Forecasts.” *Meteorological Applications* 6 (1999): 301-12.

[16] Eldukair, Z.A., and B.M. Ayyub. “Analysis of Recent U.S. Structural and Construction Failures.” *Journal of Performance of Constructed Facilities* 5.1 (1991): 56-73.

[17] Ellingwood, B.R., and P.B. Tekie. “Wind Load Statistics for Probability-Based Structural Design.” *Journal of Structural Engineering* 125.4 (1999): 453-63.

[18] *Factiva*. Dow Jones, 2010. <http://factiva.com>.

[19] Fish, M. “Snow’s Burden Reveals Weakness of Roof, Law the Season’s Heavy Snowfall Took Its Toll in Roof Collapses and Pointed to a Gap in Rules Governing the Safety of Public Schools.” *The Post Standard* Mar. 22, 1994: A1.

[20] Fisher, J. M., M. A. West, and J. P. Van De Pas. *Designing with Vulcraft – Steel Joists, Joist Girders, and Steel Deck*. 2nd ed. Milwaukee, WI: Nucor Corp, 2002.

[21] Geis, J., K. Strobel, and A. Liel. “Snow-Induced Building Failures.” *Journal of Performance of Constructed Facilities* (2011), Submitted.

[22] Gustafson, K. “Evaluation of Existing Structures.” *Modern Steel Construction* Feb. 2007, AISC.

[23] Hadipriono, F.C. “Analysis of Events in Recent Structural Failures.” *Journal of Structural Engineering* 111.7 (1985): 1468-81.

[24] Hadipriono, F.C., and C.F. Diaz. ‘‘Trends in Recent Construction and Structural Failures in the United States.’’ *International Journal of Forensic Engineering* 1.4 (1988): 227–32.

[25] Harris, J.R. *Case Studies: Snow-Induced Building Failures*. 9 Feb. 2011. Incident Reports. J.R. Harris & Company, Denver, CO.

[26] Holicky, M. “Safety Design of Lightweight Roofs Exposed to Snow Load.” *Engineering Sciences* 58 (2007): 51-57.

[27] Holicky, M., and M. Sykora. *Failures of Roofs under Snow Load: Causes and Reliability Analysis.* Proc. Fifth Congress on Forensic Engineering, 11-14. Washington D.C: 2009.

[28] Holtermann, T., M. Perry, and P. Green. *Specifying Steel Joists, Joist Girders, and the IBC 2006*. ASCE Conf. Proc., 2390-99. Austin, TX: Apr. 30-May 2, 2009.

[29] International Code Council, Inc. *International Building Code*. Country Club Hills, IL: International Code Council, Inc, 2009.

[30] Jackson, Kyle. "Probabilistic Models for Uniform and Non-Uniform Snow Loading on Roofs," University of Colorado. Dec. 2011. Masters of Engineering Thesis.

[31] Kiser, U. "Roof Collapse Fears Wane as Snow Melts." *Manassa Journal Messenger* Feb. 19, 2010.

[32] Levy, M., and M. Salvadori. *Why Buildings Fall Down: How Structures Fail*. New York: Norton, 2002.

[33] *LexisNexis Academic*. Reed Elsevier Inc., 2010. <http://www.lexisnexis.com/hottopics/lnacademic/>.

[34] Liel, A.B., C.B. Haselton, and G.G. Deierlein, "Seismic Collapse Safety of Reinforced Concrete Buildings: II. Comparative Assessment of Non-Ductile and Ductile Moment Frames," *Journal of Structural Engineering* (2010), In Press.

[35] Macdonald, M., M.A. Heiyantuduwa, and J. Rhodes. "Recent Developments in the Design of Cold-Formed Steel Members." *Thin-Walled Structures* 46 (2008): 1047-53.

[36] Majowiecki, M. "Snow and Wind Experimental Analysis in the Design of Long-Span Sub-Horizontal Structures." *Journal of Wind Engineering and Industrial Applications* 74-6 (1998): 795-807.

[37] Maple Valley Truss Company, Inc. "Truss Types." 2011. <http://www.maplevalleytruss.com/config.htm>.

[38] Management Computer Controls, Inc. "Estimators' Reference." 2010. <http://www.mc2-ice.com/support/estref/popular_conversion_files/steel/bar_joists.htm>.

[39] Manning, S. "Inspector: PG Toys 'R' Us Met Building Codes." *The Associated Press States & Local Wire* Feb. 25, 2003.

[40] Marotta, T.W., and C.A. Herubin. *Basic Construction Materials*. 5th ed. New Jersey: Prentice Hall, 1996.

[41] Martin, R., and N.J. Delatte. "Another Look at Hartford Civic Center Coliseum Collapse." *Journal of Performance of Constructed Facilities* 15.1 (2001): 31-6.

[42] Martinez, J. "Church Roof Collapses After Heavy Snow." *The Boston Herald* Mar. 8, 2001: 002.

[43] The Mathworks, Inc. MATLAB; 2011. < http://www.mathworks.com/products/matlab/description1.html>.

[44] McCormac, J.C. *Structural Steel Design*. 4th ed. New Jersey: Prentice Hall, 2008.

[45] Mehta, M., W. Scarborough, and D. Armpriest. *Building Construction: Principles, Materials, and Systems*. New Jersey: Pearson Prentice Hall, 2008.

[46] Meløysund, V., K.R. Lisø, J. Siem, and K. Apeland. "Increased Snow Loads and Wind Actions on Existing Buildings: Reliability of the Norwegian Building Stock." *Journal of Structural Engineering* 132.11 (2006): 1813-20.

[47] National Research Council of Canada. *National Building Code of Canada.* Ottawa: National Research Council of Canada, 2010.

[48] NESEC. "Winter Storms." The Northeast States Emergency Consortium, 2008. <http://www.nesec.org/hazards/winter_storms.cfm>.

[49] O'Rourke, M. "Snow & Rain Provisions in ASCE 7-10." *Structure* Feb. 2011: 36-40. <http://www.structuremag.org>.

[50] O'Rourke, M. *Snow Loads: Guide to the Snow Load Provisions of ASCE 7-05*. Reston, VA: ASCE, 2007.

[51] O'Rourke, M., and M. Auren. "Snow Loads on Gable Roofs." *Journal of Structural Engineering* 123.12 (1997): 1645-51.

[52] O'Rourke, M., P. Koch, and R. Redfield. *Analysis of Roof Snow Load Case Studies—Uniform Loads*. Hanover, NH: Cold Regions Research & Engineering Laboratory, 1983.

[53] O'Rourke, M., R. Redfield and P. von Bradsky. "Uniform Snow Loads on Structures." *Journal of the Structural Division* 108.ST12 (1982): 2781-2798.

[54] PEER. OpenSees (Open System for Earthquake Engineering Simulation); 2006. <http://opensees.berkeley.edu/>.

[55] PEER. *OpenSeesWiki*. 2006. National Science Foundation. <http://opensees.berkeley.edu/wiki/index.php>.

[56] Project for Excellence in Journalism. *The State of the News Media 2004*. Journalism.org, 2004. <http://www.stateofthemedia.org/2004>.

[57] Rosales, M., and L. Stallones. "Coverage of Motor Vehicle Crashes with Injuries in U.S. Newspapers, 1999-2002." *Journal of Safety Research* 39.5 (2008): 477-82.

[58] Shoemaker, W.L. "MBMA's Contributions to the Metal Building Industry." *Metal Building Manufacturers Association*, 2009 <http://www.mbma.com/>.

[59] Steel Joist Institute. *Standard Specifications—Load Tables and Weight Tables for Steel Joists and Joist Girders*. 42nd ed. Fox River Grove, IL: SJI, 2005 <http://steeljoist.org/free-downloads>.

[60] Steel Joist Institute. "Steel vs. Concrete." 2010 < http://steeljoist.org/>.

[61] Takahashi, T., and B.R. Ellingwood. "Reliability-Based Assessment of Roofs in Japan Subjected to Extreme Snows: Incorporation of Site-Specific Data." *Engineering Structures* 27 (2005): 89-95.

[62] Tang, M., E. Castro, F. Pedroni, A. Brzozowski, and M. Ettourney. "Performance-Based Design with Application to Seismic Hazard." *Structure* June 2008: 20-22. <http://www.structuremag.org>.

[63] Tucker, N., and O. Wiggins. "Screaming Shoppers Race to Escape Collapse; Parents Grab Children, Drop Toys, Flee for Exits as Store's Roof Gives Way." *The Washington Post* Feb. 23, 2003: A23.

[64] United States. Census Bureau. *The 2010 Statistical Abstract*. 17 Dec. 2009. <http://www.census.gov/prod/2009pubs/10statab/construct.pdf>.

[65] United States. Climate Change Science Program. Subcommittee on Global Change Research. *Weather and Climate Extremes in a Changing Climate*. June 2008. <http://downloads.climatescience.gov/sap/sap3-3/sap3-3-final-all.pdf>.

[66] United States. Dept. of Commerce. National Climatic Data Center. *Storm Event Database*. 2009. <http://www4.ncdc.noaa.gov/cgi-win/wwcgi.dll?wwEvent~Storms>.

[67] Wardhana, K., and F.C. Hadipriono. "Study of Recent Building Failures in the United States." *Journal of Performance of Constructed Facilities* 17.3 (2003): 151-58.

[68] Willhoit, D. "Ten Months After Collapse, Westford Church to Rebuild." *Lowell Sun* Jan. 8, 2002.

[69] Winter, S. and H. Kreuzinger. "The Bad Reichenhall Ice-Arena Collapse and the Necessary Consequences for Wide Span Timber Structures." *Engineered Wood Products Association* (June 2008).

Appendix 2

ASCE 7-05: Supplemental Information

Table 2A.1 – Occupancy category of buildings and other structures for flood, wind, snow, earthquake, and ice loads (ASCE 7-05 2005).

Nature of Occupancy	Occupancy Category
Buildings and other structures that represent a low hazard to human life in the event of failure, including, but not limited to: • Agricultural facilities • Certain temporary facilities • Minor storage facilities	I
All buildings and other structures except those listed in Occupancy Categories I, III, and IV	II
Buildings and other structures that represent a substantial hazard to human life in the event of failure, including, but not limited to: • Buildings and other structures where more than 300 people congregate in one area • Buildings and other structures with daycare facilities with a capacity greater than 150 • Buildings and other structures with elementary school or secondary school facilities with a capacity greater than 250 • Buildings and other structures with a capacity greater than 500 for colleges or adult education facilities • Health care facilities with a capacity of 50 or more resident patients, but not having surgery or emergency treatment facilities • Jails and detention facilities Buildings and other structures, not included in Occupancy Category IV, with potential to cause a substantial economic impact and/or mass disruption of day-to-day civilian life in the event of failure, including, but not limited to: • Power generating stations[a] • Water treatment facilities • Sewage treatment facilities • Telecommunication centers Buildings and other structures not included in Occupancy Category IV (including, but not limited to, facilities that manufacture, process, handle, store, use, or dispose of such substances as hazardous fuels, hazardous chemicals, hazardous waste, or explosives) containing sufficient quantities of toxic or explosive substances to be dangerous to the public if released. Buildings and other structures containing toxic or explosive substances shall be eligible for classification as Occupancy Category II structures if it can be demonstrated to the satisfaction of the authority having jurisdiction by a hazard assessment as described in Section 1.5.2 that a release of the toxic or explosive substances does not pose a threat to the public.	III
Buildings and other structures designated as essential facilities, including, but not limited to: • Hospitals and other health care facilities having surgery or emergency treatment facilities • Fire, rescue, ambulance, and police stations and emergency vehicle garages • Designated earthquake, hurricane, or other emergency shelters • Designated emergency preparedness, communication, and operation centers and other facilities required for emergency response • Power generating stations and other public utility facilities required in an emergency • Ancillary structures (including, but not limited to, communication towers, fuel storage tanks, cooling towers, electrical substation structures, fire water storage tanks or other structures housing or supporting water, or other fire-suppression material or equipment) required for operation of Occupancy Category IV structures during an emergency • Aviation control towers, air traffic control centers, and emergency aircraft hangars • Water storage facilities and pump structures required to maintain water pressure for fire suppression • Buildings and other structures having critical national defense functions Buildings and other structures (including, but not limited to, facilities that manufacture, process, handle, store, use, or dispose of such substances as hazardous fuels, hazardous chemicals, or hazardous waste) containing highly toxic substances where the quantity of the material exceeds a threshold quantity established by the authority having jurisdiction. Buildings and other structures containing highly toxic substances shall be eligible for classification as Occupancy Category II structures if it can be demonstrated to the satisfaction of the authority having jurisdiction by a hazard assessment as described in Section 1.5.2 that a release of the highly toxic substances does not pose a threat to the public. This reduced classification shall not be permitted if the buildings or other structures also function as essential facilities.	IV

[a]Cogeneration power plants that do not supply power on the national grid shall be designated Occupancy Category II.

Table 2A.2 – Ground snow loads at 204 National Weather Service locations where load measurements are made (ASCE 7-05 2005).

Location	Ground Snow Load (lb/ft²)			Location	Ground Snow Load (lb/ft²)		
	Years of record	Maximum observed	2% Annual probability[a]		Years of record	Maximum observed	2% Annual probability[a]
ALABAMA				MICHIGAN			
Birmingham	40	4	3	Alpena	31	34	48
Huntsville	33	7	5	Detroit City	14	6	10
Mobile	40	1	1	Detroit Airport	34	27	18
ARIZONA				Detroit-Willow	12	11	22
Flagstaff	38	88	48	Flint	37	20	24
Tucson	40	3	3	Grand Rapids	40	32	36
Winslow	39	12	7	Houghton Lake	28	33	48
ARKANSAS				Lansing	35	34	36
Fort Smith	37	6	5	Marquette	16	44	53
Little Rock	24	6	6	Muskegon	40	40	51
CALIFORNIA				Sault Ste. Marie	40	68	77
Bishop	31	6	8	MINNESOTA			
Blue Canyon	26	213	242	Duluth	40	55	63
Mt. Shasta	32	62	62	International Falls	40	43	44
Red Bluff	34	3	3	Minneapolis-St. Paul	40	34	51
COLORADO				Rochester	40	30	47
Alamosa	40	14	14	St. Cloud	40	40	53
Colorado Springs	39	16	14	MISSISSIPPI			
Denver	40	22	18	Jackson	40	3	3
Grand Junction	40	18	16	Meridian	39	2	2
Pueblo	33	7	7	MISSOURI			
CONNECTICUT				Columbia	39	19	20
Bridgeport	39	21	24	Kansas City	40	18	18
Hartford	40	23	33	St. Louis	37	28	21
New Haven	17	11	15	Springfield	39	14	14
DELAWARE				MONTANA			
Wilmington	39	12	16	Billings	40	21	15
GEORGIA				Glasgow	40	18	19
Athens	40	6	5	Great Falls	40	22	15
Atlanta	39	4	3	Havre	26	22	24
Augusta	40	8	7	Helena	40	15	17
Columbus	39	1	1	Kalispell	29	27	45
Macon	40	8	7	Missoula	40	24	22
Rome	28	3	3	NEBRASKA			
IDAHO				Grand Island	40	24	23
Boise	38	8	9	Lincoln	20	15	22
Lewiston	37	6	9	Norfolk	40	28	25
Pocatello	40	12	10	North Platte	39	16	13
ILLINOIS				Omaha	25	23	20
Chicago-O'Hare	32	25	17	Scottsbluff	40	10	12
Chicago	26	37	22	Valentine	26	26	22
Moline	39	21	19	NEVADA			
Peoria	39	27	15	Elko	12	12	20
Rockford	26	31	19	Ely	40	10	9
Springfield	40	20	21	Las Vegas	39	3	3
INDIANA				Reno	39	12	11
Evansville	40	12	17	Winnemucca	39	7	7
Fort Wayne	40	23	20	NEW HAMPSHIRE			
Indianapolis	40	19	22	Concord	40	43	63
South Bend	39	58	41	NEW JERSEY			
IOWA				Atlantic City	35	12	15
Burlington	11	15	17	Newark	39	18	15
Des Moines	40	22	22	NEW MEXICO			
Dubuque	39	34	32	Albuquerque	40	6	4
Sioux City	38	28	28	Clayton	34	8	10
Waterloo	33	25	32	Roswell	22	6	8
KANSAS				NEW YORK			
Concordia	30	12	17	Albany	40	26	27
Dodge City	40	10	14	Binghamton	40	30	35
Goodland	39	12	15	Buffalo	40	41	39
Topeka	40	18	17	NYC - Kennedy	18	8	15
Wichita	40	10	14	NYC - LaGuardia	40	23	16
KENTUCKY				Rochester	40	33	38
Covington	40	22	13	Syracuse	40	32	32
Jackson	11	12	18	NORTH CAROLINA			
Lexington	40	15	13	Asheville	28	7	14
Louisville	39	11	12	Cape Hatteras	34	5	5
LOUISIANA				Charlotte	40	8	11
Alexandria	17	2	2	Greensboro	40	14	11
Shreveport	40	4	3	Raleigh-Durham	36	13	14
MAINE				Wilmington	39	14	7
Caribou	34	68	95	Winston-Salem	12	14	20
Portland	39	51	60	NORTH DAKOTA			
MARYLAND				Bismark	40	27	27
Baltimore	40	20	22	Fargo	39	27	41
MASSACHUSETTS				Williston	40	28	27
Boston	39	25	34	OHIO			
Nantucket	16	14	24	Akron-Canton	40	16	14
Worcester	33	29	44	Cleveland	40	27	19

Table 2A.2 – Ground snow loads at 204 National Weather Service locations where load measurements are made (ASCE 7-05 2005).

Location	Ground Snow Load (lb/ft²)			Location	Ground Snow Load (lb/ft²)		
	Years of record	Maximum observed	2% Annual probability[a]		Years of record	Maximum observed	2% Annual probability[a]
Columbus	40	11	11	Austin	39	2	2
Dayton	40	18	11	Dallas	23	3	3
Mansfield	30	31	17	El Paso	38	8	8
Toledo Express	36	10	10	Fort Worth	39	5	4
Youngstown	40	14	10	Lubbock	40	9	11
OKLAHOMA				Midland	38	4	4
Oklahoma City	40	10	8	San Angelo	40	3	3
Tulsa	40	5	8	San Antonio	40	9	4
OREGON				Waco	40	3	2
Astoria	26	2	3	Wichita Falls	40	4	5
Burns City	39	21	23	UTAH			
Eugene	37	22	10	Milford	23	23	14
Medford	40	6	6	Salt Lake City	40	11	11
Pendleton	40	9	13	Wendover	13	2	3
Portland	39	10	8	VERMONT			
Salem	39	5	7	Burlington	40	43	36
Sexton Summit	14	48	64	VIRGINIA			
PENNSYLVANIA				Dulles Airport	29	15	23
Allentown	40	16	23	Lynchburg	40	13	18
Erie	32	20	18	National Airport	40	16	22
Harrisburg	19	21	23	Norfolk	38	9	10
Philadelphia	39	13	14	Richmond	40	11	16
Pittsburgh	40	27	20	Roanoke	40	14	20
Scranton	37	13	18	WASHINGTON			
Williamsport	40	18	21	Olympia	40	23	22
RHODE ISLAND				Quillayute	25	21	15
Providence	39	22	23	Seattle-Tacoma	40	15	18
SOUTH CAROLINA				Spokane	40	36	42
Charleston	39	2	2	Stampede Pass	36	483	516
Columbia	38	9	8	Yakima	39	19	30
Florence	23	3	3	WEST VIRGINIA			
Greenville-Spartanburg	24	6	7	Beckley	20	20	30
SOUTH DAKOTA				Charleston	38	21	18
Aberdeen	27	23	43	Elkins	32	22	18
Huron	40	41	46	Huntington	30	15	19
Rapid City	40	14	15	WISCONSIN			
Sioux Falls	39	40	40	Green Bay	40	37	36
TENNESSEE				La Crosse	16	23	32
Bristol	40	7	9	Madison	40	32	35
Chattanooga	40	6	6	Milwaukee	40	34	29
Knoxville	40	10	9	WYOMING			
Memphis	40	7	6	Casper	40	9	10
Nashville	40	6	9	Cheyenne	40	18	18
TEXAS				Lander	39	26	24
Abilene	40	6	6	Sheridan	40	20	23
Amarillo	39	15	10				

Sloped Roof Snow Loads

For warm roofs ($C_t \leq 1.0$ as determined from Table 2.2 in Chapter 2) with an unobstructed slippery surface that will allow some snow to slide off the eaves, C_s is determined using the dashed line in Figure 2A.2a. For these types of warm roofs, it is assumed that their thermal resistance (R-value) equals or exceeds 30 ft2 h °F/Btu and 20 ft2 h °F/Btu for nonventilated roofs and ventilated roofs, respectively. Ventilated roofs should be vented in such a way as to allow exterior air to circulate freely from the eaves to the ridges.

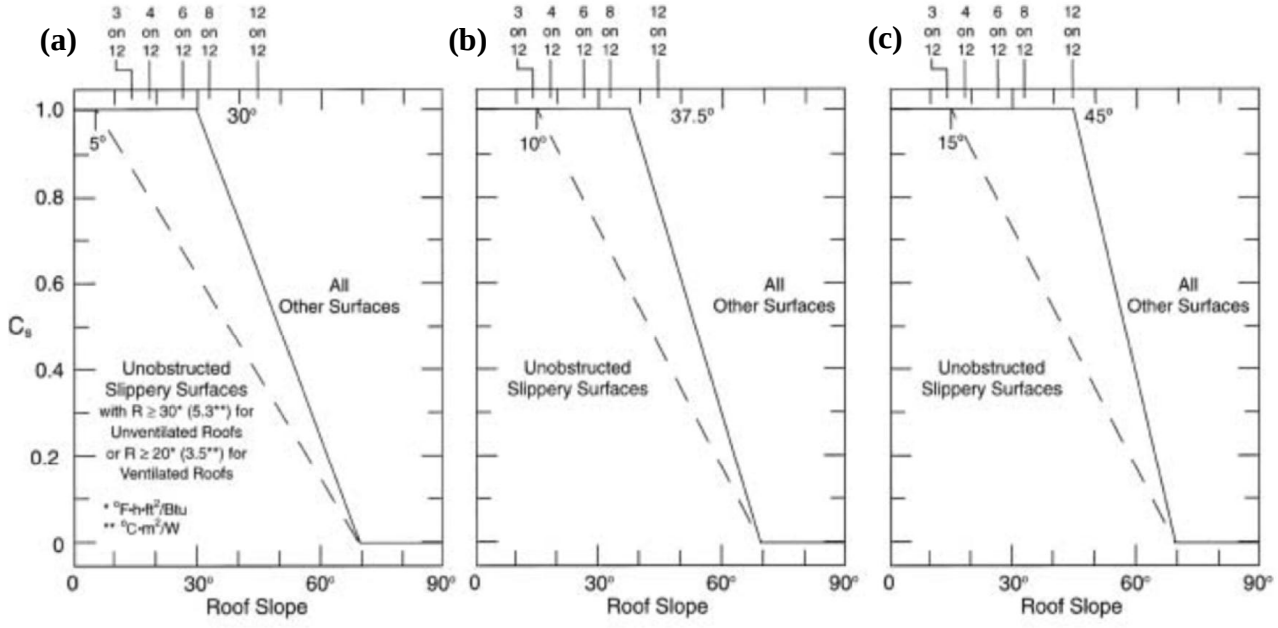

Figure 2A.2 – Graphs for determining roof slope factor C_s for warm and cold roofs for (a) warm roofs with $C_t \leq 1.0$, (b) cold roofs with $C_t = 1.1$, and (c) cold roofs with $C_t = 1.2$ (ASCE 7-05).

If any of the aforementioned conditions are not met, the solid line is used in Figure 2A.2a (ASCE 7-05 2010). For cold roofs ($C_t > 1.0$) with $C_t = 1.1$ and an unobstructed slippery surface that will allow some snow to slide off the eaves, C_s is determined using the dashed line in Figure 2A.2b; all other cold roofs with $C_t = 1.1$, C_s is determined using the solid line. If $C_t = 1.2$ and the

roof has an unobstructed slippery surface, C_s is determined using the dashed line on Figure 2A.2c; for all other cases with C_t = 1.2, Cs is determined using the solid line (ASCE 7-05 2005).

Portions of roofs with slopes greater than 70° shall be considered free of snow. For multiple folded plate, sawtooth, and barrel vault roofs, C_s shall be 1.0. Obstructions along the eaves may occur, such as ice dams and icicles. For these cases, unventilated warm roofs that have an R-value less than 30 ft2 h °F/Btu and ventilated warm roofs that have an R-value less than 20 ft2 h °F/Btu should be designed to withstand a uniformly distributed load of 2 psf on all overhanging portions of the eaves. Only dead loads should be present when this uniformly distributed load is applied (ASCE 7-05 2005).

Drifts on Lower Roofs

Snow drifts form when wind blows the snow from a higher roof or when the wind from the opposite direction causes the snow to drift along an obstruction. These two types of drifts are called leeward drifts and windward drifts, respectively, and are shown in Figure 2A.3.

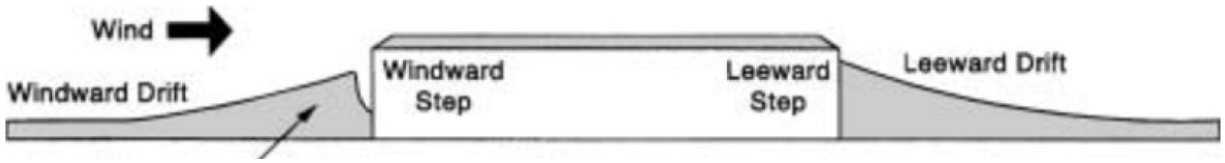

Figure 2A.3 – Drifts formed at windward and leeward steps (ASCE 7-05 2005).

Loads from the surcharged drifted load shall be approximated by the triangle in Figure 2A.4. Drift loads are superimposed on the balanced snow load case. If the ratio of the drift width to the height of the balanced snow load (determined by dividing p_s by γ), h_c/h_b is less than 0.2, drift loads need not be applied.

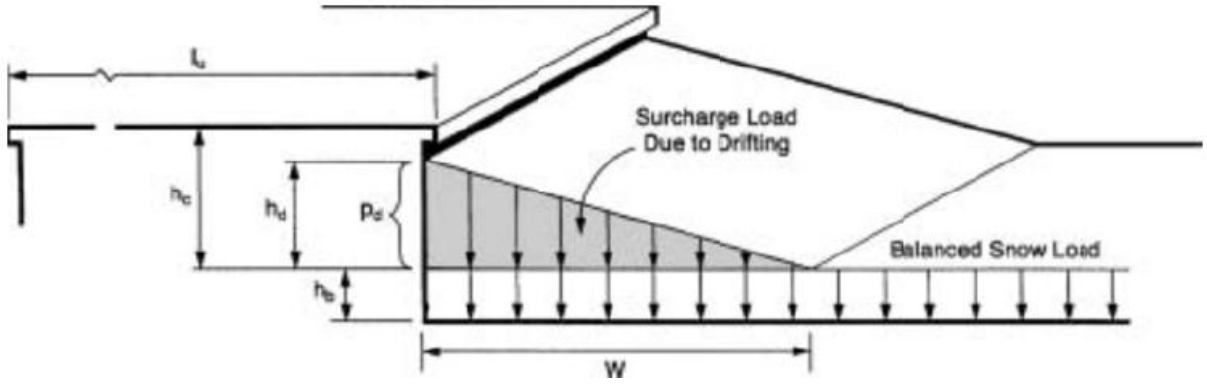

Figure 2A.4 – Configuration of snow drifts on lower roofs (ASCE 7-05 2005).

For leeward drifts, the drift height is determined from Figure 2A.5, using the upper roof length. For windward drifts, l_u in Figure 2A.5 is replaced by the length of the lower roof, and the drift height is taken as ¾ h_d. If the drift height is equal to or less than h_c, the drift width, w, is equal to $4h_d$ and the drift height is h_d. However, if the height is larger than h_c, the drift width is equal to $4h_d/h_c$ and the drift height shall be taken as h_c. The drift width is never to exceed $8h_c$. The maximum intensity of the drift surcharge load, p_d, is equal to $h_d\,\gamma$, where γ is equal to $(0.13p_g + 14)$ but not more than 30 pcf (ASCE 7-05 2005).

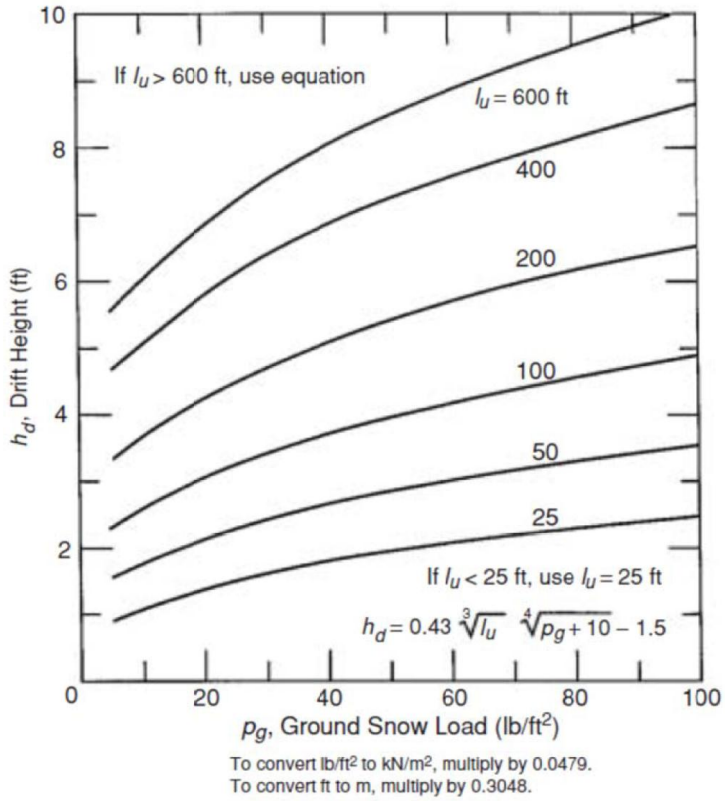

Figure 2A.5 – Graph and equation for determining drift height (ASCE 7-05 2005).

Roof Projections

The same method used above for drifting snow shall be applied to calculate drift loads on all sides of roof obstructions, such as parapet walls and roof projections. The drift height is ¾ h_d and l_u is equal to the length of the roof upwind of the projection or parapet wall. Drift loads shall only be calculated for roof projections that are 15 ft long or more (ASCE 7-05 2005).

Sliding Snow

Some roof geometries allow snow to slide easily onto ground or perhaps, lower roofs. Situations in which snow slides from upper roofs to lower roofs should be avoided, if possible. If these instances cannot be avoided, the extra load from the sliding snow should be considered. For nonslippery upper roofs with slopes greater than 1:6 and slippery upper roofs with slopes greater than ¼:12, the sliding snow load shall be determined, where the total sliding snow per

unit length of the eave is 0.4pf ·W. The sliding snow shall be applied as uniformly distributed load over a distance of 15 ft from the upper roof eave. Sliding snow shall be reduced proportionately if the distance is less than 15 ft. In all cases, sliding snow shall be added to the balanced load case (ASCE 2005).

Rain-on-Snow Surcharge

For locations where the ground snow load is less than 20 psf (but not zero) and the roof slope is less than *W*/50 (in degrees), a five psf rain-on-snow surcharge shall be added to the balanced roof snow loads. W is defined as the horizontal distance from the eave to the ridge of the roof (ASCE 7-05 2005).

Ponding Instability

Without proper roof pitch or when drains become clogged, ponding is likely to occur on building roofs. Ponding can be a recurring event: as water ponds in one part of the roof, the roof deflects, which causes more water to pond at that spot, and the cycle continues. Instability due to ponding shall be investigated from rain-on-snow or melting snow if slopes on buildings are less than ¼ in./ft. (1.19°) (ASCE 7-05 2005).

7.3.1 Partial Loading

In addition to balanced roof snow load cases, unbalanced snow load cases must also be investigated. Balanced snow loads are assumed to be uniformly distributed along the entire roof span in design, while unbalanced snow loads vary across the roof span. For multi-span roof systems, partial loading shall be investigated for selected spans loaded with the balanced snow load. Remaining spans in the multi-span roof systems shall be loaded with half the balanced snow load for the following continuous beam system cases: (1) full balanced snow load on either exterior span and half the balanced snow load on all other spans; (2) half the balanced snow load

on either exterior span and full balanced snow load on all other spans; and (3) all possible combinations of full balanced snow load on any two adjacent spans and half the balanced snow load on all other spans. For Case (3) there will be (n-1) possible combinations, where n equals the number of spans in the continuous beam system (ASCE 2005). See Figure 2a and Figure 2b for Case (1) and Case (2), respectively, for a structure with three spans. Since the building is symmetric, Case (3) will not have to be examined. For more information on the design of non-uniform and drifted snow loads, see Appendix 2. At this stage, partial loading was not considered in the design of the buildings analyzed in this study.

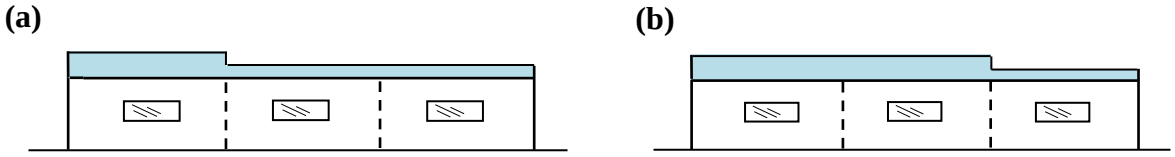

Figure 2A.6 – Elevation views depicting snow loads on a three-span structure with (a) full balanced snow load on either exterior span and half the balanced snow load on all other spans, and (b) half the balanced snow load on either exterior span and full balanced snow load on all other spans.

Snow Provisions in ASCE 7-10

The most recent version (2010) of ASCE 7 contains important changes and updates to the provisions of ASCE 7-05. The most notable updates include the clarification of minimum roof snow loads and RTU drifts, the addition of one thermal factory category for freezer building and cold roofs, the revision of lower and upper bound roof slopes for unbalanced loads, the deletion of the consideration of drift loads outside the wind shadow region for lower roofs, the consideration of sliding loads from upper to lower roofs, and the consideration of ponding for buildings with roof geometries not included in ASCE 7-05 (O'Rourke 2011).

Minimum Roof Snow Load

As per ASCE 7-05, the minimum roof snow load to be considered for design shall be the smaller of $I \cdot p_g$ or the ground snow load. Confusion arose when determining whether to include this value in the combination of drifting loads or sliding loads. The minimum roof snow load is distinctly different than the flat roof snow load and should not be included in the combination of drifting or sliding loads. ASCE 7-10 created a new symbol for the minimum roof snow load, pm, which is separate from the flat roof snow load and the sloped roof snow load (O'Rourke 2011).

Drift Loading at Roof Top Units (RTUs)

With ASCE 7-05, confusion arose when determining which fetch distance to use with windward drifts at Roof Top Units (RTUs). The designer was expected to consider two different drift distances upwind and downwind from the RTU, but it was unclear which distance to use at the location of the windward drift. ASCE 7-10 simplified the fetch distance as the greater of these two distances, thereby requiring the same drift on both sides (O'Rourke 2011).

Thermal Factor

Even if the worst case scenario is used (I = 1.0, C_e = 1.2, and C_t = 1.2), the roof snow load would always be smaller than the ground snow load with the ASCE 7-05 provisions ($1.008p_g$). In most situations, this phenomenon is accurate. However, observations by the Structural Engineers Association of Washington (SEAW) revealed larger roof snow loads than ground snow loads after one winter storm on freezer buildings and cold rooms. Investigation revealed heat transfer as the reason for the larger roof snow load values due to retention of the snow pack and potential for additional buildup. Roof snowpack on a heated building (heated air at the base of the snowpack and ambient air above) causes the snow to melt, while roof

snowpack on a freezer building (cold air at the base of the snowpack and above) causes the snow to build up. Ground snow load values fall somewhere in the middle of these two due to the warm ground and ambient air above. Therefore, ASCE 7-10 created an additional thermal factor for structures intentionally kept below freezing (C_t = 1.3), while the 1.2 thermal factor for unheated and open air structures of ASCE 7-05 remained (O'Rourke 2011).

Unbalanced Loads

ASCE 7-05 requires the consideration of drifted snow for hip and gable roofs with slopes greater than 70 degrees. However, independent observations from the Tahoe-Truckee Engineers Association (TTEA) and insurance company files suggest that unbalanced loads only form on roof slopes of 6 on 12 or less. Therefore, ASCE 7-10 does not require unbalanced loads to be applied to roof slopes exceeding 7 on 12. For hip and gable roofs with slopes less than ½ on 12, unbalanced snow loads are not required to be applied (O'Rourke 2011).

In ASCE 7-05, the empirical relationship between drift height, ground snow load, and upwind fetch distance (Equation 2 of ASCE 7-05, Chapter 6) for the calculation of the drift height is based on a fetch distance of hundreds of feet. Although ASCE 7-05 provided a lower bound fetch distance of 25 feet, the empirical relationship proved problematic and produced negative fetch distances for gable roofs since most eave-to-ride distances of single-family residences were less than 25 feet. Tests of simulated drifts revealed that lowering the limit by five feet was sufficient. ASCE 7-10 requires designers to use a fetch distance of 20 feet if less than or equal to 20 feet in the approximation for drift height (O'Rourke 2011).

Separated Structures

Although ASCE 7-05 required the consideration of drift loads on lower level roofs if the roof separation is less than 20 feet, it does not require any specific geometric consideration for the drift loads. Therefore, ASCE 7-10 added a requirement for the consideration of leeward drifts if a portion of the lower roof is in the area of aerodynamic shade or wind shadow of the upper level roof, as shown in Figure 2A.6a by slope 1 to 6. The geometry of the drift surcharge load should have a height of the smaller of h_d (drift height based on the upper roof fetch distance) and (6*h*-*S*)/6 (based upon a snow drift filling the wind shadow space on the lower level roof), a length of the smaller of 6h_d and (6*h*-*S*), and should match the shadow boundary slope in Figure 2A.7b (O'Rourke 2011).

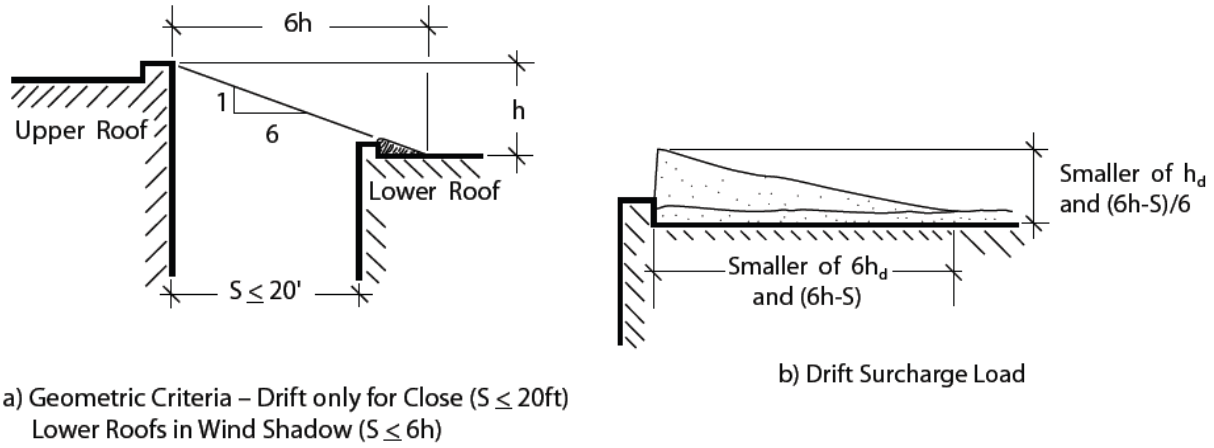

Figure 2A.7 – Leeward and drift on separated roofs (O'Rourke 2011).

Although ASCE 7-05 does require lower roofs to be designed for sliding snow, it fails to account for sliding snow on separated roofs. The sliding snow load provisions were expanded in ASCE 7-10 to include separated roofs within 15 feet if the elevation distance is greater than the horizontal separation distance based on a 1 to 1 sliding load shadow, as shown in Figure 2A.8a. The load per unit length in ASCE 7-05 is $0.4 \cdot p_f \cdot W_s$ and the load per unit length in ASCE 7-10 is $0.4 \cdot p_f \cdot W(15 - s)/15$, as shown in Figure 2A.7b (O'Rourke 2011).

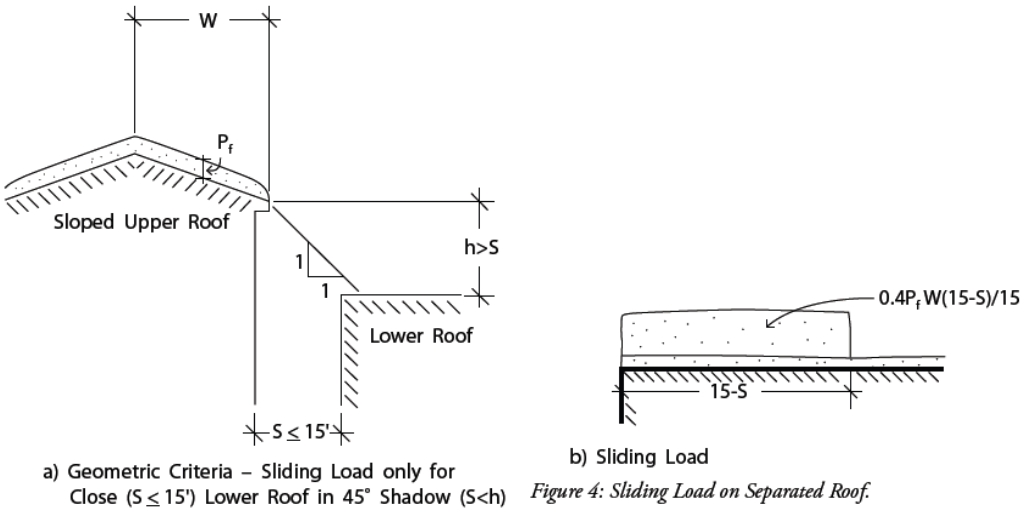

Figure 4: Sliding Load on Separated Roof.

Figure 2A.8 – Sliding load on separated roof (O'Rourke 2011).

Ponding

Although ASCE 7-05 considers ponding for roofs with slopes less than ½ to 12, it does not consider ponding for roofs where water could build up, irrespective of the slope. Therefore, ASCE 7-10 altered the provisions to account for these different cases.

Appendix 5

Geometric Transformations

The local coordinate system is defined first by the x-axis, which connects the two element nodes. In OpenSees, "the y- and z- axes are then defined using a vector that lies on a plane parallel to the local x-z plane and the local y-axis is defined by taking the cross product of the unit vector and the x-axis" (PEER 2006). Geometric transformations are specified in OpenSees by defining how much a unit vector in local elemental xz space contributes to overall global X, Y, and Z space. For the upper chord of the joist shown below in Figure A5.2, the unit vector in local xz space contributes only to the positive global Z degree of freedom. Therefore, the geometric transformation is defined as [0 0 1], which are the global X, Y, and Z contributions. If the beam is rotated 180 degrees, as in the bottom chord case, the geometric transformation will be [0 0 -1], since the unit vector will be contributing to the negative global Z direction (Figure A5.3). The web and end rods members are defined by the following: X-contribution = sin(Θ); Z-contribution = cos(Θ). The unit vector xz lies in the global XZ plane, and therefore does not contribute to the global Y direction. The geometric transformation of the

web member is [0.866 0 0.5] (Figure A5.4), while the geometric transformation for the end rod member is [0.5 0 0.866] (Figure A5.5).

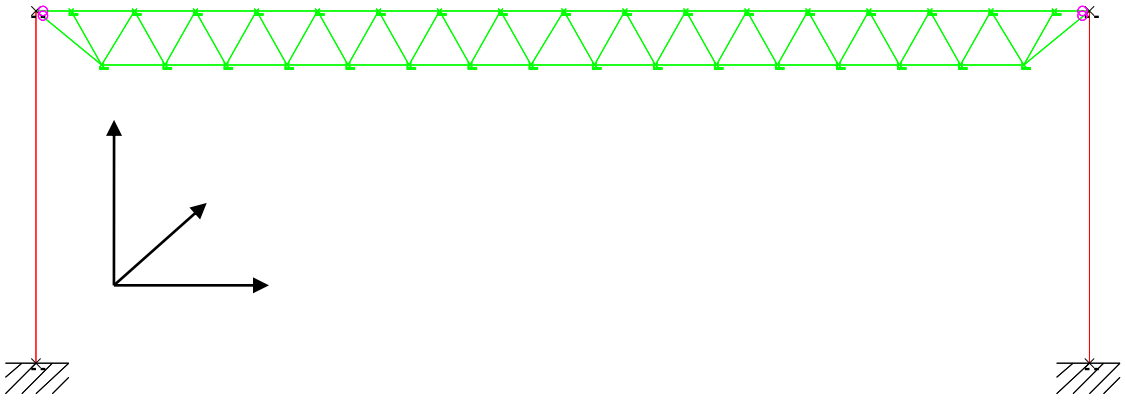

Figure A5.1 – Front elevation view of one joist from the building models.

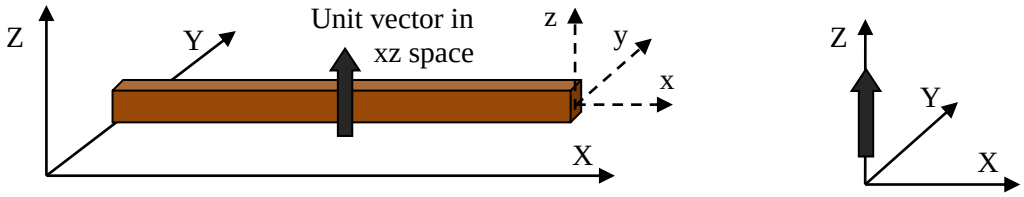

Figure A5.2 – Geometric transformations for upper chord elements.

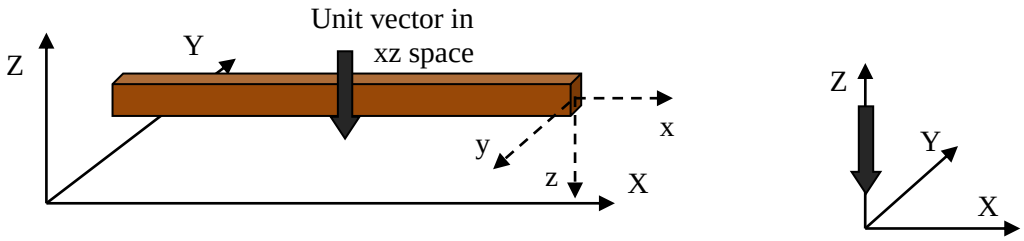

Figure A5.3 – Geometric transformations for lower chord elements.

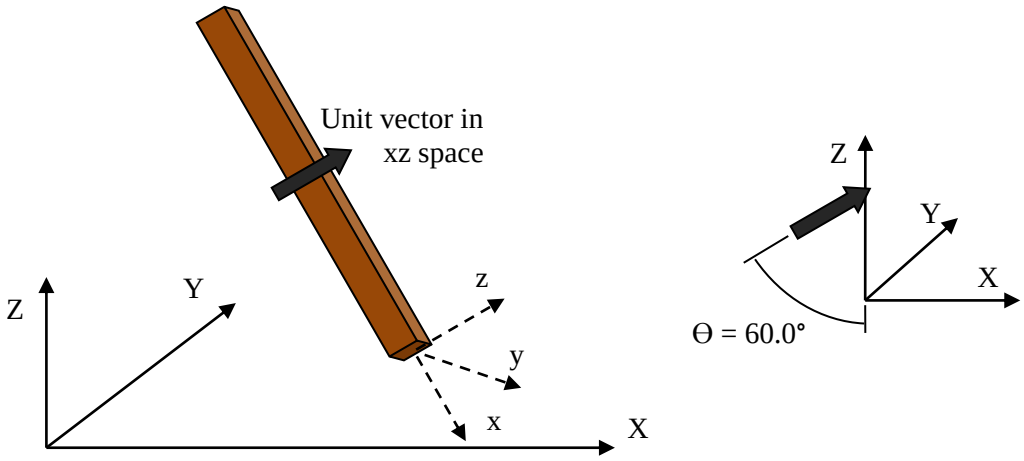

Figure A5.4 – Geometric transformations for interior web elements.

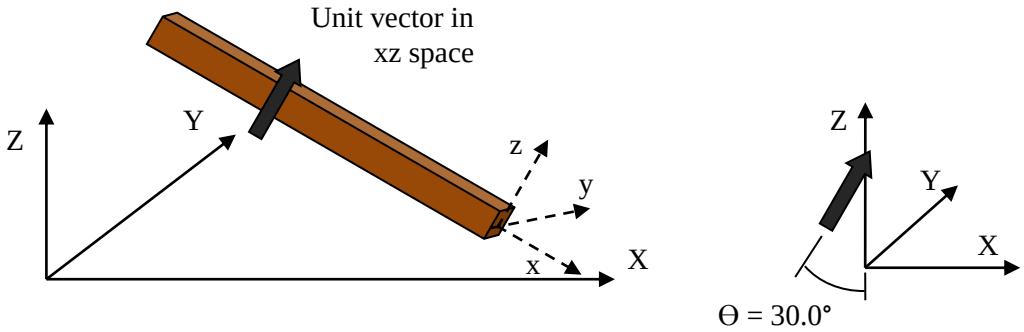

Figure A5.5 – Geometric transformations for end rod elements.